Vysoké učení technické v Brně
Fakulta strojního inženýrství
Ústav konstruování

Brno University of Technology Faculty
of Mechanical Engineering Institute
of Machine and Industrial Design

THE EFFECT OF SYNOVIAL FLUID CONSTITUENTS ON FRICTION AND LUBRICATION OF ARTICULAR CARTILAGE

Ing. Pavel Čípek
Autor práce
Author

doc. Ing. Martin Vrbka, Ph.D.
Vedoucí práce
Supervisor

Disertační práce
Dissertation Thesis

Brno 2021

STATEMENT

I hereby declare that I have written the PhD thesis The Effect of Synovial Fluid Constituents on Friction and Lubrication of Articular Cartilage on my own according to advice of my supervisor doc. Ing. Martin Vrbka, Ph.D., and using the sources listed in references.

.....

Author's signature

BIBLIOGRAPHICAL REFERENCE

ČÍPEK, P. *The Effect of Synovial Fluid Constituents on Friction and Lubrication of Articular Cartilage*. Brno, 2021, 109 p. PhD thesis. Brno University of Technology, Faculty of Mechanical Engineering, Institute of Machine and Industrial Design. Supervisor: doc. Ing. Martin Vrbka, Ph.D.

ACKNOWLEDGEMENT

There are many people who deserve thanks, but it is impossible to express thanks to everyone who deserves it. At first, I would like to thank my supervisor doc. Ing. Martin Vrbka, Ph.D. as well as the head of Tribology research group prof. Ing. Ivan Křupka, Ph.D. for their support, opportunity and advice during my doctoral study. Special thanks must go to Ing. David Nečas, Ph.D. for his help, motivation, and discussions. Of course, many thanks include to all my colleagues at Institute of Machine and Industrial Design for friendly and positive atmosphere. Finally, I express my huge thanks to my parents and family and also to my wife Anna!

ABSTRACT

The present PhD thesis deals with the lubricating mechanism within a model of synovial joint. The aim of this thesis is to describe the effect of individual components of synovial fluid on lubricating film formation in the model of synovial joint; for this purpose, the experimental analysis of friction coefficient and observation of adsorbed lubricating film using the fluorescence microscopy were performed. The special self-designed reciprocating tribometer allowing for simultaneous friction measurement and contact observation was designed. The tribometer was calibrated and verified using a commercial tribometer. Furthermore, the methodology of experiments was developed including a design of evaluation procedure. In order to process the visualization record, the software based on the image segmentation was developed. The last part of the thesis introduces a novel methodological approach together with a new self-designed tribometer enabling to assess the role of components contained in the model synovial fluid in relation to the formation of lubricating film based on in situ observation of the contact area and simultaneous frictional measurement. The thesis presents original results extending the knowledge in the natural synovial joint biotribology towards the further development of effective treatment for patients with diseased joints.

KEYWORDS

Biotribology, cartilage, reciprocating tribometer, friction, lubrication, fluorescence microscopy

ABSTRAKT

Práce se zabývá problematikou biotribologie modelu synoviálního kloubu. Cílem práce je popsat vliv složek synoviální kapaliny na formování mazacího filmu v modelu synoviálního kloubu. Práce je zaměřena na experimentální analýzu součinitele smykového tření a jeho propojení s pozorováním adsorbovaného mazacího filmu v kontaktu pomocí fluorescenční mikroskopie. Součástí práce je návrh tribometru, který umožňuje vizualizaci v průběhu experimentů. Tribometr je vyroben, kalibrován a verifikován pomocí komerčního tribometru. Dále je součástí práce návrh metodiky experimentů včetně návrhu postupu pro zpracování a hodnocení výsledků. Pro zpracování záznamu z vizualizace kontaktu byl navržen speciální software, který pracuje na principu segmentace obrazu. Poslední část práce je zaměřena na aplikaci vyvinuté metodologie spolu s nově navrženým tribometrem, což umožňuje posoudit roli složek modelové kapaliny u formování mazacího filmu v modelu synoviálního kloubu. Experimentální část je založena na měření tření za současné vizualizace kontaktu. Tato práce prezentuje originální výsledky rozšiřující oblast biotribologie synoviálního kloubu, které mohou pomoci dalšímu rozvoji účinné léčby pacientů s nemocnými klouby.

KLÍČOVÁ SLOVA

Biotribologie, chrupavka, reciproční tribometer, tření, mazání, fluorescenční mikroskopie

CONTENTS

1 INTRODUCTION

One of the keys to a quality and painless life is the opportunity to be active. Physical activities in our lives can reduce stress and help us to stay mentally balanced [1], [2]; however, it requires a healthy natural musculoskeletal system, which ensures the movement of the human body. Despite the fact that the human society takes it for granted, the natural human joint can be affected by a variety of diseases that can damage it and limit its function. The proper function of human natural musculoskeletal system requires, from a tribological point of view, well lubricated contact surfaces of natural joints, which is closely related to a very low friction coefficient (CoF) and low wear on cartilaginous surfaces of the natural joint. The diseases disrupt the tribological environment in the joint, and the unique properties deteriorate. There are many types of joint diseases (arthrosis, arthritis, osteoarthritis, etc.) and each of them affects and degrades the natural joint differently. The natural joint is gradually damaged and, if a professional medical intervention is not performed, the joint can be damaged to the degree where movement is not possible. The disease of unfunctional natural joint is almost healed with total replacement, when the joint is replaced for the artificial one [3]. The joint replacement fully compensates the natural joint but its lifetime is limited. When the lifetime of the replacement ends, the artificial joint is too damaged, and it needs to be replaced with a new one. In this case, the correct function of human movement system is preserved; nevertheless, the artificial joints have an average lifetime of 10 – 20 years [4]. When the disease and damage of the natural joint occurs in young patients, the artificial joint will need to be replaced more than once. The human body does not have the ability to handle the artificial joint reoperation repeatedly , because of bone degradation , and the surgery also has an impact on the overall health condition of the patient [5], [6], [7]. Therefore, if the patient's natural joint is damaged at young age, these patients, in old age, remain with an incurable artificial joint, and their movement system is unfunctional.

Due to the acute problems with longevity of endoprosthesis, scientists have come up with non-invasive treatment (intervention that does not require surgery) of diseased natural joints (viscosupplementation). The supplement is a gel-like liquid, based on hyaluronic acid (HA) and it is injected into the joint gap [7]. Its primary function is to restart the lubrication processes in the synovial joint, which can improve the protection of the cartilage surface; Ideally, the disease progression is stopped, or there is at least a slowdown in the process of joint degradation. The general effort of viscosupplementation is to postpone the necessity of the surgery of damaged natural joint for as long as possible [7], [8]. The supplement therapy is usually effective, unfortunately this is not guaranteed in every patient; therefore, it is obvious that the principles of the viscosupplementation function have not yet been fully understood [9], [10], [11]. For better understanding of viscosupplementation principles, a full description of the lubricating processes in the natural synovial joint is necessary. The description of lubricating film formation in the cartilage contact (a model of natural synovial

joint) holds a key role in understanding the viscosupplementation function; therefore, a full understanding of this issue can help us to develop an effective supplement for the whole spectrum of patients with diseased joints.

2 STATE OF ART

2.1 Synovial joint

The natural synovial joints (NSJ) are one of the key components of human musculoskeletal and movement system. The joint consists of two bones facing each other, which surfaces are covered by articular cartilage tissue (AC) and the articular gap is lubricated by the synovial fluid (SF) [12], see Fig. 2.1. The main role of NSJ is transmission of load, while preserving movement with very low CoF, which is allowed due to the unique tribological and mechanical properties of AC in combination with unique tribological properties of SF [13].

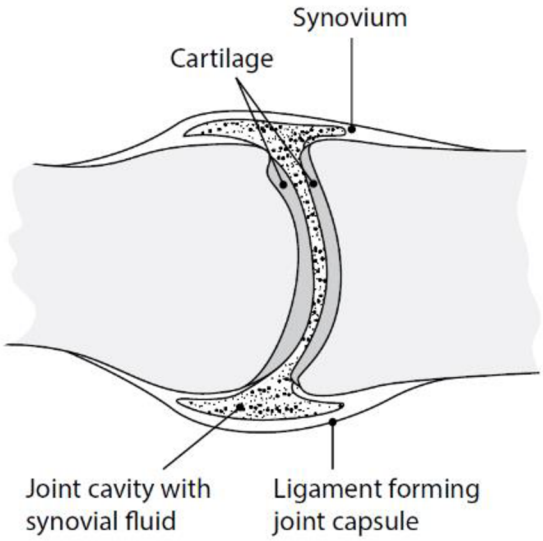

Fig. 2.1 - Natural synovial joint [14]

2.1.1 Articular cartilage

The AC is a spongy tissue with porous structure, mostly formed by water (60-80%) and the extracellular matrix (ECM) contains mostly type II collagen fibres, proteoglycans, lubricin, HA, etc. [12], [15], [16], [17]. The AC structure has very low cell density, only 2 – 10%, and it does not contain blood vessels. The cells have a low regenerative capacity, because the nutrient intake allows only for diffusion, which causes poor transmission of nutrients into the AC structure; therefore the AC nutrients are largely supplied by SF [12], [15].The AC is anisotropic and heterogeneous material, which structure changes through the thickness (depth from the surface), especially the orientation of collagen fibres and representation of individual components [18]. The thickness of the AC can be divided into three zones; each of them characterized by different structure, especially by varying orientation, shape and amount of collagen fibres [12], [18]. The first, surface zone, is characterized by greatest cell density and the chondrocytes and collagen fibres are flat in shape. Thanks to these properties,

the surface zone of the AC is most resistant to shear and normal load, and the collagen fibres are orientated parallel to the surface. The surface zone occupies 10-20% of the AC thickness (see Fig. 2.2) [18]. The second, middle zone, occupies the greatest part of the AC thickness, 40-60%. The collagen fibres are not regularly oriented, they have a random direction and shape. The last depth zone is characterized by collagen fibres orientated perpendicular to the AC surface and they are flat in shape. The depth zone forms a transition, connection between the AC and subchondral bone (see Fig. 2.2).

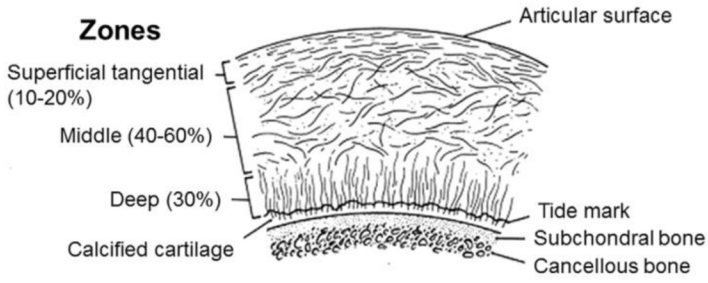

Fig. 2.2 - AC structure divided into zones

The AC is a mechanically robust materiel that can carry load up to 18 MPa, such as the load occurring in hip joint [19]. The elasticity modulus (EM) of the AC ranges between 1 and 20 MPa and it depends on the type of joint, place on the AC surface (especially if the place is loaded or not), etc. [13], [20]. The value of EM depends on the degree of AC hydration. The water content rate (hydration) in the AC structure varies with cartilage depth. It is caused by negatively charged glycosaminoglycans that are included in surface zone of the AC structure, and they attract water [21]. The water is stored in the AC pores together with other components of the SF, however the pores store only particles smaller than themselves, and the rest remains on the AC surface [22].

2.1.2 Synovial fluid (SF)

The SF is an indispensable part of NSJ. It sources the lubrication of the AC surface and surrounding tissues, that are in mutual contact. The combination of AC and SF provides transferring of load, which the NSJ is loaded with. The unique tribological and mechanical properties of SF and AC allow mutual movement of individual bones with very low CoF. The SF is a blood plasma dialysate, which is mainly composed of HA [23]. It also contains protein components, however the concentration is only about 2%, which is identical with blood plasma [24]. The other components contained in SF are in particular proteoglycans and surface active phospholipids [25]. The SF is secreted by chondrocytes in the AC and by synovium. The resulting SF is concentrated in the joint gap and synovial space. A deficiency or change in composition of the SF can lead to damage to the AC surface, and therefore to joint diseases [26]. Main components contained in the SF, defining the unique lubricating ability, are proteins and HA. These components hold the same role as additives in technical

lubricants, and they also determine the rheological properties of the SF [27]. The viscosity of the SF varies with shear rate, and it is higher in healthy joint [28].

2.2 Tribology of natural synovial joint (NSJ)

Even though tribology is relatively young scientific field, the tribology of NSJ is a field with abundant number of publications. The first publication appeared at the beginning of the last century. This research field, dealing with tribology of biological components, has to deal with impossibility of simulation of real situations. The real biological subject has to be replaced with model situation, in this case a replacement of the real human synovial joint with a model of synovial joint, in order to simulate the contact of synovial joint. The experimental models vary depending on the focus of the experimental task, however one half of the contact pair of the experimental model is always an AC sample removed from an animal joint.

2.2.1 Friction in the synovial joint

Most works published so far, are experimental tasks focused on friction detection. The tasks are focused on determining the CoF in different contact pairs, types of motion, lubricants, etc. The whole portfolio of the "friction" works forms a comprehensive state of knowledge, summarizing the friction behaviour of the AC under different conditions. All experiments show unique character of CoF trend, and very low value of CoF, usually ranging in hundredths. Extensive review study overviewing CoF values was published by Jarrett M. L. et al. [29]. The values of CoF vary depending on used material combinations, lubricant, operational conditions or used experimental device. The choice of experimental lubricant has great impact on the value of CoF in the AC contact. Many authors found the best tribological properties while using synovial fluid as the experimental lubricant [30], [31], [32]. Stachowiak G. W. et al. in [30]performs the experimental set with rat AC. All experiments were focused on friction detection between AC sample and a metal disk, while the experimental condition varied (load and lubricants). The pin-on-disk tribometer was used as an experimental device, however the reciprocating motion (sliding) was not considered. One set of sliding speed was used for all of the experiments (40 mm/s), which corresponds with the real conditions in human joints. The load was sets on two levels 2.7 N and 4.9 N, which corresponds with two different contact pressures. The first value represents average weight of a young person, and the second one was set for testing of the impact of load. The best tribological properties were demonstrated in contact lubricated by SF (see Fig. 2.3). Load variation causes increase of CoF values in the contact lubricated by SF (Fig. 2.3-C, D) and the change of lubricant to saline solution causes the opposite trend of CoF and it's increase. The dry contact shows values of CoF comparable to those showing in SF,

nevertheless only in the beginning of the experiment (see Fig. 2.3). This phenomenon points to the ability of self-lubricating properties of the AC, but only for a short time.

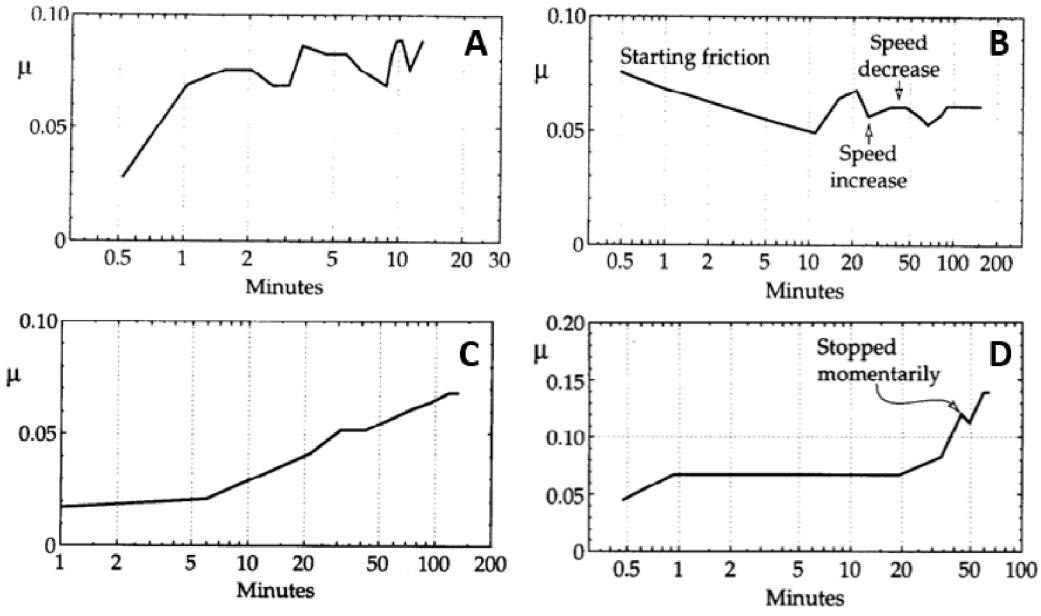

Fig. 2.3 – CoF trends between cartilage and stainless steel. Temperature 38°C, sliding speed 40 mm/s. A - dry contact, load 2.7 N; B – saline solution 0.9 mg/100 ml, load 4.9 N; C – SF, load 2.7N; D – SF, load 4.9 N [30]

Merkher Y. S. et al. [31] published work focused on testing of human AC under varying experimental conditions in order to clarify the difference between static and dynamic CoF. The experimental device was formed by a pair of AC samples, where the upper sample was smaller, diameter 4 mm, while the lower sample had 8 mm in diameter. The upper sample was pressed on to the lower one, and after specified time interval (dwell time), a sliding motion between samples has been created. The authors defined wide range of varying experimental conditions, experimental temperature 24 and 37°C, sliding speed 0.5; 1 and 2 mm/s and the loads equivalent to physiological loads were changed to values 5, 10 and 30 N, which correspond with equivalent pressure 0.4, 0.8 and 2.4 MPa. Three lubricants were used for the experiments – saline solution, histidine buffer (H.B.) and SF (in this publication I.F.S.). The results show that the I.S.F. reports the smallest difference between static and dynamic CoF; it is obvious from Fig. 2.4, and this difference is smaller the temperature is higher (Fig. 2.4-B). This impact of temperature is clear for all used lubricants. The values of CoF decrease with increasing load (the difference between CoF values in Fig. 2.4-A and B). The I.S.F. shows the lowest values of static CoF with 10 N load, but also with 30 N load, nevertheless the lowest dynamic CoF is presented by H.B. Authors also evaluate general impact of load to both kinds of the CoF, which is shown in Fig. 2.5. The dependency between dynamic CoF and load is steeper than dependency between static CoF and load. This work shows the unique tribological properties of the AC, where the CoF decreases with load.

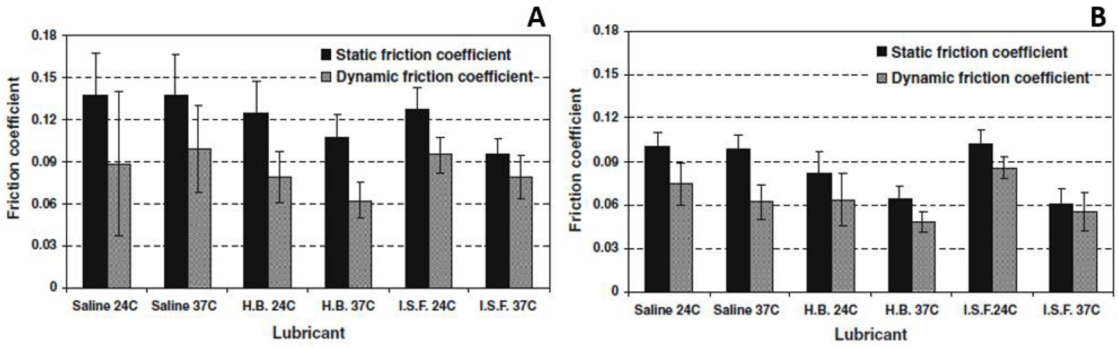

Fig. 2.4 – The comparison of static and dynamic CoF. Both experiments with dwell time 5 s and subsequent sliding speed 1 mm/s. A – load 10 N, B – load 30 N [31]

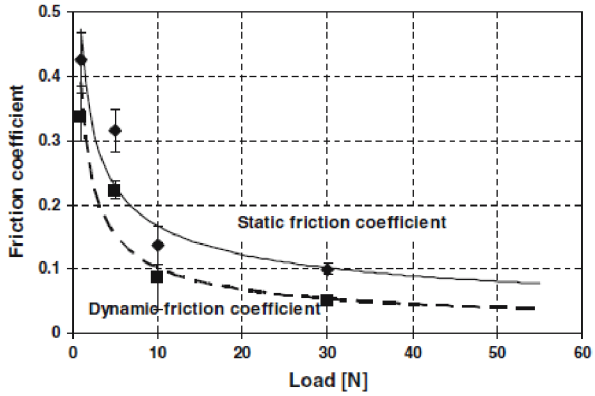

Fig. 2.5 – Dependency between load and static/dynamic CoF [31]

A research focused on simulating of real joint was performed by Teeple E. et al. [32] or Mccan L. et al. [33]. Teeple E. et al. performed research focused on determining of dependency between CoF values and disease rate by osteoarthritis (OA). The hind knees of guinea pigs were used for testing. Tests were performed using swinging simulator, simulating the knee motion. Three degrees of disease rate were determined, the fully healthy joints, joints slightly damaged by OA and joints with extensive damage. The results confirmed higher values of CoF in joints with excessive damage, however the difference between joints with no and slight damage caused by OA was almost negligible. Mccan L. et al. [33] also simulated real joint contact using swinging simulator, and two material combinations were tested within this work. The first one represents real joint (cartilage on cartilage (AC-AC)) and the second one represents the partial endoprosthesis (cartilage on stainless steel (AC-SS)). Authors used medial femoral condyles dissected from the bovine femur as samples. The walking cycle of loading was used during testing, and two levels of maximum load were used (259 N and 1036 N). These experiments show higher values of CoF with higher load, which suggests that higher load does not always mean lower values of CoF (see Fig. 2.6-A). The contact, which was simulated by cartilage vs stainless steel (AC-SS) shows much higher values of CoF than AC-AC contact (see Fig. 2.6-B). The dispersion of CoF values that is shown in Fig. 2.6 implies poor measurement repeatability, which is clear even in present studies.

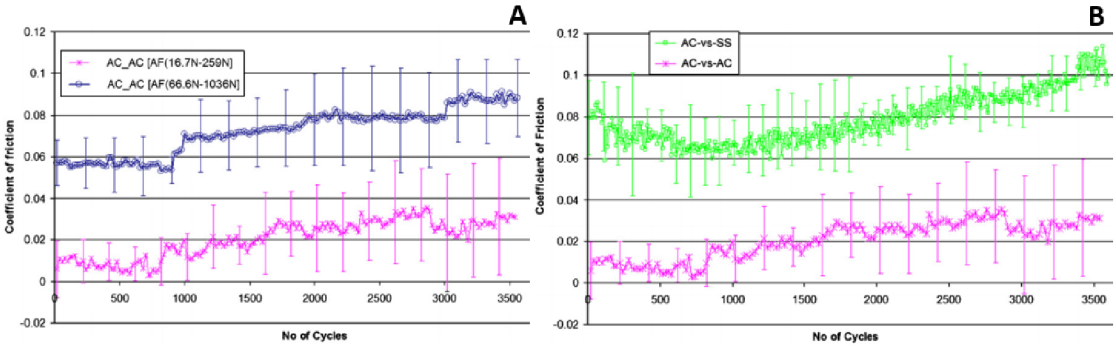

Fig. 2.6 - CoF trend A – load dependency, B – cartilage vs stainless steel – maximum load 259 N [33]

The CoF is affected not only by load, lubricant or material combination of testing samples, but also by region on the AC surface from which the sample is removed. Dependency between values of CoF and region from which the sample is removed is described for example in study from Chan S. M. T. et al. [34]. The study used samples removed from knee joint of calves. The samples were removed from two places; medial anterior (M1) and posterior (M4), see Fig. 2.7. The Position M1 represents region with relatively high contact pressure in vivo and M4 represents region with relatively low contact pressure in vivo. The removed samples had a diameter of 4 mm. As follows from previous literature [13], these regions are characterized by different mechanical properties, which study [34] put into context with CoF level.

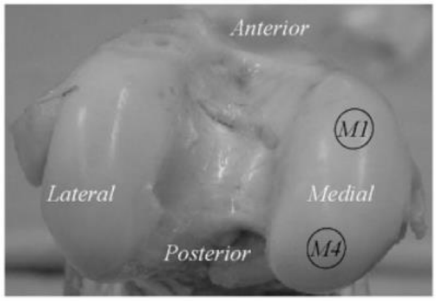

Fig. 2.7 - Positioning of sample removing [34]

The phosphate buffered saline (PBS) was used as a lubricant, and all experiments were performed on the pin-on-disk tribometer with reciprocating motion. The sliding speed was set to 0.5 mm/s with stroke 7.85 mm. The load of AC sample varied and its values were between 0.9 – 24.3 N, which corresponds with 0.32 – 0.96 MPa of contact pressure. All experiments were performed in the still loaded mode (without rehydration) and also in mode when the sample was unloaded always before sliding motion (rehydration). There is a significant difference between CoF with and without rehydration. The results showing CoF values are shown in Fig. 2.8-A,B,C. The CoF value is lower with shorter duration of experiments (comparison of Fig. 2.8- A,B,C). The experiments with sample from highly loaded region M1 show significantly better values of CoF than samples removed from M4. The dependence between load and CoF is shown in Fig. 2.8-D,E,F, and it corresponds with most previous works; the values of CoF decrease with increasing load.

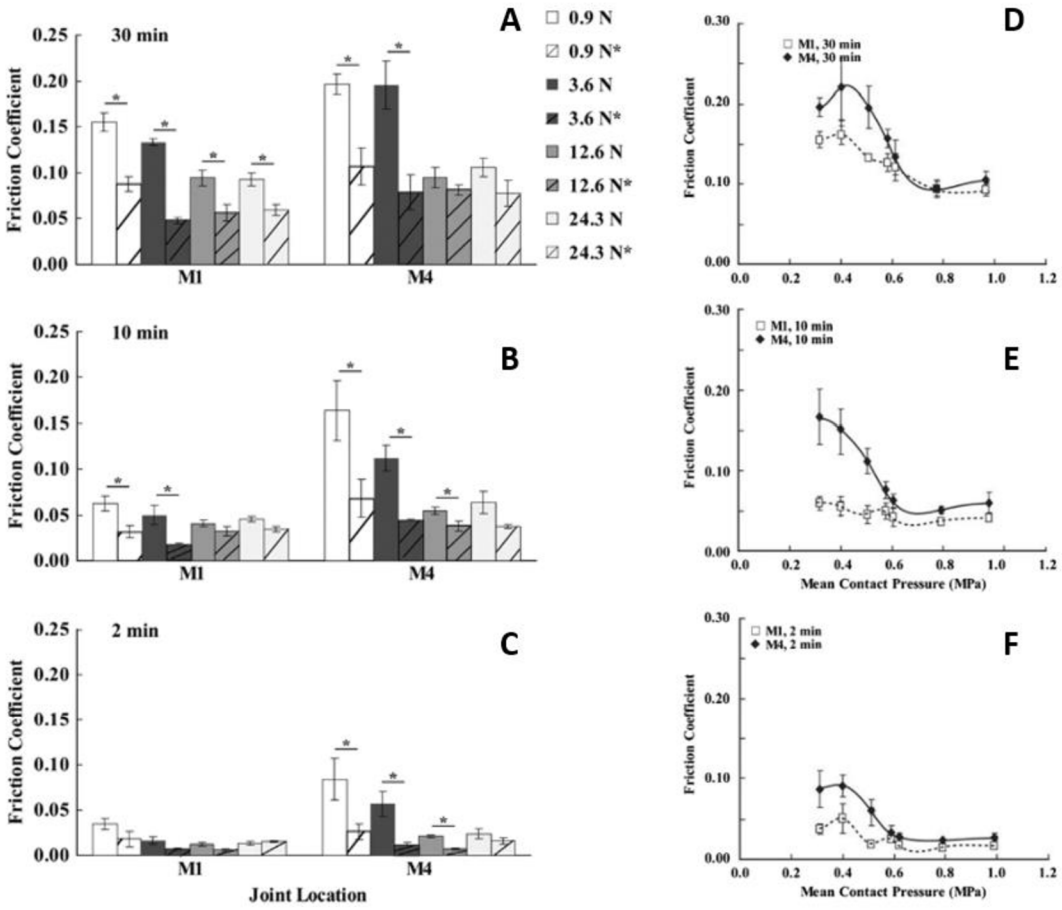

Fig. 2.8 – CoF values. A, D, C – dependence of CoF on the sampling region; D, E, F – dependence of CoF on the load; A, D duration of experiments 30 min; B, E – duration of experiments 10 min; C, F – duration of experiments 2 min. The load values marked with an asterisk represent rehydration [34]

There are also studies that deal with the effect of material combination on friction. A wide range of materials were used, nevertheless combinations as glass vs AC (e.g. [35], [36]) or steel vs AC (e.g. [30] - already mentioned, [35]) were used most often. Glass as a contact pair with AC, has the potential to further visualize the AC contact (explained below). Recently, there have also been studies focused on research of material combination of AC vs PVA hydrogel (e.g. [37]), which show promising results in terms of tribological properties. Author Oungoulian et al. [35] tested different material combinations in his study. They were testing materials that are usually used for manufacturing of artificial joint heads or articular sockets, in contact with the AC. Several types of steel (CoCr (high carbon), CoCrLC (low carbon), 316SS (low vacuum melt stainless steel)) and optical glass in contact with AC sample were used. All combinations of materials were tested under the same experimental conditions on the pin-on-plate tribometer, load 2.2 N (contact pressure 0.18 MPa), sliding speed 1 mm/s with stroke ±5 mm. In addition to impact of material combination to friction, authors also followed the degree of the AC tissue destruction after experiments (creep). The authors found the least wear in the AC vs glass configuration, and

the greatest one was observed in the case of 316SS (see Fig. 2.9-B). The results from friction tests are shown in Fig. 2.9-A.

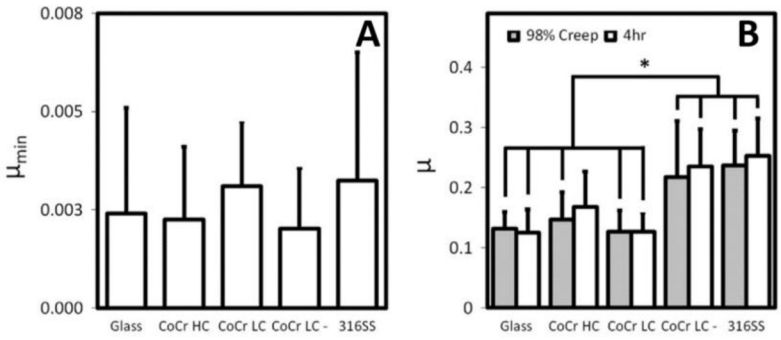

Fig. 2.9 – A – minimal CoF depending on the material; B – CoF in the 98% state of creep and after 4 hour of testing [35]

PVA hydrogel provides interesting alternative, similar to AC. These materials have almost similar tribological and mechanical properties, and the scientists are trying to improve hydrogel for use as artificial cartilage. Author Li F. et al. [37] introduced interesting and comprehensive study dealing with PVA hydrogel testing, and impact of experimental conditions to CoF levels. The impact of load (10 and 22 N, which is assuming contact pressure not higher than 0.4 MPa), sliding speed (10 and 20 mm/s) and lubricant (hyaluronic acid (HA) 2.5 g/l and Ringer´ solution) were observed on the pin-on-plate tribometer. Compared to previous studies, the results show a similar dependence of the load on CoF; the CoF decreases with increasing load, and the sliding speed causes increase of CoF, which is obvious also in Fig. 2.10-A. The authors performed a long-term test within this study, the results of which are shown in Fig. 2.10-B. The impact of lubricant change is evident from both figures in Fig. 2.10, they suggest that HA as a lubricant shows lower CoF values than the second lubricant. The analysis of the AC surface after the experiment is also part of this study. There wasn't any noticeable damage of AC after the friction test, but the PVA hydrogel reported scratches and scars. The long-term test, however, shows greater damage to both contact samples.

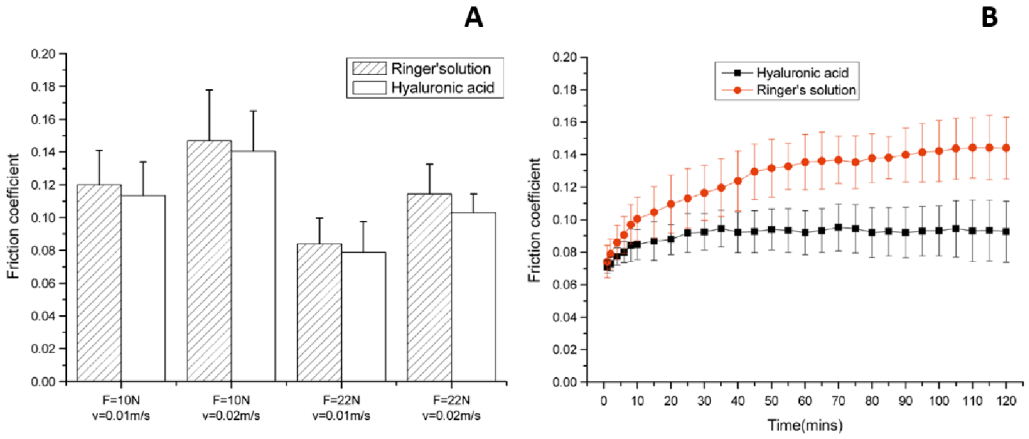

Fig. 2.10 – A – the impact of load, lubricant and sliding speed on CoF; B – the long-term test, load 22 N, sliding speed 10 mm/s [37]

The contact pair of glass and AC sample is also tested by Moore A. C. et al. [36] in his study. Author tested different diameters of AC samples (6, 12 and 19 mm) and its impact on the CoF trends, and further there are experiments focused on the rehydration and its description, resulting in theoretical explanation of hydrodynamic hypothesis of tribological rehydration. The tests were carried out on the pin-on-plate tribometer, where the AC sample under a glass plate, which allows for in situ view of the contact. The authors used it for measuring of the diameter of the contact area. The contact load was set to 5 N, which corresponds with 0.25 ± 0.05 MPa and 5 ± 0.4 mm diameter of contact area. The experiments were performed with a sliding speed of 60 mm/s and stroke of reciprocating motion 20 mm. The results show significant decrease of CoF levels in AC samples of diameters 12 and 19 mm (see Fig. 2.11-A). The authors explain this phenomenon by the contact size ratio and size of AC sample. If the diameter of the contact area is larger than the diameter of the AC sample, friction will strongly increase (Fig. 2.11-A), and similar situation occurs with the compression rate (Fig. 2.11-B).

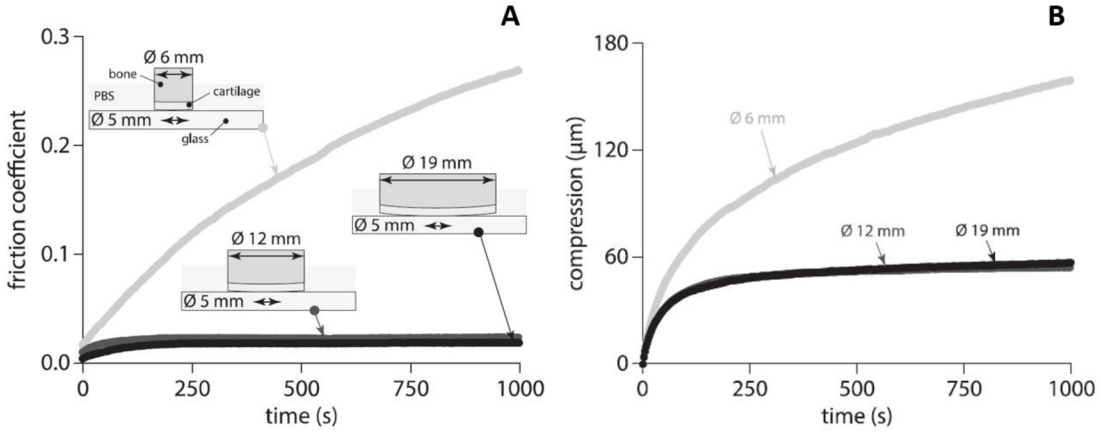

Fig. 2.11 – Friction tests – load 5 N, sliding speed 60 mm/s, stroke 20 mm, A – The impact of AC sample diameter change on CoF level; B – compression of AC samples by the same load 5 N [36]

Authors of this study also focused on the effect of rehydration due to hydrodynamic effect to friction and compression of AC sample. The experiments were carried out on sample with diameter 19 mm. As the Fig. 2.12 shows, rehydration through the experiment has positive impact on the CoF value and also on the compression ratio. When the rehydration occurs, the CoF value drops to its initial value; however, the compression ratio is reduced by only about a third (see Fig. 2.12). The authors offer a schematic description of the rehydration due to phenomenon of hydrodynamic effect (see also in Fig. 2.12). The initial phase (no sliding speed – phase (1)) is characterized by the highest rate of fluid flowing from the AC pores to the bath, therefore the compression rate rises steeply. The fluid flowing from the AC pores is slower in the second phase (still no sliding speed – phase (2)), which causes the compression to approach an asymptote. When the sliding speed in the contact occurs, raising of the compression rate stops, the trend of compression ratio begins to decrease, and the CoF trend falls down (phase (3) – sliding speed 60 mm/s). Authors explain this change by hydration of the AC pores by fluid due to hydrodynamic pressure, therefore the compression

ratio decreases. After a certain time (phase (4) – still sliding speed 60 mm/s), the compression ratio, again, approaches an asymptote, nevertheless from the other side, and the imbibition rates balance the exudation rates. The CoF level does not change. When the sliding speed changes to lower level, the compression rates again begin to raise along with the CoF value (phase (5) – change of sliding speed to 10 mm/s). The flowing of fluid into the AC pores goes down, which causes the raise of compression and friction.

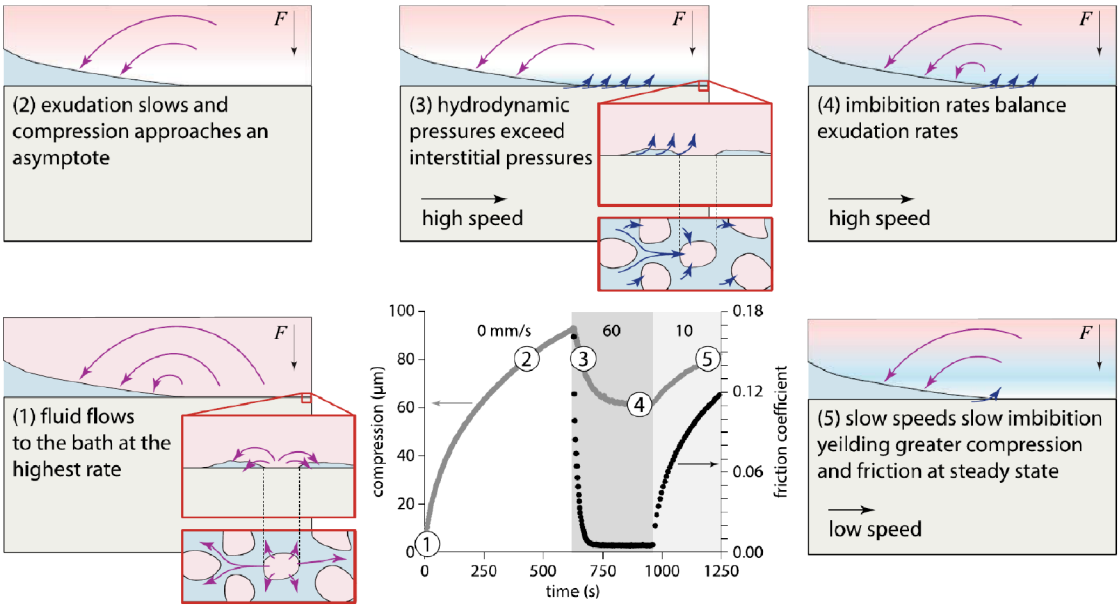

Fig. 2.12 – Tribological rehydration and the proposed recovery mechanism [36]

2.2.2 Lubrication in the synovial joint

The field of biotribology of NSJ does not only include studies dealing with the friction behaviour of the AC, but there are also studies focused on defining the lubrication system prevailing in the AC contact. Studies with this focus are not very common, especially in further past, however, they are starting to appear in increasing numbers. The basis of understanding of lubricating system of the AC is described by porous structure influence, due to which the AC has unique tribological and mechanical properties. Greene G. W. et al. [22] performed a study dealing with SF flowing through the AC structure. The AC structure contains negatively charged proteoglycans, which cause proteoglycans to bind to HA, making the AC structure very highly hydrophilic (attracting water) [21]. This combination is entangled in collagen fibres on the AC surface, creating the gel-like layer on the AC surface. The diameter of pores in uncompressed state is less than 10 nm, and after compression of the AC, the diameter decreases. Size of the pores is an order of magnitude smaller than the collagen fibres, therefore the water is flowing or defunding through them [38]. When the AC is compressed, the size of the pores decreases and the flowing of water is limited. This aspect causes retention of water in the AC pores which allows for better load transfer. The pressured AC structure allows for the fibrous tissue to be held together,

therefore, the mechanical properties in tension are improved [39]. The authors in [22] performed experiments with pork AC removed from knee and the AC sample was placed between two glasses plates. Fluorescently marked lubricants were used for the experiment. The AC sample was compressed by the glass and the contact was excited by laser. The fluorescence microscope was used as an observational optical device. The observation was focused on flowing of lubricant from the AC pores and the intensity of emitted light from contact was recorded. The authors also studied recovering ability (hydration) of the AC, where the amount of lubricant in dependency on time were observed. The results given in Fig. 2.13 confirmed the hydration ability of the AC in uncompressed state, however the hydration in compressed state has also been demonstrated (compressed curve in Fig. 2.13).

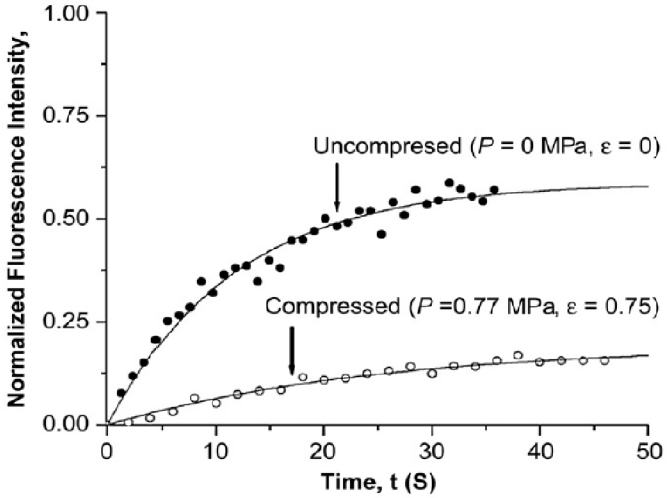

Fig. 2.13 – Recovery (hydration) ability of cartilage in uncompressed and compressed state [22]

Uncompressed state of the AC allows for flowing of lubricant through the AC structure in both horizontal and vertical direction. This phenomenon is allowed by two types of pores, vertical and horizontal. The flowing of lubricant through and out of structure fundamentally affects the EM through compression process. The scheme of this is given in Fig. 2.14. In the first state (uncompressed state Fig. 2.14-A), the AC has high EM and high load is required to open the structure to flowing. When the AC is subjected to compression, the horizontal pores begin to expand at the expense of the vertical pores, which shrink with compression. The flowing of lubricant out of the structure begins, especially from the vertical pores (Fig. 2.14-B). When larger compression occurs, the EM is low due to low lubricant volume in the AC structure. The horizontal pores are flattened and the flowing or diffusion of lubricant is difficult, therefore limited (Fig. 2.14-C). The last state of compression process is a state in which the collagen fibres are touching each other. The content of lubricant is very limited and the whole load is transferred by the solid phase of the AC structure. The load required for deformation is higher, which causes the increase of EM. The last state of compression process is shown in Fig. 2.14-D. The compression of the AC structure causes weeping of lubricant out of the AC pores, creating the lubricating film in the contact. This phenomenon

is allowing the extrusion of the lubricant out of the AC structure, which works as a pump of lubricant to the AC contact. This principle is the basis of lubricating processes in the SF. It creates the basis of all models of lubricating modes and theories.

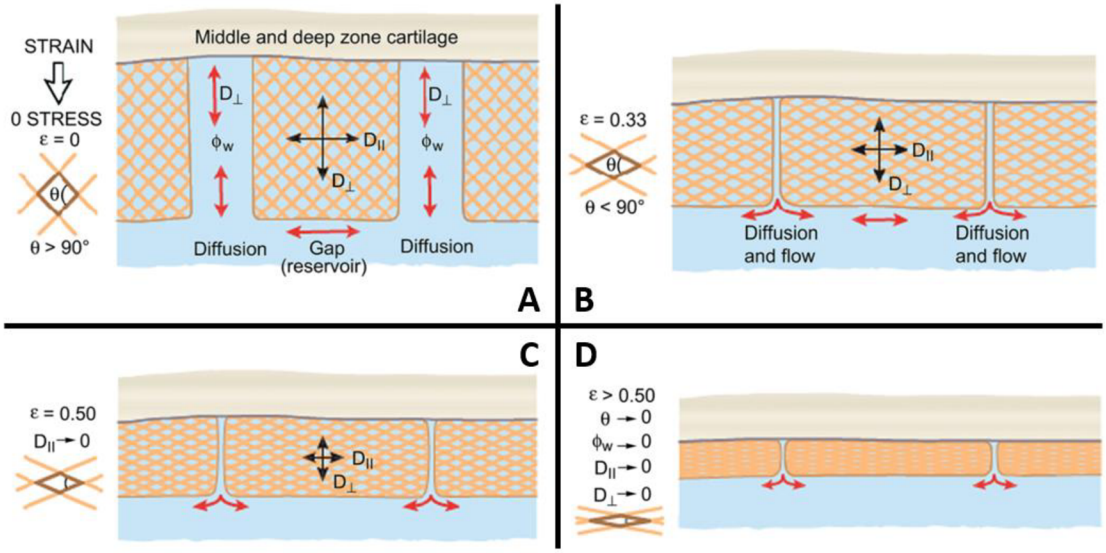

Fig. 2.14 - Compression process [22]

A similarly focused study was published by Wu T-T. et al. [40]. The authors developed a model of physical lubrication mechanism based on the rotary tests on the reciprocating tribometer. The AC sample was located above the ZrO_2 ball, which was doing the reciprocating rotary motion. Two loading and three stroke levels were set (5 and 10 N; 2.5, 5 and 10°). Four types of lubricants were used, PBS, HA with molecular weight 6 - 15x10^5 kD, CS – chondroitin sulphate extracted from beef, with molecular weight 5x10^4kD, and the combination of HA and CS dissolved in PBS – CH. The results show that the PBS gives the highest friction, defined by dissipated energy, of all tested lubricants (see Fig. 2.15) and the best tribological behaviour was shown by CH.

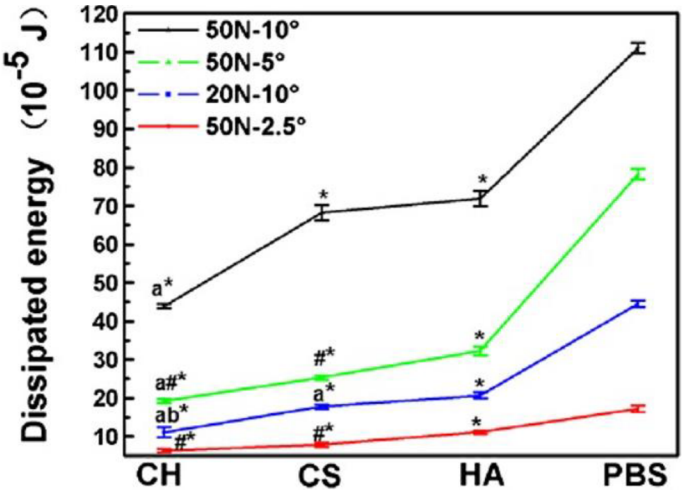

Fig. 2.15 - Dissipated energy of the reciprocating rotary tests [40]

The surface wear was also observed; it showed that the surface of the AC sample lubricated by PBS reports the most extensive wear. The AC surface with contact lubricated by HA or CH was more damaged than the surface lubricated by CS. Based on the test results, the authors developed a model presenting lubrication mechanisms of different lubricants (see Fig. 2.16). The PBS used as lubricant contains only small molecules, which are not able to create the gel-like layer on the AC surface. The molecules penetrate the AC structure and if the AC is loaded, the PBS lubricant flows out of the structure. Due to the absence of surface layer, the AC is almost unprotected (Fig. 2.16-A). CS and HA used as lubricants give better results, therefore these lubricants contain larger molecules, which are able to create the gel-like layer on the AC surface, and only the smaller molecules penetrate the structure (Fig. 2.16-B,C). The best protection ability is shown by the combination of CS and HA (Fig. 2.16-D). Results show that higher molecular weight helps in creation of the surface protecting gel-like layer.

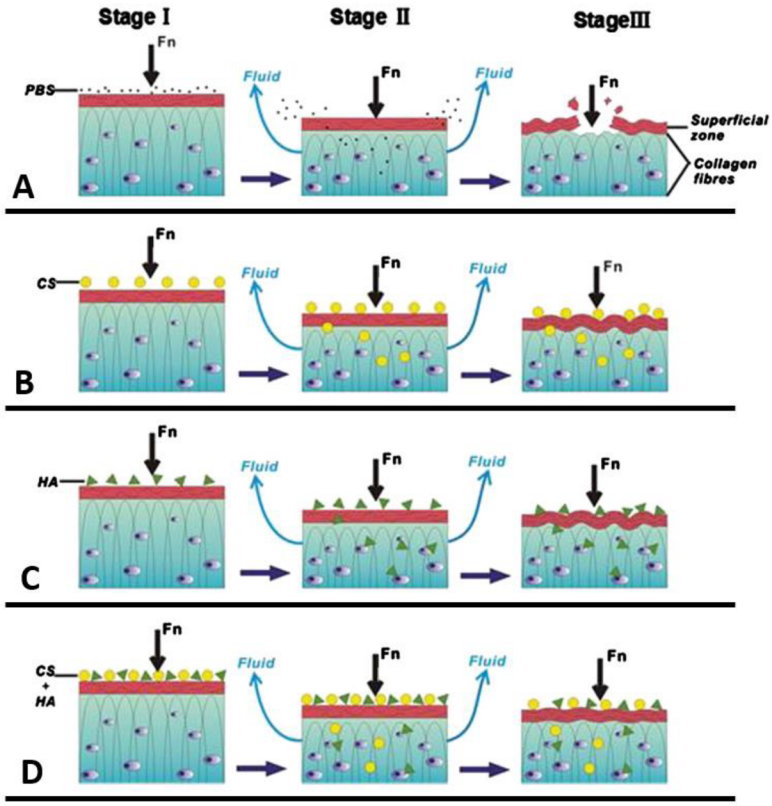

Fig. 2.16 - Physical lubrication mechanism model [40]

Flowing of lubricant out of the AC structure was simulated by mathematical model of Accardi M. A. et al. [41], where reciprocating tests focused on clarification of the lubricating regimes were also performed. The authors defined four types of experimental conditions, which correspond with four sections of Stribeck curve (two boundary sections - Fig. 2.17-A1, A2, mixed - Fig. 2.17-A3, and hydrodynamic section - Fig. 2.17-A4). All tests were performed in reciprocating tribometer in pin-on-plate configuration, where the AC sample was a plate and the pin was represented by a steel ball. The evolution of CoF during experiments was evaluated (see Fig. 2.17-B). As expected, the CoF level through

experiment, representing the hydrodynamic regime is the lowest, and conversely, the boundary CoF is the highest. The CoF trend representing boundary regime, shown in Fig. 2.17-B, is similar to CoF trends from previous studies, nevertheless the trends representing mixed and hydrodynamic regimes show trend with almost constant value.

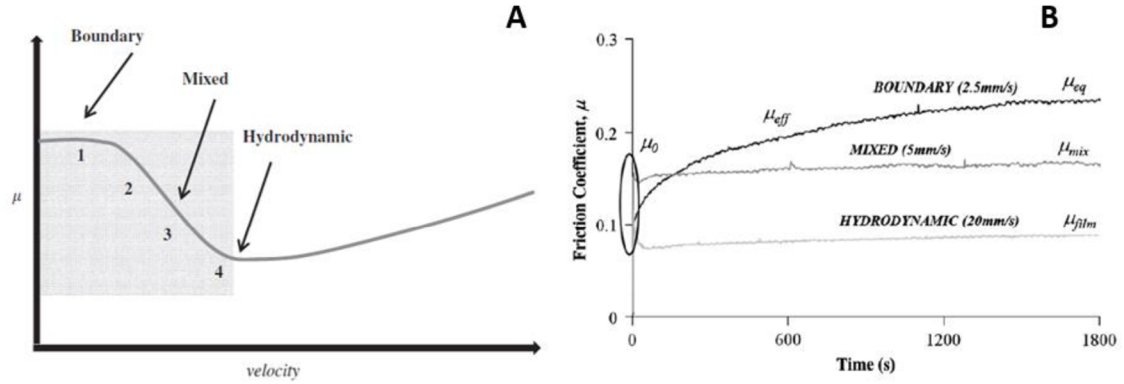

Fig. 2.17 – A – Stribeck curve – definition of experimental sections (1 – stroke 0.25 mm, frequency 10 Hz, velocity 2.5 mm/s; 2 - stroke 0. 5 mm, frequency 10 Hz, velocity 5 mm/s; 3 - stroke 1 mm, frequency 10 Hz, velocity 10 mm/s; 4 - stroke 2 mm, frequency 10 Hz, velocity 20 mm/s); B - Evolution of the CoF for boundary, mixed and hydrodynamic regime [41]

The influence of static loading was also observed in this study. The dependency of CoF on time shows increase of the initial CoF when the loaded state lasts longer. Authors performed a mathematical simulation of statically loaded state (Fig. 2.18-A) and statically loaded state with reciprocating sliding (Fig. 2.18-B). The results show flowing of lubricant similar to the one published in their previous study; the flowing of lubricant out of the AC structure is the basis of the unique function of the AC.

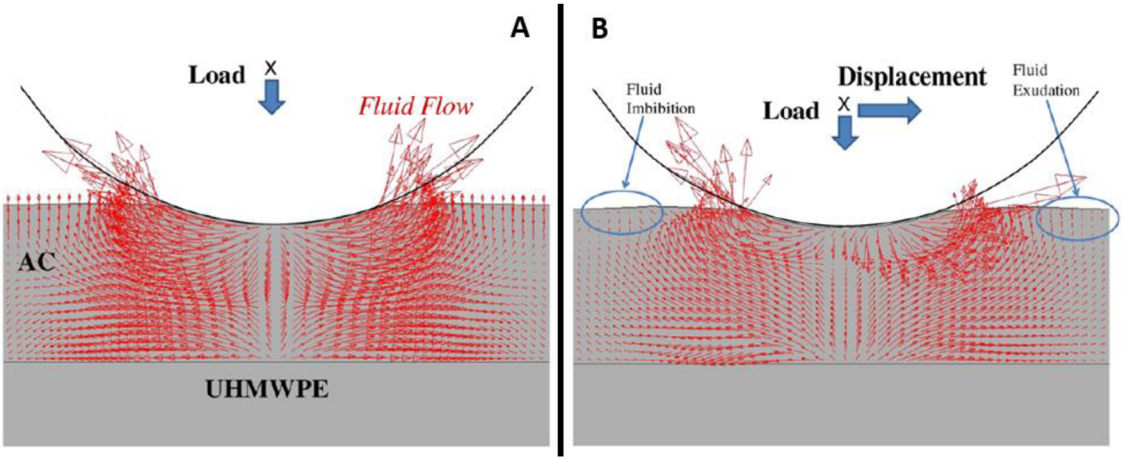

Fig. 2.18 - Fluid exudation predicted by the FEM, A – loaded state without reciprocating motion; B – loaded state with reciprocating sliding [41]

The Stribeck curve is an important tribological criteria, based on which the tribological properties are evaluated. The Stribeck surfaces were used in [42] by Gleghorn J. P. et al. to evaluate the tribological properties of the AC. The authors set two configurations of testing sample of AC (pivoted rod system (Fig. 2.19-A) and cylindrical rod system (Fig. 2.19-B)) and wide range of experimental conditions, from which the Stribeck surfaces were

composed. The experiments were carried out with three types of lubricants, PBS, bovine synovial fluid (BFS) and unique synovial fluid (ESF). The authors constructed the Stribeck surfaces for both types of testing samples and for PBS and ESF. If the AC sample is mounted by cylindrical rod, the Stribeck surface shows a significant break between the boundary and mixed regions (Fig. 2.19-C), which the sample mounted on pivoted rod does not report (Fig. 2.19-D). The authors justify the significant break of Stribeck surface, in case of the tests with cylindrical rod, by presence of wedge gap, which causes the hydrodynamic pressure in the AC contact. The experiments with PBS (Fig. 2.20-A) and ESF (Fig. 2.20-B) show that the ESF used as a lubricant gives several times lower values of CoF in the boundary region than PBS, nevertheless the CoF values in the hydrodynamic region are similar.

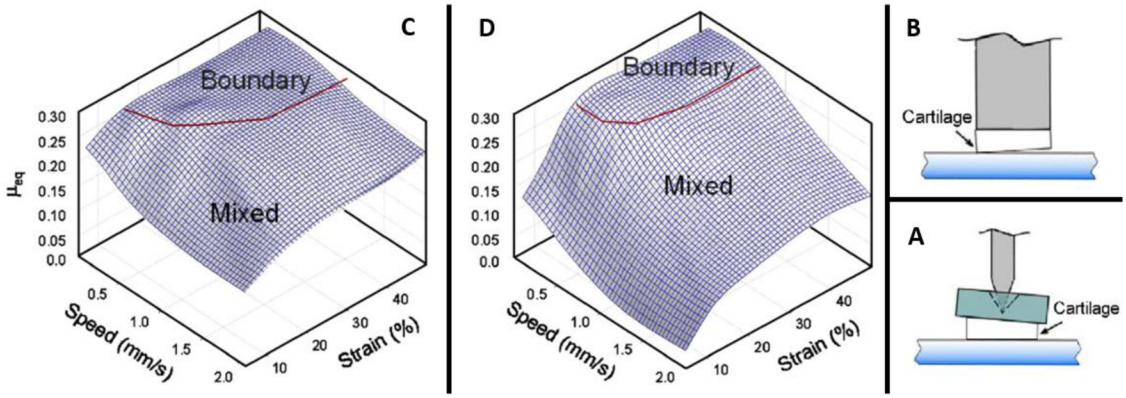

Fig. 2.19 – A - AC mounting by pivoted rod; B - AC mounting by cylindrical rod; C, D - Stribeck surfaces from

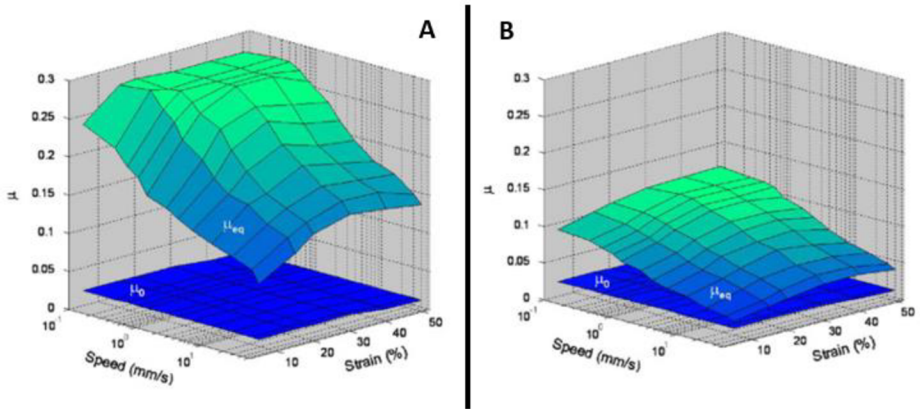

mean CoF, lubricant PBS. C - pivoted rod; D - cylindrical rod [42]

Fig. 2.20 – Stribeck surfaces for tests with A – PBS, B – ESF. [42]

In addition to the basic types of lubricating regimes that were mentioned e.g. in [41], [42], there are only few studies focused on the description of lubricating regimes, that were published so far. Until recently, there were only a few basic models of AC lubricating, weeping [43], boosted [44], biphasic [45] and boundary [46] AC lubricating regime, and only recently have these been expanded by Murakami T. et al. in [47], which adds another model - adaptive multimode lubrication mechanism (see Fig. 2.21). The adaptive multimode lubrication mechanism draws all mentioned regimes together into one group, and it says that the regime changes with operation conditions. The NSJ can respond to change of

operation conditions and adapts the lubricating mechanism, while maintaining the protection of the AC. The adaptive multimode lubricating mechanism explains the difference between the Stribeck curve for hard contact (e.g. artificial joints) and AC contact. Due to the unique structural properties of the AC, the CoF stays at low levels, despite the sliding speed being very low; in this case the biphasic lubrication is active. The load is transmitted by reaction from solid phase of AC on one hand, and on the other hand the load is transmitted by reaction force from pressure of SF captured in the AC structure. When low sliding speed occurs in the AC contact and it is loaded by low force, the lubricating regime is different in each place, depending on the surface irregularities of the AC. The places that are in contact operate in boundary, hydration or gel-film lubrication; these places are the most prone to damage. The rest of the surfaces that are not in direct contact with the second cartilage, are lubricated by weep lubricant from cartilage structure. The hydrodynamic pressure begins to gain importance when the AC contact is loaded with high sliding speed, and the adaptive multimode mechanics is suppressed, therefore the hydrodynamic lubricating regime occurs.

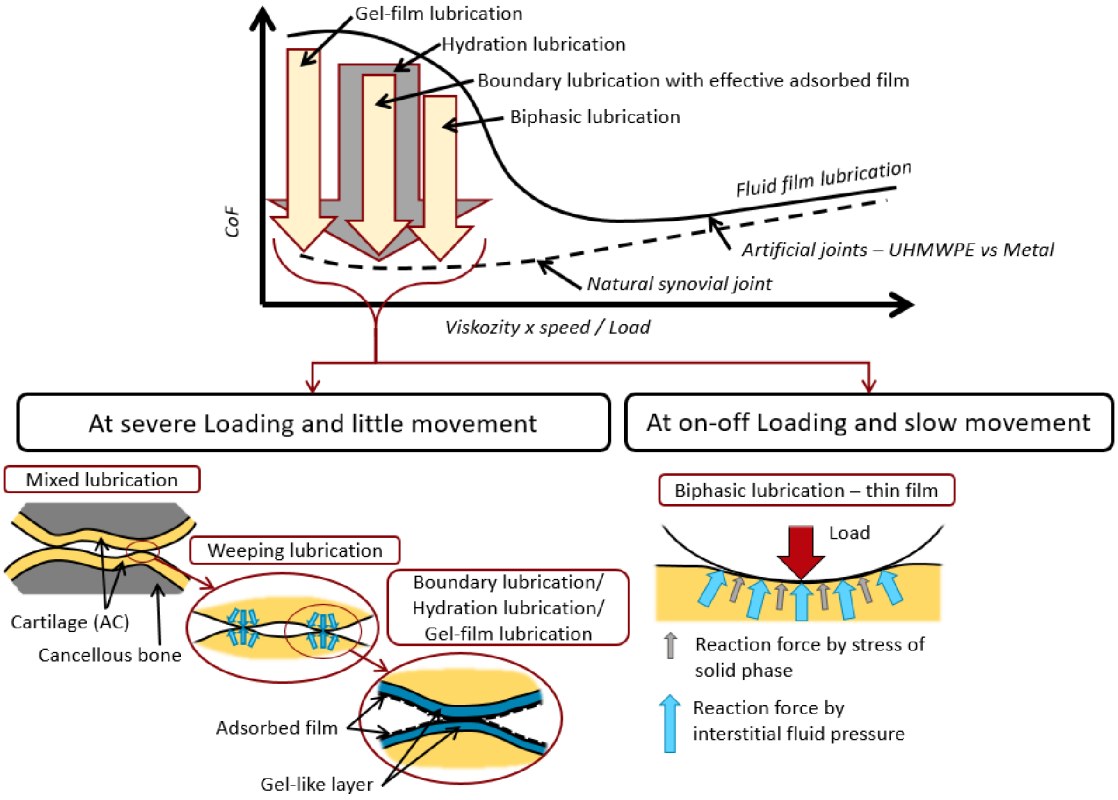

Fig. 2.21 - Adaptive multimode lubricating mechanism [47]

The principle of hydration lubrication was described by Jahb S. et al. [48]. The study was focused on modelling the NSJ by two plates of mica opposite each other. The mica plates represent the AC surfaces with similar hydrophilicity properties, which allows the specific chemical properties of lubricating film. The authors simulated the lubricating model by AFM; therefore, in micro scale. Friction effects were monitored, and based on them, the theoretical model of hydration lubrication mechanism was described. Due to similar hydrophilicity of mica and AC, the bonding of lubricant components is possible. The HA

creates surface layer on the mica plate due to its hydrophilicity, which creates suitable conditions for bonding of phospholipids. The phospholipids bond the HA and also bond themselves with lipid tails, which creates the phospholipidic bilayer (see Fig. 2.22). When both mica surfaces are covered by phospholipidic bilayers, the so-called hydration shell is formed (see Fig. 2.23-B). If sliding occurs between the mica plates, the slip phase is on the borderline between both phospholipidic bilayers in the middle of hydration shell (see Fig. 2.23-B). Due to charge of phosphate core, the water in vicinity (lubricant) bonds to phosphate core. Sliding between plates causes exchange of water molecules between individual phosphate cores (Fig. 2.23-A); therefore, the friction process takes place here (Fig. 2.23-B). High energy is necessary to break the hydration shell, therefore it can transfer high load.

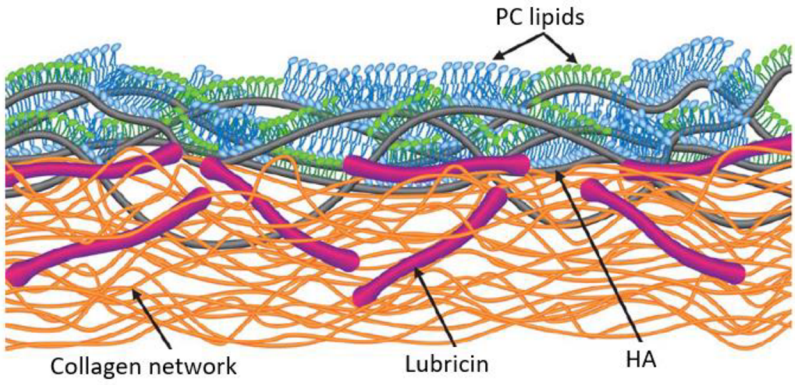

Fig. 2.22 – Phospholipidic bilayer on the cartilage surface [48]

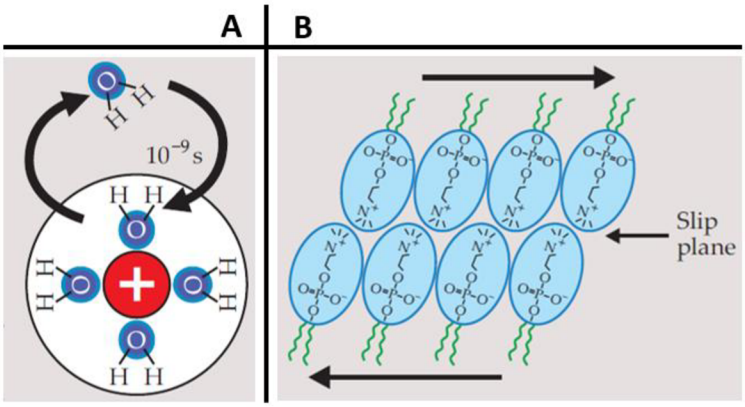

Fig. 2.23 – Hydration shell – the principle of hydration lubrication. A – exchange of water molecules from the vicinity and between phosphate cores; B – the hydration shell – position, where the sliding occurs [48]

The unique structure of AC is undoubtedly one of the basis properties allowing the movement of NSJ nearly without friction, however, for long-term movement, the protection of AC surface, in which the gel-like layer fulfils its role, is necessary. The significance and impact of individual lubricating mechanisms have been investigated by several authors in the past; however, the main focus was on the importance of the gel-like layer and adsorbed film. The presence of the gel-like layer was presented e.g. by Forsey R. W. et al. [49], where the reciprocating experiments between cartilage pin and plate were performed. Furthermore, the AC samples were evaluated on penetration of AC surface by HA, which creates the

gel-like layer. The evaluation was allowed due to fluorescently marked HA. The results show that the HA targets defects on the AC surface and it tends to cling to chondrocytes under the AC surfaces, which is allowed only to smaller molecules of HA and the rest remains on the surface and creates the gel-like layer (Fig. 2.24-A). Therefore, the HA plays important role in damaged NSJ, where the damaged regions are protected by it (Fig. 2.24-B).

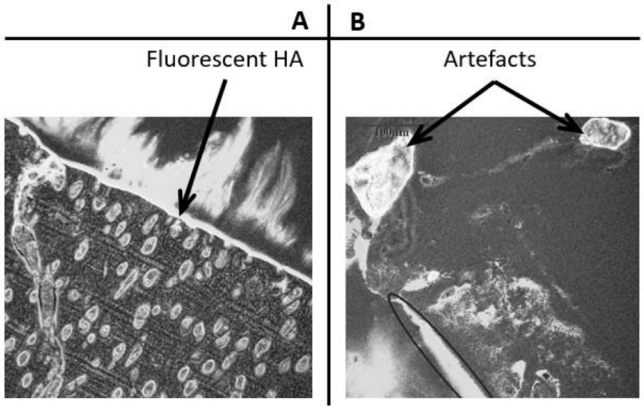

Fig. 2.24 – The bovine AC surfaces in 600x magnification; A – AC surface is coated by HA; B – HA targets to the artefacts [49]

The importance of the gel-like layer on the AC surface and its function at protecting the AC was published by Murakami T. et al. [50]. Authors carried out the experiments and based on them. the impact of the gel-like layer on the AC surface was specified. The presence and importance of the gel-like layer and adsorbed protein film on the AC surface were approached by Higaki H. et al. in their study [51]. The surfaces are covered by gel-like layer, and the protein film is adsorbed on it (see Fig. 2.25). The importance of gel-like layer in the role of a wear protector were proven, and frictional tests confirm this, as is obvious from Fig. 2.26.

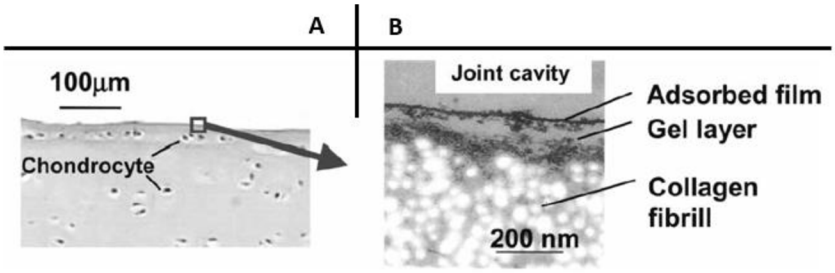

Fig. 2.25 - Surface structure; A - snap from optical microscope; B - AC transverse section [51]

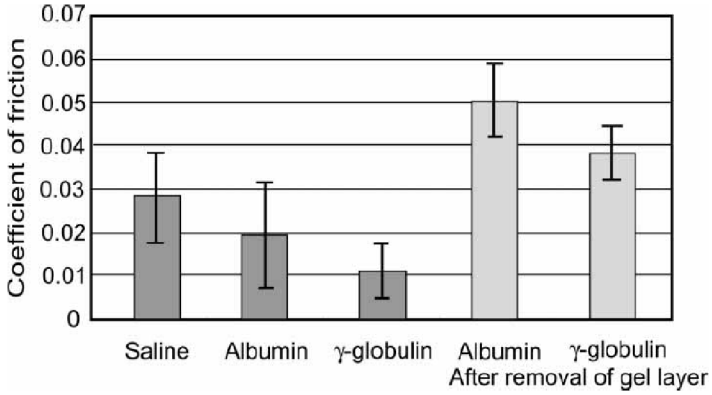

Fig. 2.26 - Minimum CoF in the case with without gel-like layer [51]

2.2.3 Visualization of the cartilage contact

Several studies investigate the AC contact using more methods simultaneously, as was mentioned earlier. However, one of the methods is always the friction measurement, which the authors combine with the other methods. For better understanding of lubrication mechanism in the AC contact, the visualization of its contact is the most useful method. The studies focused on simultaneous friction measurement and visualization are rare and the PVA hydrogel is predominantly used instead of the AC sample. Such focused research was published by Seido Y. et al. in studies [52] and [53]. Both of these studies are focused on visualization of the PVA hydrogel contact during reciprocating test, and the impact of different lubricants (especially the role of individual parts of the lubricant in film formation) was examined. The reciprocating tribometer in pin-on-plate configuration was used as an experimental device. The PVA hydrogel was used as a pin sample doing the motion, while glass was used as a plate. The fluorescence microscopy was used as a suitable optical method for visualization. The fluorescent snaps of the contact were taken always after fixed time, always before and after experiments; the visualization was not performed during the reciprocating experiment. The results show the importance of γ-globulin protein in formation of the lubricating film. As evident in the Fig. 2.27-A and B, the lubricants containing γ-globulin protein report more protein clusters, nevertheless there is a strong dependence on the ratio of lubricant components, as is obvious from Fig. 2.27-C, where the lubricant composition is the same as B; however, the ratio between components is different. Authors monitored number of particles in the contact during the experiments, and the dependency between number of particles and lubricant composition arose (see Fig. 2.28). The clusters created by the γ-globulin also show higher amounts (Fig. 2.28-A) than the clusters created by albumin proteins (Fig. 2.28-B). The simple protein solutions show no significant gradual adsorption during the experiment, which is the same in both cases in which both components are marked (lubricant A, B, E, F in Fig. 2.28). When the lubricant is more complex, such as the solution of albumin and γ-globulin, the number of particles is rising during experiments, nevertheless this phenomenon only applies to specific concentration of both components of the lubricant (albumin – 0.7 wt%, γ-globulin – 1.4 wt%), Such concentration is shown by lubricant C_G and C_A. in Fig. 2.28. The lubricant, with marked γ-globulin gives higher values of particles in the contact, therefore the increase is steeper. The lubricants that contain both components in the same ratio (D_G and D_A) show also increase of adsorbed particles in the contact; however, the increase stops during the experiment. Although more complex lubricants show lower number of particles, the gradual increasing of the number of particles is guaranteed. The highest number of particles in the contact is shown in simple lubricant B and F, both of which contain higher concentrations of components; consequently, a higher concentration of simple solution means a higher number of particles. The results show that

the γ-globulin proteins adsorb in the contact first, and only then the albumin proteins adsorb on the γ-globulin layer.

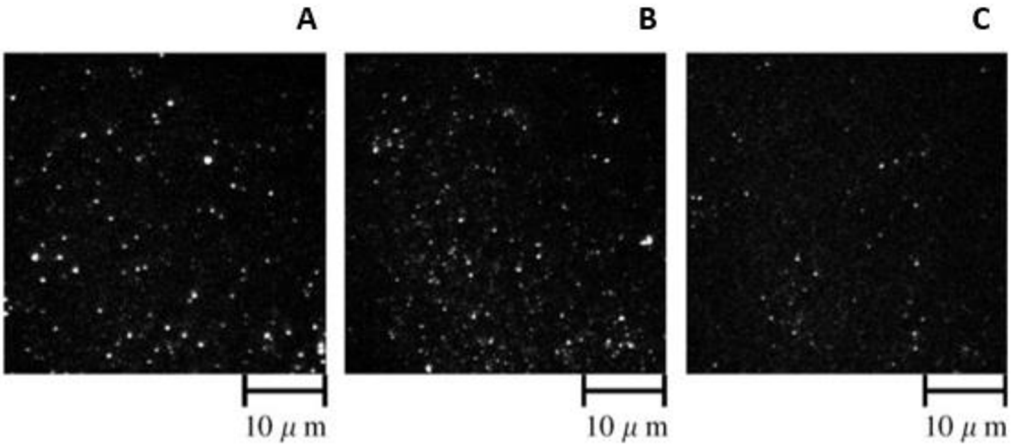

Fig. 2.27 – Snaps of PVA hydrogel contact, marked component - γ-globulin. A – only γ-globulin solution (1.4 wt%); B – albumin + γ-globulin solution (0.7 and 1.4 wt%); C – albumin + γ-globulin solution (1.4 and 1.4 wt%) [52]

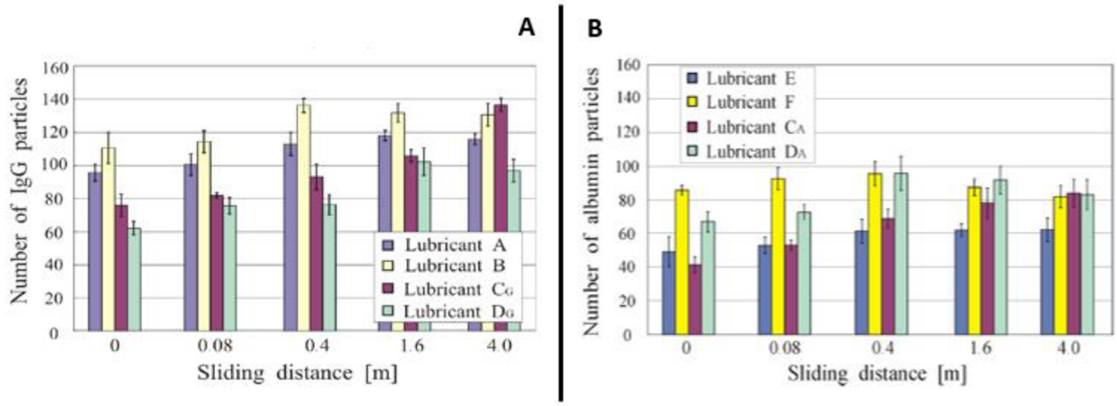

Fig. 2.28 - Number of particles during friction reciprocating test. A - marked component - γ-globulin solution (A, B - simple γ-globulin solutions - A – 0.7 wt%; B – 1.4 wt%;C_G – albumin 0.7 wt% + γ-globulin 1.4 wt%; D_G - albumin 1.4 wt% + γ-globulin 1.4 wt%)); B – marked component – albumin (E, F - simple albumin solutions - E – 0.7 wt%; F – 1.4 wt%;C_A – albumin 0.7 wt% + γ-globulin 1.4 wt%; D_A - albumin 1.4 wt% + γ-globulin 1.4 wt%) [53]

A schematic model of formation of the lubricating film by the protein components contained in the SF was published by Nakashima K. et al. [54]; however, the model is valid for hydrogel contacts. The authors performed reciprocating test and the additional analysis was performed after the test. The analysis was focused on composition of the adsorbed film from PVA hydrogel vs glass reciprocating test. The glass sample was observed after the experiments, and the adsorbed film was gradually removed. After each removing of the adsorbed film, the analysis of the film was performed using fluorescence microscope. Authors divided removal of the adsorbed film into three steps – the surface zone, the middle zone and the deep zone. Several configuration of lubricant were used for testing; each one combined albumin and γ-globulin protein in different ratio. The snaps from fluorescence microscope were taken sequentially, and both snaps were put together in the end. The best

results were shown by the lubricant containing both proteins (albumin and γ-globulin); however, the specific ratio is required (0.7 wt% of albumin and 1.4 wt% of γ-globulin). The snap of this experiment is shown in Fig. 2.29-A. The lubricant with reversed composition (1.4 wt% of albumin and 0.7 wt% of γ-globulin) does not show such good results (see Fig. 2.29-B) compared to Fig. 2.29-A. based on the results of gradual analysis of the glass plate, a lubricating formation model was compiled (see Fig. 2.30). The best variation is the already mentioned lubricant shown in Fig. 2.29, and the model of film formation is shown in Fig. 2.30-A. The situation with the lubricant being only a simple protein solution is shown in Fig. 2.30-B – the wear is reduced, but only a little. The last variation shows the model of lubricant with too much protein content, which causes increase in wear, see Fig. 2.30-C.

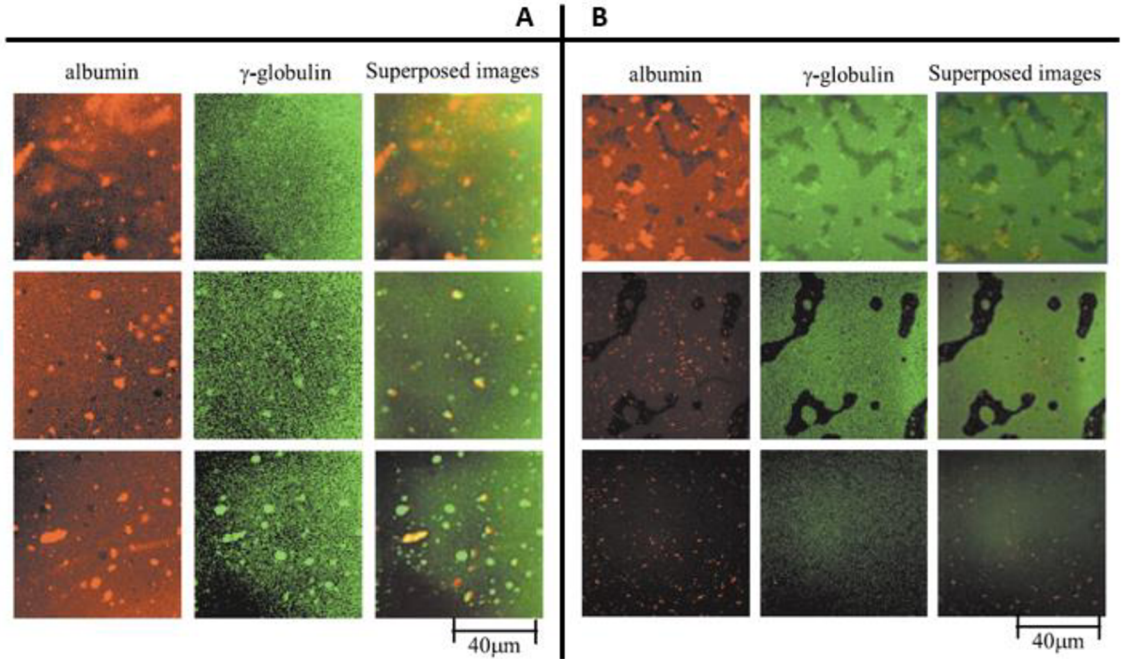

Fig. 2.29 – Fluorescence snaps of glass plate after the reciprocating experiment. A – lubricant composition - albumin 0.7 wt%, γ-globulin 1.4 wt%; B - lubricant composition - albumin 1.4 wt%, γ-globulin 0.7 wt% [54]

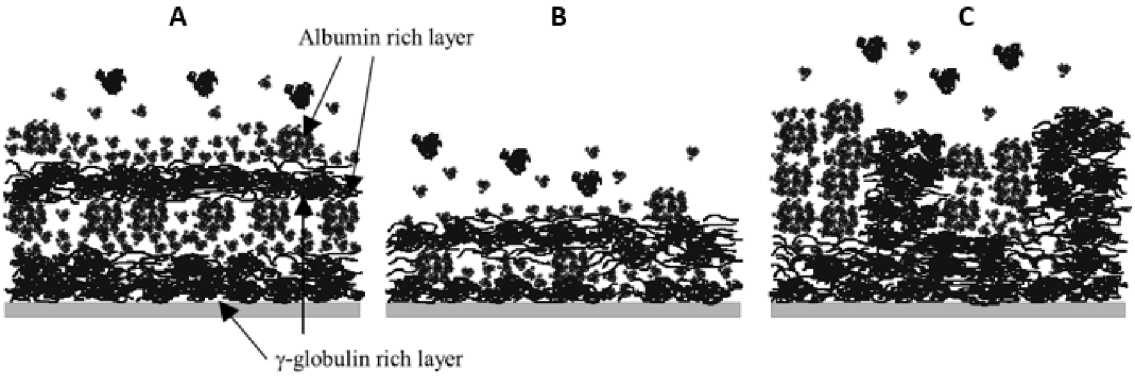

Fig. 2.30 – schematic model of lubricating film formation. A – lubricating film observed in lubricant with composition - albumin 0.7 wt%, γ-globulin 1.4 wt%; or albumin 1.4 wt%, γ-globulin 0.7 wt%; B - lubricating film that reduced wear little ; C – increasing wear due to addition of excessive protein [54]

3 ANALYSIS AND CONCLUSIONS OF LITERATURE REVIEW

From the literature review, it is obvious that biotribology of NSJ is very important and currently developing field, trying to describe the lubrication processes prevailing in the NSJ. The review shows that the lubricating processes in the NSJ are not fully described, nor fully understood yet. The field of biotribology of NSJ has a very close connection to joint diseases. The NSJ can be affected by the disease causing a damage to NSJ, i.e., to AC. If the NSJ is damaged to a degree where it can no longer work, using a conventional procedure, it is replaced with an artificial joint (endoprosthesis). The artificial joints have a limited service life. This leads to reoperation of a worn-out artificial joint and replacement of such joint with a new one. The human organism is not able to tolerate too many reoperations, because the surgery greatly affects physical and also psychological health [5], [6], [7]. The general effort of NSJ treatment is to postpone the necessity of replacing the NSJ with an artificial joint as the next reoperation might not possible due to its impact on the patient's health. The up-to-date non-invasive method of treating the NSJ degradation is the viscosuplementation, which can at least slow down the disease progression [7], [8]. The effects of the supplement therapy are not guaranteed, which implies that the viscosupplementation has not yet been fully understood [9], [10], [11]. Full understanding of lubrication processes in the NSJ has a great importance for viscosupplementation, and it can help in developing new effective treatments. Physical activities in our lives can reduce stress and help us to stay mentally balanced [1], [2],

The NSJ is a unique tribological object allowing for movement with very low friction [13]. The basis of friction properties of NSJ is the AC in combination with SF [12]. The AC is a compliant porous material allowing for fluid retention, and the EM is very low [13], [20], [22]. Studies focused on the tests of AC confirmed that the SF is a unique lubricant, most frequently reporting the lowest CoF [30], [31], [32]. The extraordinariness of NSJ was also confirmed by the studies focused on friction tests between AC samples, because when both samples are from AC, the frictional properties report the best results [33]. The AC shows a dependency between CoF and load, the CoF is decreasing with increasing load [30], [31], [34], [37]. The CoF is also affected by the region from which the samples are removed. The samples removed from a more loaded region show better frictional properties than the samples removed from the regions outside the loaded region; this phenomenon is linked with mechanical properties of the samples [13], [34]. Furthermore, rehydration of AC in between friction tests positively affected the CoF trend. The CoF trend is restarted to the initial value [47], [34], [36]. Increasing sliding speed in the AC contact causes the CoF to decrease, which authors justify by hydrodynamic pressure that pushes the lubricant into the contact [36]; nevertheless, this phenomenon is only valid for high sliding speed while in the case of

low sliding speed, the phenomenon is opposite [37]. The positive impact of hydrodynamic pressure in the AC contact is described also by [41], [42].

The efficiency of the AC lubrication is express by CoF; however, the explanation why the CoF is uniquely low is important for full understanding of the NSJ lubrication. The basis of NSJ lubrication are the structural properties of AC, which allow flowing of the lubricant into, away from, and through the structure of the AC [22], [40], [41]. This phenomenon allows for the hydration of cartilage, and the weeping of the lubricant from the AC structure is the basis of the lubricating theories [47], [22], [36], [43], [44]. The flowing of the lubricant through the porous structure is dependent on the lubricant composition [40]. The amount of lubricant contained in the structure influences the EM of the AC, which varies with compression rate [22]. The size of molecules of individual components in relation to the size of pores is a crucial criterion for penetrating the porous structure. The components with larger size of molecules create the layer on the AC surface [47], [40], [48], [49], [51], [54]. The surface layer is the basis for low friction, and it is very important for AC protection [40], [51]. The layer, which is created on the AC surface is composed of two basic component – gel-like HA layer and adsorbed protein film [47], [48], [49], [51], [54]. The gel-like layer bonds the chondrocytes in the AC structure located directly on the AC surface [49], [50], [51]. This layer is responsible for protection of the AC covering the defects on the AC surface [49], [51].The adsorbed protein film is formed on the gel-like layer and is an order of magnitude thinner [48], [51]. The adsorbed film causes the specific function of AC lubrication, such as the hydration lubrication [48]. The adsorption rate depends on the lubricant composition, especially on the ratio between the protein components in the lubricant; however the studies were focused only on testing of PVA hydrogel [52], [53], [54]. The main role in the formation of the lubricating film in the PVA hydrogel contact is played by the protein γ-globulin, but also by the right composition and the ratio between the components to adhere to [53], [54].

Based on the literature review, the only suitable optical method for simultaneous visualization of the AC contact lubricated by SF is fluorescence microscopy [49], [51], [52], [53], [54]. This method allows for the observation of individual components marked by fluorescence die [52], [53], [54]. The observation of individual components allows for the description of lubricating film formation in the AC contact. The visualization limitation is the necessity of using a transparent material as one part of the testing pair; in this case, it is mostly glass, which, of course, affects the contact area e.g. from the point of view of the EM or contact pressure [36], [52], [53], [54]. Such focused studies are very rare; however, the authors used PVA hydrogel instead of AC [52], [53], [54], or simultaneous visualization is not performed [36]. The studies dealing with the evaluation of the adsorbed film exist but the evaluation is performed after the experiments [49], [51].

The literature review shows that the research dealing with tribological behaviour is very widespread, and its tradition dates back several decades. There are many studies dealing with friction behaviour of AC, especially the studies that have been published further in the past. Topics of these studies are diverse and it is obvious that the frictional behaviour of NSJ is well described. On the other hand, there are works focused on the lubricating issues of the NSJ. These works deal with formation of the lubricating film in the AC contact. There are many theories trying to describe and explain the mechanism of AC lubricating; however, only a few of them have an experimental background. There are also studies that perform tests to describe the lubricating film formation in the AC. These studies use the method of simultaneous visualization of the contact and friction measurements; however, they use PVA hydrogel samples instead of AC samples. There is no study, which would use the simultaneous visualization and friction measurements in the AC contact to describe the lubricating film formation. It follows that the lubricating issues are not fully understood, and there is no study that would provide a full description of lubricating film formation in the AC contact.

4 AIM OF THESIS

The aim of this PhD thesis is to describe the effect of individual components of synovial fluid on lubricating film formation in the model of synovial joint. The thesis is focused on the experimental analysis of friction coefficient and observation of adsorbed lubricating film with the use of the principle of fluorescence microscopy. To achieve the main goal of this thesis, the solution to the following sub-aims is necessary:

- Development and design of the experimental device.
- Development of the methodology for removing and storing of the articular cartilage samples.
- Design of the methodology of experiments.
- Design of data processing and evaluating.
- Series of experiments focused on the analysis of the influence of individual components of synovial fluid.
- Data analysis.
- Discussion and publication of obtained results.

4.1 Scientific questions

- What is the influence of the individual components contained in the model synovial fluid on the lubricating film formation in the model of synovial joint?
- How is the friction coefficient affected by the number of dominant protein particles in the model of synovial joint?

4.2 Hypotheses

- A simple protein solution does not create a stabile lubricating film with high friction coefficient. A combination of simple proteins causes the proteins to bind to each other. Forming of the lubricating film is mostly affected by hyaluronic acid and phospholipids; these components contribute to the stability of lubricating film and increase its thickness.
- It is expected that a higher particle count of dominant proteins component adsorbed in the contact causes a higher friction coefficient whereas the thickness and area of lubricating film increases.

4.3 Thesis layout

The PhD thesis is composed of one paper published in peer-reviewed journals and two papers published in journals with impact factor. The first article is focused on development and design of the experimental device. The design of reciprocating tribometer that allows for simultaneous visualization and friction measurement is described. The experimental device containing a fluorescence microscopy is introduced. Initial experiments involving simultaneous friction measurements and AC contact visualization are performed. The second article is focused on the methodology of the experiments. Evaluation of the experimental data is described. Furthermore, processing of the experimental data from the fluorescence visualization is described, including the software for evaluation. The principle of the snap processing is described in detail, and calibration of the fluorescence method is examined. The last article is focused on the application of designed experimental approach. The experimental set focused on determining the influence of the albumin protein on lubricating film formation was performed. The analysis of the influence of individual components and their role in lubricating film formation is described. This article is a combination of two previous ones, where the main aim of this dissertation thesis is answered.

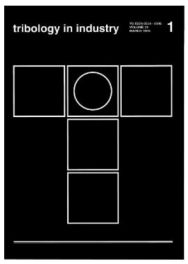

[55] ČÍPEK, P.; REBENDA, D.; NEČAS, D.; VRBKA, M.; KŘUPKA, I.; HARTL, M. Visualization of Lubrication Film in Model of Synovial Joint. *Tribology in Industry*, 2019, 41, 387-393.
Author's contribution: 70%
CiteScore = 1.09

[56] ČÍPEK, P.; VRBKA, M.; REBENDA, D.; NEČAS, D.; KŘUPKA, I. Biotribology of Synovial Cartilage: A New Method for Visualization of Lubricating Film and Simultaneous Measurement of the Friction Coefficient. *Materials*, 2020, 13, 1-20.
Author's contribution: 50%
Journal impact factor = 3.057, Quartile Q2, CiteScore = 3.26

[57] ČÍPEK, P.; VRBKA, M.; REBENDA, D.; NEČAS, D.; KŘUPKA, I. Biotribology of synovial cartilage: Role of albumin in adsorbed film formation. *Engineering Science and Technology, an International Journal*, 2022, 34: 101090.
Author's contribution: 50%
Journal impact factor = 4.36, Quartile Q2, CiteScore = 9.00

5 MATERIALS AND METHODS

In order to answer the scientific questions asked in the previous chapter, experimental investigation on several devices was performed. All used experimental devices, including the experiment focusing are shown in Fig. 5.1. The mini traction machine was used for verification of the AC sample storing method, where the CoF of the AC samples before and after freezing was examined. Furthermore, the Bruker UMT TriboLAB as a verification and calibration device was used. The comparative experimental set for verification of the new designed reciprocating tribometer was carried out. Finally, the new self-designed reciprocating tribometer was used for simultaneous visualization and friction measurements in the model of the NSJ, which allowed for observation and description of the lubricating processes in the AC contact. This experimental device uses fluorescence microscopy for in-situ contact observation – visualization. The third experimental device is the culmination of this thesis, the other devices are only auxiliary.

Research in the field of biotribology usually uses only one of the approaches – either frictional measurement or visualization. There are only a few studies connecting these two approaches, and if they do, the approaches are not performed simultaneously [49], [50], [51], or the PVA hydrogel was used instead of the AC sample [52], [53], [54].

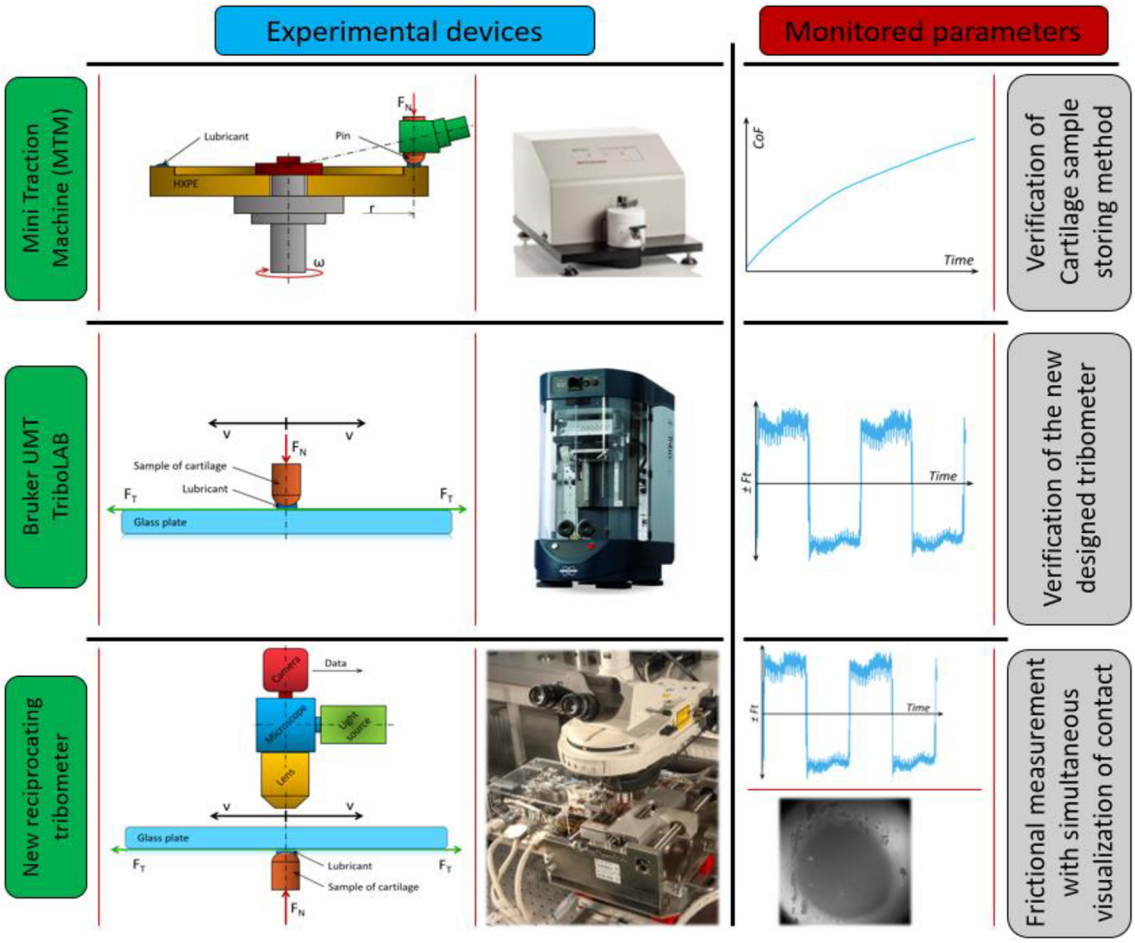

Fig. 5.1 - Used experimental methods

5.1 Experimental device

5.1.1 Ball-on-disc friction tribometer – Mini Traction Machine

This experimental device is commercial – Mini Traction Machine (MTM, PCS Instruments, United Kingdom) and it allows to evaluate the frictional properties between the rotating disc and rotating ball (see Fig. 5.2-B). It is possible to set the required slide-to-roll-ratio (SRR), or used the static sample mounted in the special holder (see Fig. 5.2-A). This device was used as a verification device for storing methodology in the configuration of pin-on-disc, where the pin is represented by the AC sample. The MTM offers a wide range of useful operating conditions and it is equipped by two load cells for evaluation of CoF between the samples. One sensor detects the load force, and the second one detects the friction force. The frequency of detecting the forces is 1 Hz. This thesis used the experimental set with sliding velocity of 100 mm/s and load of 5 N. PBS was used as a lubricant and the AC samples had a diameter of 5 mm. For comparability, all AC samples were tested under the same conditions.

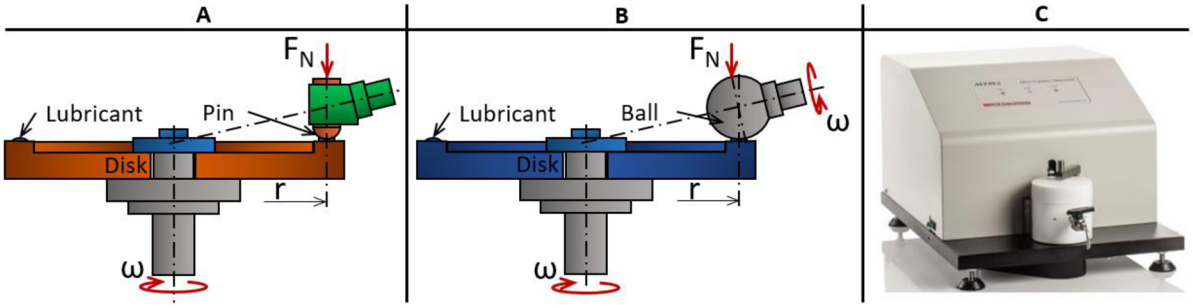

Fig. 5.2 – Scheme of MTM configuration options. A – Pin-on-disc; B – Ball-on-disc; C – MTM tribometer

5.1.2 Pin-on-plate friction tribometer – Bruker UMT TriboLAB

The Bruker UMT TriboLab (Fig. 5.3-C) is also a commercial tribometer for evaluating CoF within a wide range of test configurations. The pin-on-plate configuration was used in this thesis (Fig. 5.3-A). This tribometer is equipped by a biaxial load cell for evaluation of the CoF in the tested contact. The sensor allows detecting of the normal load and the frictional effects. The sensor with load capacity of 50 N in both axes was used. There are many variations of useful modules for testing, with a wide range of adjustable conditions. Only the reciprocating module was used for the tests. The reciprocating motion of tested sample is allowed either by the reciprocating module equipped with crank mechanism, or slider, to which the load cell is mounted. The reciprocating motion induced by the module is non-linear, it is sinusoidal, but the high frequency of motion is possible. The slider allows for the linear motion, which is provided by the stepper motor. This experimental arrangement used the slider for application of the reciprocating motion, because the motion is constant.

This device was used as a verification tribometer for calibrating of the developed reciprocating tribometer. For this purpose, a self-designed bath was manufactured in order to achieve a similar configuration as the developed tribometer (Fig. 5.3-B). The PTFE G400 pin was tested on a glass plate under loads of 15 and 20 N with sliding speed of 5 and 10 mm/s and the stroke of 20 mm. These experimental conditions respect the conditions commonly used during the NSJ testing. All performed experiments used the PBS as lubricant.

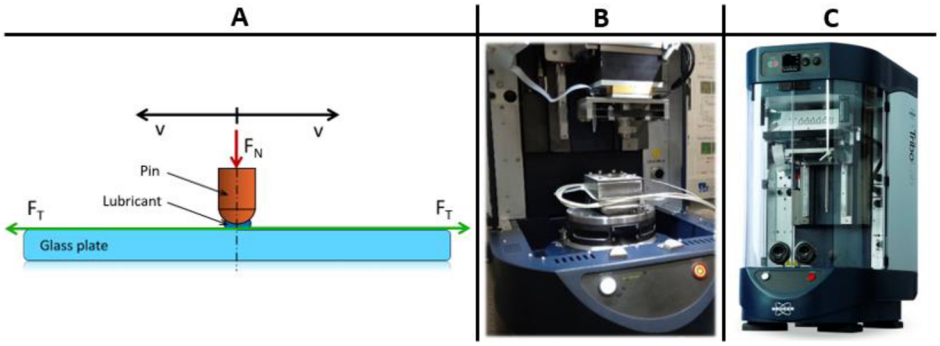

Fig. 5.3 - Tribometer Bruker UMT TriboLAB. A - Scheme of used configuration pin-on-plate; B – Bruker tribometer

5.1.3 Pin-on-plate reciprocating tribometer for friction measurements and visualization

None of the commercial tribometer allowed for simultaneous visualization of the contact area and friction measurements. Furthermore, the reciprocating motion and low loading are necessary to accomplish the aims defined in the previous chapter. In order to comply with all of these requirements, the self-designed tribometer was developed. The conception of the tribometer was inspired by the previous studies where the visualization of the contact area was performed. The experimental device used in [36] fulfils the requirements for simultaneous visualization and frictional measurements, and the location of the contact area corresponds with the optical device used by our department [58], [59]. The requirements for experimental conditions were set based on the previous studies and real conditions prevailing in the human natural joints [17], [19], [36], [37], [60].

The scheme of the self-designed reciprocating tribometer is shown in Fig. 5.4-A. The AC sample is located under a glass plate, and it is static. This arrangement allows for continuous observation of the AC contact by fluorescence microscope, and the contact area is recorded by a high-speed camera. The contact is flooded with the lubricant (model synovial fluid in this case) and the bath is heated to the human body temperature. The second part of the contact pair is the glass plate, which is the movable part producing the reciprocating motion. The AC sample is mounted to a lever, which is fixed by a shaft and bearings. The load on the contact is applied through the AC sample by lifting of the lever by the linear stepper motor placed under the lever. The basis of the tribometer is a rigid frame, allowing for rigid

mounting of the movable parts, and movement without clearance. The movable glass plate is mounted on the carriage, which is fitted by a ball sleeve. The carriage motion is allowed due to its mounting on the guide bars and the carriage is reciprocally propelled using a ball screw and stepper motor. The sealing between the glass plate and the heated bath prevents leaking of tested lubricant from the bath. The device is equipped with two load cells to examine the CoF during the experiment. One sensor detects the load force (normal) and the second one the friction effects. The whole device is placed under the fluorescence microscope allowing the contact observation during the experiments (see Fig. 5.4-A and Fig. 5.5-B). The Arduino MEGA 2560 microcomputer (Atmel Corporation, San Jose, USA) is responsible for controlling of the movable parts of the tribometer; detection of the effects of the forces is allowed by the measuring card NI USB 6001 (National Instruments, Austin, Texas, USA). The effects of the forces are recorded by computer and LabVIEW software (National Instruments, Austin, Texas, USA) using a measuring card. The measuring and controlling equipment are located in the control box connected with the tribometer by cables. The experimental conditions (e.g., sliding velocity, stroke, load during the experiment, etc.) can be modified on the control box using control buttons and display.

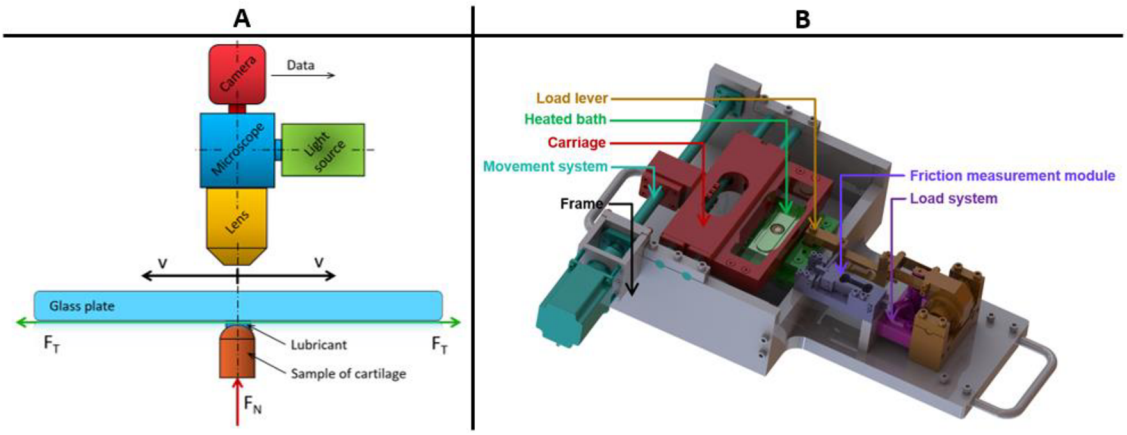

Fig. 5.4 – Self-designed reciprocating tribometer. A – Scheme of tribometer arrangement; B – Design of device

5.1.4 Fluoresce microscopy – visualization method

The optical method based on fluorescence principle was used for the observation of the AC contact. Fluorescence is the light emission of the substance. The fluorescence emission occurs when the substance is excited by light or other electromagnetic radiation; the excited substance begins to emit light. The fluorescence phenomenon can be divided into three basic phases (the states from the beginning of excitation to emission):

- **Excitation**: The light source, representing the source of electromagnetic radiation, supplies photons into the substance with the fluorophore. This process inducts the fluorophore to the excited electronic single state.

- **Excited-state lifetime**: The state of molecule relaxation occurs - the energy dissipates. This state usually lasts 1 – 10 ms, and after this time, the molecules are left in the state in which they can emit fluorescence.
- **Fluorescence emission**: When the fluorophore is returning to the ground state, the photon is emitted. The emitted photon has a longer wavelength due to energy dissipation, which took place in the previous phase.

A detailed description of fluorescence microscopy is provided in [61]. The scheme and the experimental apparatus in the laboratory are shown in Fig. 5.5. The light source is represented by a mercury lamp emitting white light. The Fluorescein Isothiocyanate (FITC) and Tetramethylrhodamine (TRITC) filters were used for the purposes of this thesis. The filters allow for the change in the wavelength of excited and emitted light; FITC (excitation on 490 nm, emission on 525 nm) and TRITC (excitation on 557 nm, emission on 576 nm). The axial resolution of the FITC filter is approximately 290 μm, and 320 μm for the TRITC filter. The filter is mounted to the carousel located above the lens. Due to the large size of the compliant contact of AC, the double magnification lens was used for observation. The depth of field of the apparatus is approximately 200 μm, which was sufficient with respect to the sliding speed and the estimated film thickness. The image focusing is performed by the field diaphragm and a slight refocusing by the z-feed of the optical system. The observation of the AC contact was performed through a glass plate made from optical glass B270; therefore, the optical properties of the glass did not affect neither fluorescence excitation, nor emission. The same apparatus was used for observation of the artificial joint contact represented by glass acetabulum and stainless steel hip joint. A description of the optical system and its use are published in [58], [59].

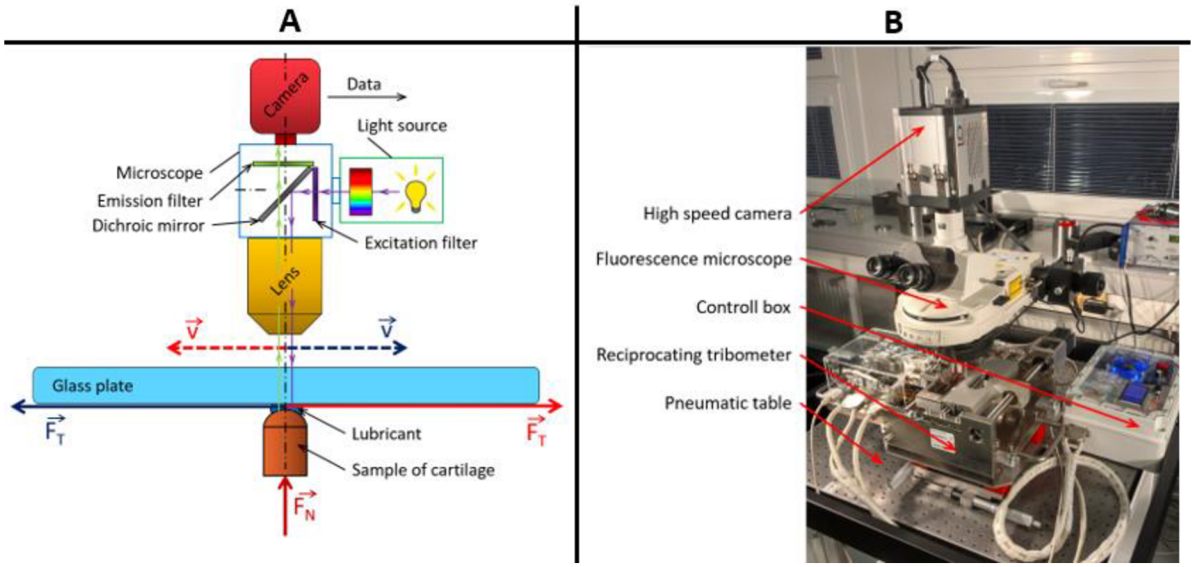

Fig. 5.5 - Fluorescence microscopy. A - Scheme of fluorescence apparatus conception; B - Experimental apparatus in laboratory

5.2 Specimens and conditions

5.2.1 AC specimens

The pin samples removed from the femoral hip head of mature pigs were used. The samples were removed as soon as possible after the slaughter of the animal from the canopy of the femoral head, and the emphasis was placed on the same location of the sampling region through all sampling femoral heads. The emphasis was also placed on preserving the undamaged surface of the sampling region. This procedure ensures that the removed samples had as similar properties as possible because the mechanical and tribological properties strongly depend on the location of the sampling region [13], [34]. The ejector and hollow drill bit were used for sample removal. At the beginning of this thesis, the hollow drill bit was used to remove the samples [55], [56] but these samples had frayed edges. To avoid this, the ejector was preferred [57]. The diameters of the samples were 5.7 and 9.7 mm. The deviation between the AC samples with different diameters was published by Moore A. C. et al. [36], where the analysis of the CoF influence on the diameter of the sample was described. The basis of the contact visualization is that the contact area has to be of a lesser diameter than the diameter of the sample itself. For the experimental tasks focused on visualization, the samples with 9.7 mm diameter were used. The removed samples were stored in PBS, deeply frozen (-20 ˚C) immediately after sampling, and the testing samples were defrosted immediately before the experimental set. This sampling procedure was used in [62], [63] and verified in [64], [65]. The sampling procedure performed by the ejector is given in Fig. 5.6.The second sample of the contact pair was the glass plate, which fulfils the important premise of transparency, in order to ensure an insight into the contact area. The glass plate is 154 mm long, 43 mm wide, and 4 mm thick.

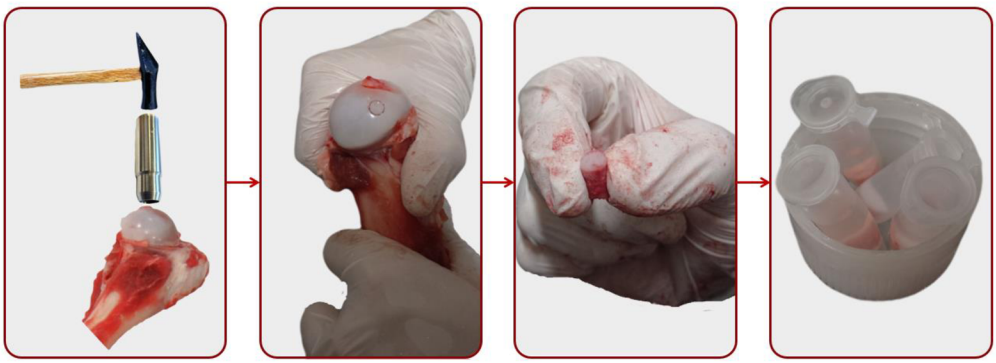

Fig. 5.6 - Sampling process

5.2.2 Lubricants

The PBS was used as a lubricant for the verification phase of this thesis (verification of the sampling process, verification and calibration of the reciprocating tribometer). Furthermore,

the model synovial fluids were used for the experimental sets, where the simultaneous visualization and friction measurements were performed. The lubricants are shown in Tab. 5-1. The basis of visualization is the labelling of observed components; in this case, it was bovine serum albumin or γ-globulin. The albumin (Sigma-Aldrich, A7030) was labelled by Rhodamine-B-isothiocyanate (283924, Sigma-Aldrich). In the second case, γ-globulin from bovine blood (Sigma-Aldrich, G5009) was labelled by Fluorescein-isothiocyanate (F7250, Sigma-Aldrich). The other components containing the model SF are HA with molecular weight of 1000 kDa and phospholipids. The experimental lubricant was prepared by mixing of all the components with PBS. The prepared experimental lubricants were wrapped in the aluminium foil to prevent degradation of the labelled components by light. The lubricant samples were stored in frozen state at -20°C. Defrosting was performed immediately before the experiment. Lubricants 1 – 4 were used in the last study attached to this work [57] for clarification of the albumin impact on the lubrication film formation in the NSJ. Lubricants 1, 5 and 3 were used in the study [55] to examine the device functionality; the study [56] used lubricants 1, 3 and 6.

Tab. 5-1 - Lubricant composition

Lubricant label	Composition, concentration (mg/ml)				Labelled component
	Albumin	γ-globulin	HA	Phospholipids	
Lubricant 1	20	-	-	-	Albumin
Lubricant 2	20	3.6	-	-	Albumin
Lubricant 3	20	3.6	2.5	-	Albumin
Lubricant 4	20	3.6	2.5	0.15	Albumin
Lubricant 5	-	3.6	-	-	γ-globulin
Lubricant 6	20	3.6	2.5	-	γ-globulin

5.2.3 Experimental conditions

All experiments were performed under the conditions which correspond with the real conditions in the NSJ; they were inspired by previous studies [17], [19], [60]. Contact pressure of 0.8 MPa was used for all experiments, which corresponds with 10 N of load. The value of contact pressure was determined by the Hertz theory and corresponds with the contact pressure prevailing in the hip joint [19]; however, the value is strongly dependent on the EA of removed sample, which varies through all specimens [13], [34]. The experimental conditions are given in Tab. 5-2. All experiments in this thesis were performed using the same load, sliding velocity, and stroke of reciprocating motion. Variations in the duration of experiments occur. Longer duration of experiment was used for the second study attached to this thesis to verify the newly developed method of visualization of the AC contact [56].

Sliding velocity was also determined in correlation with the real conditions prevailing in the NSJ during human movement. A set sliding velocity of 10 mm/s corresponds with slow human walk. The constant velocity during every stroke is possible due to the movement system based on the stepper motor and a ball screw (see Fig. 5.7). The constant part of the velocity trend is approx. 97% of every cycle. The temperature of the human body was maintained during all experiments performed with the AC.

Tab. 5-2 - Experimental conditions

Load	Contact pressure	Velocity	Temperature
N	MPa	mm/s	°C
10	0.8	10	37

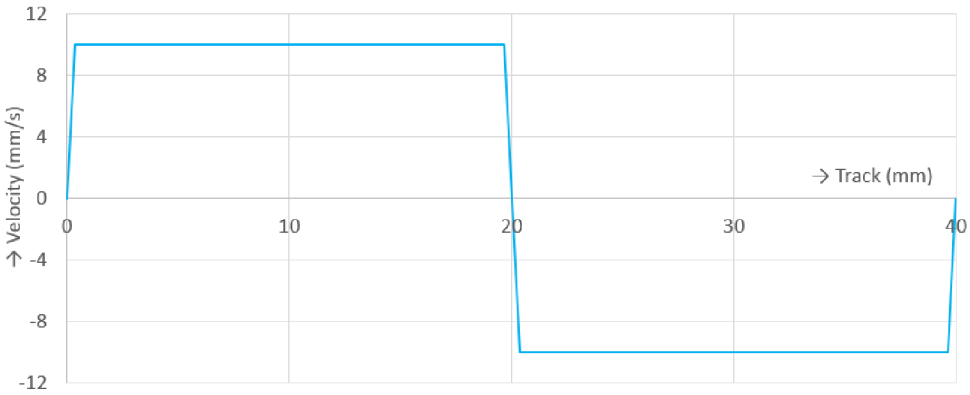

Fig. 5.7 - Sliding speed trend

5.3 Methodology and experimental design

A strictly-defined procedure before, during, and after each experiment was defined and followed. The procedure allows for comparability of experiments and helps to achieve a better repeatability. Before each experiment, the sample was hydrated in PBS to avoid drying out. Due to differences between the AC samples, the run-in cycle of each tested sample was used. This cycle is composed from 20 reciprocating cycles at load of 10 N, and after that the AC sample is unloaded in order to rehydrate. This cycle allows weeping of the original SF, which was contained in the structure of the AC before the experiment. The SF is retained in the structure and comes from the NSJ of slaughtered animal. The composition of this SF may be different; therefore, it is necessary to remove it. The run-in cycle is also used when one AC sample is tested repeatedly, for same reasons mentioned before; the lubricant

contained in the AC structure needs to be removed not to affect the experiments. One AC sample is repeatedly tested to achieve comparable results from several experiments. Before each experiment, the heated bath was cleared by protein removal solution (SDS) to achieve a non-affected lubrication bath. The experimental device is covered with a dark tarpaulin to prevent access of light from the outside; therefore, the fluoresce excitation and emission are not affected during the experiments. Repeated experiments, performed in the third study attached to this thesis [57], were carried out with a rehydration cycle between experiments. The aim of these experiments was to determine the impact of rehydration together with verification of repeatability. Nine experiments were performed in each set, which is defined by designed arrangement of the experiments (see Fig. 5.8). The experimental set was divided into three repeated experiments. The rehydration lasting 2 minutes was carried out after each experimental task. The rehydration causes restarting of CoF to the initial value, which allows for the use of this phenomenon to perform each experimental task as a unique one. This arrangement allows for the comparison between the experiments in terms of repeatability, while maintaining the comparability between them (experiments with one sample).

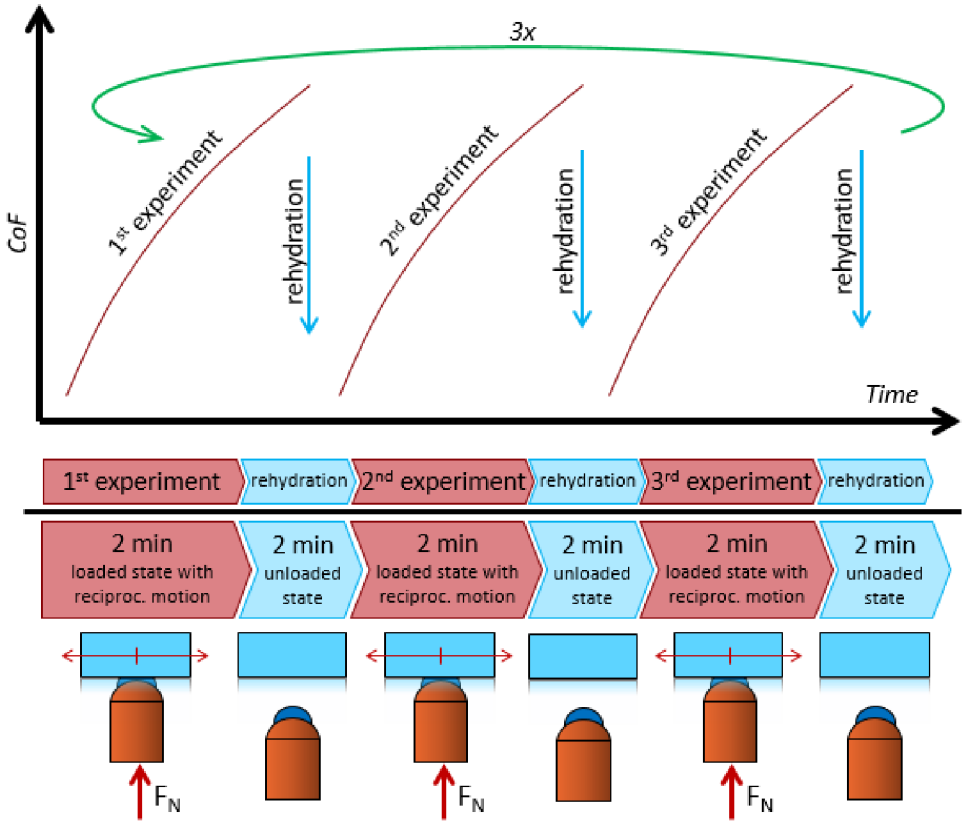

Fig. 5.8 - Scheme of repeatedly experiments

The outputs of each experiment are the records of forces representing their effects, and recorded snaps represent visualization. One of the aims of this thesis was to design the methodology of experimental data evaluation. The evaluation scheme is given in Fig. 5.9. Each experimental output has to be post-processed in two ways, the friction data processing and the visualization data processing. Raw data from the forces effects are time, normal load

and friction forces. This data is saved by computer with sampling frequency of 50 Hz. The friction force is shifted due to preloading of the friction sensor. This allows measuring of the friction forces in both directions during reciprocating motion. The offset of friction force trend is deducted using deduction of mean value (Fig. 5.9-A). It causes shifting of the friction force trend around the zero axis. Furthermore, the CoF is calculated by dividing the friction and load force. Due to the reciprocating motion, CoF has an alternating trend around the zero axis. An absolute value is created from all CoF values. The reciprocating motion causes that the CoF takes the zero value when the carriage is in the extreme positions. These values are deleted based on the difference between two adjacent values; when the difference is greater than the decision value, the CoF value is deleted (Fig. 5.9-B). The decision value was set based on the experience from the tuning phase of the evaluation process. The determining process of CoF in the NSJ was published in [66]. Recordings of trends of the effects of forces start immediately before and after the experiment. The overlap has to be cropped. Based on the initial movement of the sample during the experiment, a peak of friction force appears in its trend, which allows us to determine the moment of the beginning of the experiment. The CoF trend is the first criterion that is evaluated from the effects of forces (Fig. 5.9-C). The second one is the percentage difference between the beginning and the end, which is determined from the average of the last 1000 and first 1000 values of CoF.

The second parallel input into the evaluation procedure is a visualization record. The high-speed camera saves the record with the sampling frequency of 8 snaps per second, which can be modified based on the needs of the user and the capacity of hardware. Recorded snaps are saved with resolution of 2560 x 2140 pixels, which creates the pixel size of 3.75 micrometres with double magnification lens (Fig. 5.9-D). The specially designed software for snap evaluation was designed to remove the background and highlight lighter points (labelled proteins). The background is caused by optical noise and the lubricant contained in the porous structure of AC (Fig. 5.9-E). A description of the evaluation software principle is given in the paragraph bellow, and in the third study it is attached to this thesis [56]. The evaluation software calculates the particle count and their average size, which are values important for the forthcoming evaluation. The evaluation software processes every snap on record, which allows for determination of the particle count trend and the trend of average size of the particles (Fig. 5.9-F). Similar to evaluation of the effect of the forces, the values are saved immediately before the experiment, and the saving stops when the experiment ends. The beginning is detected due to the initial movement of particles on the snap. Furthermore, the trends, which are the outputs of the snap evaluation, are processed, and the percentage deviations between the beginning and the end are calculated (Fig. 5.9-G). The evaluation of the influence of SF composition is possible due to determination of deviations and trends, which were evaluated using both evaluation methods (effects of forces and visualization).

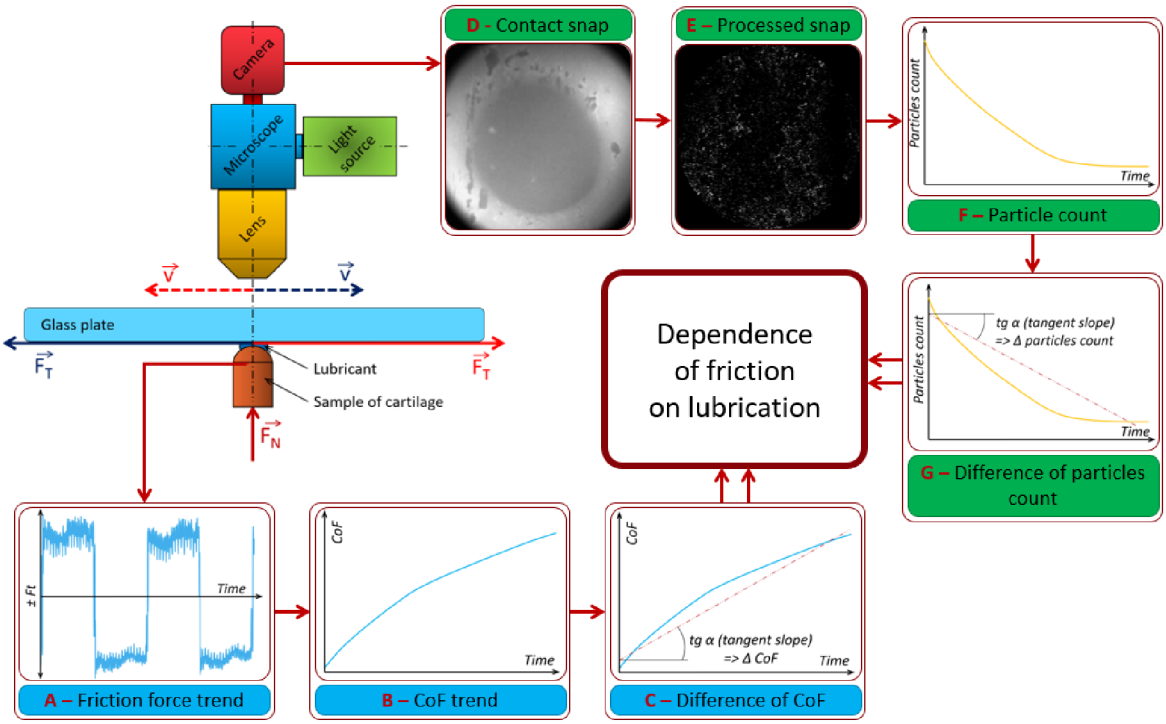

Fig. 5.9 - Evaluation scheme. A - Friction force trend; B - CoF trend; C - Difference of CoF; D - Contact snap; E - Processed snap; F - Particle count; G - Difference of particle count

The processing of snaps was based on the unique design of the software (Fig. 5.11), using the segmentation principle of image processing. Segmentation is the process of transforming the individual parts of the snap into meaningful regions or objects [67], [68]. This software removed the background and highlighted the labelled proteins from snaps in several steps. The whole procedure of snap processing is shown in the diagram in Fig. 5.10. First, the contact area was defined by a circle (Fig. 5.10-B and Fig. 5.10-C), and the surrounding area was suppressed, i.e., the surrounding area did not enter the future processing. The contact area was defined based on visual observation; the contact area was clearly visible in each snap. In the second step, dual operations, erosion and dilation, were carried out (this combination is called morphological opening, Fig. 5.10-D); therefore, at first, the structuring element (SE) was searched for in the examined area, and if SE was detected, the pixel was added into the center of SE (i.e., the examined area was reduced by the SE radius). After that, the overlap of SE in the examined area was determined. If SE, at least partially, overlapped with the examined area, the center of the resulting area was added (i.e., the examined area was magnified by the SE radius) [67]. The opened snap was subtracted from the original snap (Fig. 5.10-D and Fig. 5.10–E). Finally, thresholding was carried out (see Fig. 5.10-F and Fig. 5.10-G); according to the threshold value, all points that were below the threshold were suppressed. This principle was used in [69]. The author used the morphological opening for processing of microscope snaps of metallic alloy to highlight some parts of the snap and remove the background.

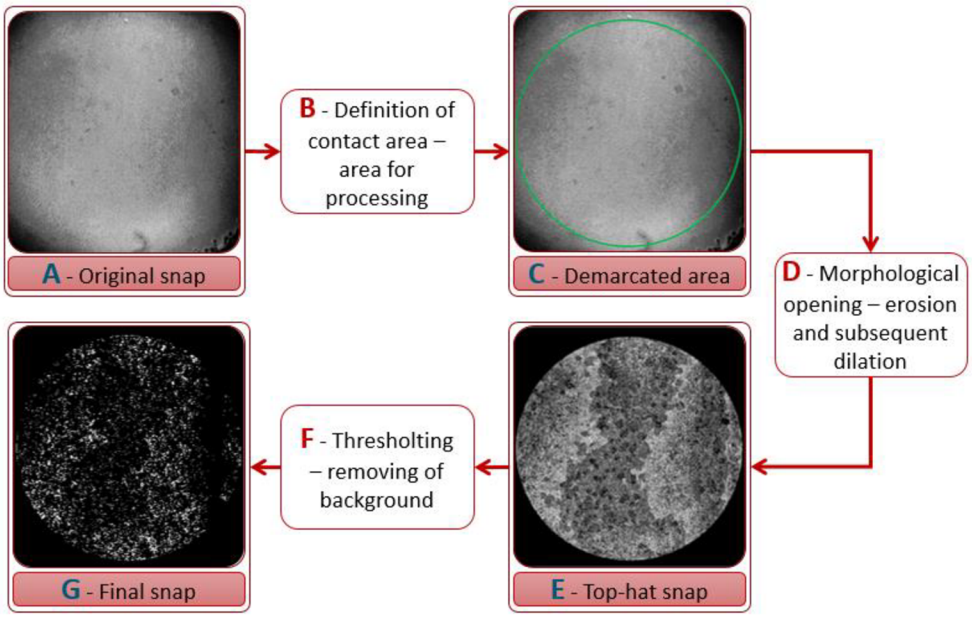

Fig. 5.10 - Snap procedure. A - Original Snap; B - Definition of contact area-area for processing; C - Demarcated area; D - Morphological opening-erosion and subsequent dilation; E - Tophat snap; F - Thresholting-removing of background; G - Final snap

A snapshot of the evaluation software is shown in Fig. 5.11. In the top right corner, there are fields for input parameters. Functions "Mask width" and "Mask center" define the circular area by which the size and position of the contact are defined. The "TopHat width" value defines sensitivity to the local snap maximum, and consequently, the areas for morphological opening are defined. The last box "Threshold" defines the threshold to determine the background. The processing steps of snaps are shown under the boxes with input parameters. The software determined the count of detected proteins and their average size; this is shown under the images with processing steps. The graph in the lower right corner describes the count and the size of particles found. The final processed snap is shown on the left side of the software window.

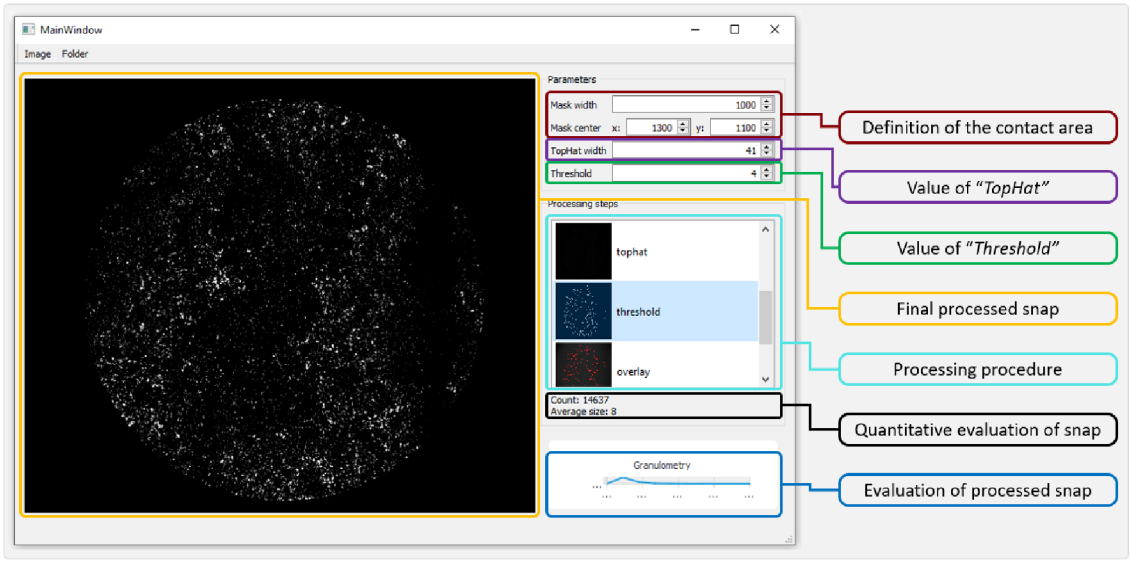

Fig. 5.11 – Evaluation software

6 RESULTS AND DISCUSSION

6.1 Verification and Calibration of the Experimental Device

The storing method has been experimentally verified using MTM. The scheme of experimental arrangement is given in chapter 5.1.1, and the scheme of experimental device is shown in Fig. 5.2-A. An experimental analysis of the impact of freezing was performed with 5 types of AC samples:

- sample freshly removed
- sample stored in the refrigerator for 2 and 6 days, temperature 4°C
- sample stored in the freezer for 6 and 12 days, temperature -20°C

The analysis of experimental results shows that fresh samples give almost the same results as the sample stored in frozen state. A standard deviation between these results is 10% at the maximum. The samples that were stored in the refrigerator already show an increase of CoF after being stored for 2 days. CoF increase by more than double was observed in samples stored for 6 days. These results agree with previous publications [62], [63], [64], [65]; therefore, storing of AC samples in frozen state is possible, and conversely, storing without freezing is impossible.

The second step of the preparatory phase was calibration and verification of reciprocating tribometer. The experimental arrangement is described in chapter 5.1.2 and the scheme of experimental device is shown in Fig. 5.3. The specially designed reciprocating tribometer was calibrated using a pulley system and weights. The verification was performed using a comparative pin-on-plate friction test, where a pin was made from PTFE G400 and PBS was used as a lubricant. The CoF results were compared between the developed reciprocating tribometer and the Bruker UMT TriboLAB (commercial tribometer). Both tribometers were in the same experimental arrangement. Two experimental conditions were tested (see chapter 5.1.2) and the results show that the accuracy of both tested devices was very similar; the standard deviation was 20% at the maximum. The description of the developed reciprocating tribometer was published in the first study attached to this thesis [55]. The study introduces a new reciprocating tribometer and its principle. Furthermore, the essence of the construction was described in this study, and the AC sampling process was introduced. The initial experiments verifying the functionality of the device were carried out in this study, which means that the simultaneous visualization and friction measurement were performed; however, the visualization has not been processed yet. This study also presents the basis of the methodology of experiments, the procedure of experiment preparation, and the basis of the visualization evaluation.

6.2 Verification and Calibration of the Method

The verification of the AC contact using a spectrometer was carried out. Labelled proteins, used for mixing of the model SF, were tested using a spectral analysis. The combination of labelled albumin and Y-globulin in one solution without AC sample, the AC sample itself without lubricant and the AC sample with lubricant were tested. The FITC and TRITC filters were used for testing, and the emission was monitored. The results are published in the second study attached to this thesis [56]. The analysis shows that the individually labelled components contained in lubricants do not affect each other. Each labelled component produces light emission only in wavelength of assigned filter, and no emission was detected under other filters. The results confirm that the AC tissue emitted no light when the sample was excited by assigned filters. The conclusion from the spectral analysis is that no influence due to unwanted emission occurs. The visualization of processing procedure, including the specially designed evaluation software of snap processing, was also presented in the second study attached to this thesis [56]. This special software removes the background of snaps and highlights labelled particles (album or Y-globulin in this case). The essence of this software is given in chapter 5.3. The calibration of evaluation software is the basis of correct processing of snaps acquired from visualization records. The first step is to define the contact area, which is performed by definition of diameter and center of the contact area. The basic premise of the process of calibration is that the fluorescence intensity of the snap is higher when the contact contains more particles; therefore, the quantity of mean fluorescence intensity is the reference value for software calibration. This quantity is evaluated for each recorded snap, which gives us the trend of fluorescence intensity. The tangent slope for intensity trend is calculated, which represents a deviation in lubricating film between the beginning and end of the experiment. A wide range of input parameters for the evaluation software is determined (TopHat and Treshold, see chapter 5.3) and every recorded snap is processed. The tangent slope for each output is evaluated. Acquired tangent slopes are compared with the fluorescence intensity outputs; the setting that shows the largest similarity to the tangent slope is determined to be correct. The correct setting is valid only for the experiments in one set, using the same lubricant (the same labelled component). If a different lubricant is used, a new calibration has to be carried out. The sensitivity analysis of the evaluation software was published in the third study attached to this thesis [57]. The analysis shows the dependency of the software input parameters in correlation with fluorescence microscopy. A wide range of input parameters is given, and the correct input parameters are located approx. in the middle of the presented range. Certain parts of the input parameters (low values of Threshold) show a linear dependency. The linearity is valid also for input parameters which are close to the setting used for snap processing. Consequently, the error caused by using another setting from the linear region is linear, i.e., no deviation occurs when the same setting is used for the whole set of experiments, because the results are only mutually compared.

6.3 Lubricating film formation in the model of synovial joint

The evaluation of lubricating film formation is based on simultaneous visualization and friction measurements, which allow for more comprehensive view of the lubricating mechanism prevailing in the NSJ. This unique approach allows for the connection between the frictional behaviour and contact observation. The particle count and their average size are used as evaluation criteria of the new approach, and the connection with CoF was established. The experiments were focused on the influence of the individual components of model SF, which is possible due to individually labelled components. The tested lubricants (model SF) were mixed from simple to more complex solutions. The evaluation was performed using a combination of the effects of the individual components in differently composed solutions, and their impact to the frictional behaviour of AC contact. Consequently, it is possible to evaluate the quantity and quality of the lubricating film. This new evaluation approach was published in the second study attached to this thesis [56], and the initial results were given. A loading process of the AC contact was observed and evaluated by the new evaluation approach, and the results show a strong decrease of particle count trend during the loading process. The following particle count trend reports only a slight decrease. The dependency between the particle count and the average size of protein particles (clusters) was found, which shows the relationship between both quantities; as the particle count strongly decreases, the average size of clusters shows a steep increase. When the contact of the AC sample with glass plate occurs, the snaps of the contact area show an outflow of particles from the contact, and the size of clusters strongly increases. This phenomenon points to a better ability of the proteins clustering when a high contact pressure (load) occurs. A very similar phenomenon was detected in studies [43], [70], [71], [72], where the escape of lubricant was also observed; nevertheless, this phenomenon was described only theoretically, without the experimental background. A new evaluation approach introduced in [56] was used for the experimental set focused on albumin impact on lubricating film formation, which was published in [57]. This study represents the culmination of this thesis, where the developed reciprocating tribometer [55] and evaluation methodology [56] are used for the experimental analysis in order to describe the lubricating film formation. The experimental set with a gradually composed lubricant was performed (see chapter 5.2.2). In order to evaluate the influence of the individual lubricant components, the lubricants ranging from a simple to complex protein composition were used. The simultaneous visualization and friction measurements were performed, and the outputs were processed using the introduced methodology. The best frictional behaviour was given by the lubricant with the following composition: albumin + Y-globulin + HA; conversely, a simple albumin solution shows the worst frictional properties. The lubricant represented by a mixture of proteins (albumin + Y-globulin) shows a slight reduction of CoF. A complex model of synovial fluid (albumin + Y-globulin + HA + phospholipids) gives lower CoF values than protein solutions; nevertheless, the CoF values are higher than the values in the

lubricant represented by a mixture of proteins and HA. A similar impact of Y-globulin proteins on the frictional behaviour was found in [47], [50], where the addition of Y-globulin proteins causes a slight reduction of CoF; furthermore, the same impact of HA was observed in these studies. The criterion for evaluation of lubricant quantity was determined in the second study attached to this thesis [56]. This criterion compiles a dependency between lubrication and friction, which is expressed by a graph where the x-axis represents *Arithmetic mean of CoF x deviation of CoF*, and the y-axis represents *Protein lubrication film area*. The x-axis expresses the frictional impact, because the use of only the arithmetic mean from the measurements can be confusing; therefore, the deviation impact was implemented. The same method was used in relation to the axis y. The resulting graph gives an overview of quality and quantity of lubricating film created in the model of the NSJ. All measurements were plotted in this graph, where four areas are drawn. Each of them represents one composition of the lubricant. The size of the areas corresponds with standard deviations of measurements and represents the stability and robustness of created lubricating film. The simple albumin solution shows the greatest area size. The particle count trend of this solution declines but the trend of the average size of clusters rises; therefore, the area of lubricating film created by albumin proteins slightly expands. A count of the albumin clusters in the contact depends on the amount of albumin particles around the contact area prior to the loading process - these particles are then trapped in the contact. The greatest area size in the resulting graph points to the lowest stability of simple protein solution; however, the adsorbed film on the AC surface is created. The albumin proteins adsorb on hydrophilic surfaces, which was shown in [16]. Consequently, the structural polarity of AC causes the attraction and adsorption of water solutions [73]; therefore, the AC surface is suitable for albumin protein adsorption. The lubricant flows through the porous structure but flowing is dependent on the size of the particles, as mentioned in [22], [40], [74]. Due to the pressure gradient, the albumin proteins create clusters larger in size, which is the reason why the CoF shows higher values. The second tested lubricant (albumin + Y-globulin solution) shows lower values of CoF than the previous one, and the particle count also declines during the experiment but the decline is stepper. The adsorbed protein clusters show a lover average size, which corresponds with a lower area of lubricating film in the resulting graph. The Y-globulin proteins are much bigger than the albumin proteins, and due to its structural properties, the Y-globulin binds the albumin, which corresponds with [59]. The Y-globulin proteins separate the adsorbed albumin film; therefore, the average size of albumin clusters in the contact is lower. This phenomenon causes a greater thickness of lubricating film, which causes lower CoF values; this deduction is supported by [75]. The lubricant represented by albumin + Y-globulin + HA shows the best frictional properties and the shape area in the resulting graph is the lowest. As was mentioned in the review, HA is very important for ensuring low values of CoF, and it creates the gel-like layer on the AC surface [9], [49], [51], [74], [75]. This layer is very important in prevention of damage, and it is strongly hydrophilic [47], [49]. These properties allow a better adsorbtion of the protein

components contained in the lubricant on the AC surface, which corresponds with the largest amount of protein clusters in the contact. Although the particle count (albumins clusters) is the highest, the increase in trend of lubricating film area is slow. The area of the shape in resulting graph is the smallest, which points to high stability of created lubricating film. Albumin binds to Y-globulin, and then is adsorbed on HA gel-like layer. The AC structure is well protected from damage, and a thick protein film is created, which allows rapid reduction of CoF. The HA contained in the lubricant acts as a stabilizer. Complex model synovial fluid containing all basic components (albumin + Y-globulin + HA + phospholipids) gives a slightly higher values of CoF and lower area of lubricating film than the previous lubricant. This composition of the lubricant is the only one with constantly raising trend of lubricating film area; this phenomenon wasn't observed in any configuration. The rising trend of lubricating film area indicates stability, which allows complete protection of the AC surface for a longer period of time. Phospholipids are bonded to the HA by phosphate cores and to other phospholipids by lipid tails, which is the basis of hydration lubrication [48]. This model assures two phospholipidic layers opposite each other (phospholipidic bilayer) to achieve the hydration model which is not compliant with the model of NSJ used in this thesis. The phospholipids in the lubricant cause the imprisonment of protein clusters between them, which leads to accumulation of protein clusters [75]. This phenomenon is the reason for the increase in the lubricating film area. The higher values of CoF are caused by absence of phospholipidic bilayer. The friction process does not take place between the phospholipidic layers as mentioned in [48]. One layer of phospholipids acts as a brush, which makes the lubricant flowing through the contact difficult. The model of lubricating film formation was published and described in the third study attached to this thesis [57].

Vol. 41, No. 3 (2019) 387-393, DOI: 10.24874/ti.2019.41.03.08

Tribology in Industry

www.tribology.rs

RESEARCH

Visualization of Lubrication Film in Model of Synovial Joint

P. Čípek[a], D. Rebenda[a], D. Nečas[a], M. Vrbka[a], I. Křupka[a], M. Hartl[a]

[a]*Brno University of Technology, Brno, Czech Republic.*

Keywords:

Biotribology
Cartilage
Reciprocating tribometer
Friction
Lubrication

Corresponding author:

Pavel Čípek
Brno University of Technology, Brno, Czech Republic.
E-mail: Pavel.Cipek@vut.cz

A B S T R A C T

Synovial joint is one of the most important parts for human movement system and the right function of it is necessary. When the synovial joint is damaged by illnesses, destroyed natural joint is exchanged for artificial joint. They are commonly used in nowadays, but there are problems with their limited lifetime. Alternative treatment procedures in surgery start appearing in order to postpone acute operation of total endoprosthesis. For proper operation of the alternative treatments lubrication processes have to be understood. The understanding of the lubrication processes can assist in the development of new suitable medical treatments. This study is focused on the visualization of the synovial joint contact and simultaneous measurement of the force effects. Experimental device represents model of synovial joint, which allows pin-on-plate reciprocating tribometer. The goal of this study is to describe the contact area behaviour and to relate it to force effects in the contact.

1. INTRODUCTION

The human movement system is based on joints and muscles. The synovial joints are composed of two bones whose surfaces covers cartilage tissue [1]. The cartilage surfaces are in close contact and the space between them is filled with the synovial fluid. This arrangement, special cartilage structure and synovial fluid, allows movement with very low friction coefficient. Tissue of cartilage is porous material with heterogeneous structure containing very few cells [2]. These specific features cause the unique tribological behaviour. Extracellular matrix is the basis of cartilage structure (ECM). ECM includes type II collagen fibres and proteoglycan [3]. Hyaluronic acid (HA), proteins, decorins, chondrocytes, etc. are also included in the ECM [4]. Cartilaginous bone coating includes three zones. The first one, surface zone, has parallely orientated collagen fibres with respect to the surface. The second one, the middle zone, has randomly orientated fibres and the last one, the deep zone, has fibres perpendicularly orientated to the surface [1]. Each of them has specific composition and properties [5]. Water volume in cartilage tissue is also very important attribute regarding lubricating properties [6,7]. Special lubricating properties are caused by very low elastic module (1 – 20 MPa) of cartilage tissue regarding the position of the cartilage surface and type of the joint [4]. All of the

mentioned specific properties together allow specific lubrication processes in synovial joint with very low coefficient of friction and wear.
Obviously, there is very limited knowledge of lubrication in natural joints in terms of experimental investigation. Only a few studies were published. Topics of these works are frequently focused on visualization of hydrogels, nevertheless, complex visualization of natural cartilage has not been published yet. The majority of the studies is aimed to friction measurement, but studies dealing with visualization of cartilage contact also appear. One of the first works dealing with visualization of hydrogel contact area by fluorescence microscopy [8] was focused on determination of the amount of the fluorescently marked particles contained in the lubricant contact area. Fluorescently marked proteins were used, in each experiment, different type of protein was marked. γ globulin showed the biggest impact on the lubrication processes, therefore, the concentration of it in synovial fluid is very important. The fluorescence microscopy was used for the observation and description of the gel-like layer formation on the cartilage surface. Forsey et al. [9] dealt with impact of the HA in creation of the gel-like layer which is the main component for the formation of the film. The study revealed dependency on size of the HA. The penetration of the cartilage structure by HA was also demonstrated by these experiments. Molecules of HA are bound in the cartilage surface because they are attracted by chondrocytes contained in cartilage structure. Wu et al. [10] showed dependency between the flow of the synovial fluid through cartilage structure and compression of cartilage tissue. The results implied dependency on size of HA molecules, specifically the large molecules of HA were caught on the cartilage surface, while the smaller particles penetrated the cartilage structure. The surface of cartilage is covered by the HA with large molecules, which creates the gel-like layer. This surface layer protects the raw cartilage surface against a damage.

Visualization of joint replacement contact was also carried out with fluorescent microscopy. Number of studies were published at our department. A lot of experience with the use of optical methods was obtained within the mentioned studies. Nečas et al. [11,12] published the papers dealing with visualization of joint replacement contact and soft contact among others.

The vast majority of previous studies mostly dealt with visualization of contact area or with the friction measurements separately. It has never been measured simultaneously yet. This study combinates this two branches of biotribology science. The usage of optical methods used at workplace is described together with classical friction measurements. Specially tailored tribometer was designed for this application. It allows simultaneous visualization of soft contact and friction measurements. Concept like this new designed tribometer, which allows combination of optical methods and friction measurements have never been used yet. The goals of this study are to design the new tribometer, to develop the sampling process and experimental methodology and finally, to perform the pilot experiments.

2. MATERIAL AND METHODS

2.1 Experimental device

The tailored new tribometer allows the measurement of friction forces and insight into the contact area, both simultaneously in real time. The pin on plate configuration of tribometer was used for compliance of this requirements. As an observation method fluorescent microscopy was chosen, therefore the concept of tribometer was adapted to be able to use it. This new design is close to the concept of tribometer which was used in study [13]. The schema of newly designed experimental device is shown in Fig. 1. To allow the visualization of contact area, the cartilage sample is placed under the glass desk. The lubricant flowing through the contact is observed by the fluorescent microscope. Due to the fluorescent microscopy method the high speed camera can record fluorescently marked particles contained in lubricant, which flow through the contact. The mercury lamp was used as a light source. The contact area was flooded by a fluorescently marked lubricant. The floated bath is heated to a human body temperature to achieve comparable conditions to human body joints. The glass desk is mounted to a carriage, which was designed as a moveable part. It performs the reciprocating motion whereas the specimen is stationary.

The new design of the tribometer is outlined in Fig. 1. The essential units of the device are shown in Fig. 2.

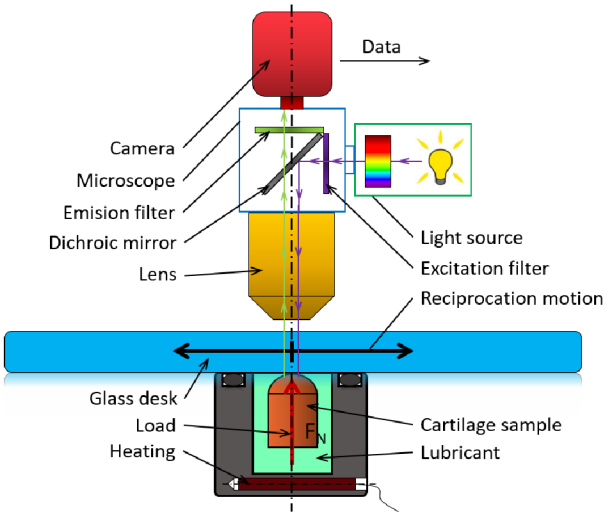

Fig. 1. Schema of the apparatus.

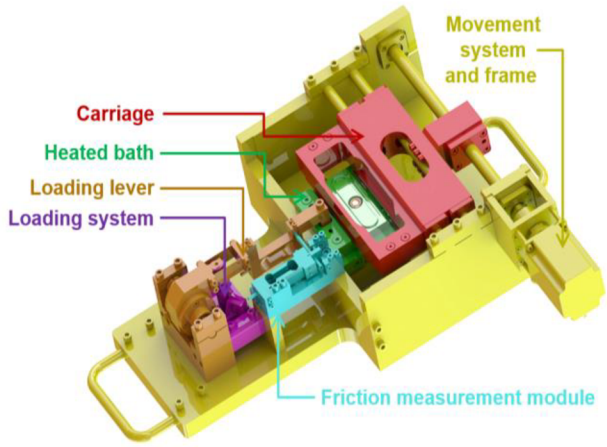

Fig. 2. Real arrangement of apparatus.

Tough frame is a basis of the tribometer, all other components are mounted on it. The carriage as a moveable part, where the glass plate is placed and which performs the reciprocating motion on the guide rods. The accurate guide rods in combination with ball screw and ball bearings in carriage body provide very accurate motion without radial and axial clearances. The heated bath enables flooding and refiling of the contact by a lubricant. The sealing is attached to the glass plate and the bath to avoid the lubricant leakage. Cartilage specimen is mounted on the end of a lever, by which the load is applied. The other end of the lever is placed in two preloaded ball bearings. This arrangement allows rotation around the axis without clearance and radial clearance is precluded too. A strain gauge is connected to the deformation member providing sufficient deformation caused by the low frictional force and great rigidity in the vertical direction (loading direction) at the same time. The first strain gauge is used for measurement of loading, the second one for measurement of friction force. It is connected parallelly to the lever behind the first gauge. Thanks to the deformation member, very low friction forces can be measured. The parallel connection of the second gauge allows its preload to the half of the measuring range, which allows measurement of friction forces during movement of carriage back and forth. The whole tribometer is situated below the fluorescent microscope on an adjustable table. The tailored tribometer is shown in Fig. 3.

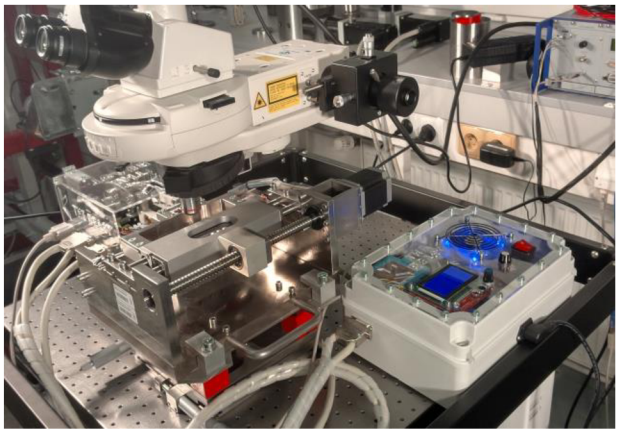

Fig. 3. Complete experimental apparatus.

National Instruments measuring card is a basis of the measuring system. Signal from the gauges is adjusted by the signal amplifier before the measuring card handles them. Data is real-time processed by LabVIEW script through connected PC. Control system is based on Arduino. The motion is ensured by the stepper motor and the load is provided by another linear stepper motor. LCD display and encoder is used as input interface. Both systems (measuring and control) work separately.

Verification and calibration was performed using standard pairs of samples (materials), in order to ensure measurement repeatability among samples. The mentioned material combination was used because the cartilage specimens show variance in results. The pin was made from PTFE-G400 and the plate was made from optical glass B270. The commercial

tribometer Bruker UMT TriboLAB was used to compare with the new tribometer. The compliance of the results obtained using the two simulators was very good.

2.2 Specimens

Specimens from mature pigs were used in the present study. The samples were removed from canopy of the femoral head as soon as possible after the slaughter of animal. The hip joint was chosen for the samples, since it is the most loaded joint, which leads to the best mechanical properties of cartilage tissue [4]. The sampling position was precisely defined through all sample bones. Strict definition assures minimization of deviation in mechanical properties through all samples. Pins of 6 mm diameter were made by the hollow drill bit and the specimens were deeply frozen (-20 ˚C) in PBS immediately after sampling. This sampling process was used in some studies before, e.g. in [14, 15] and the procedure was verified again in [16, 17]. It was proved that the tribological properties did not change. The samples were unfrozen just before testing, otherwise degradation of samples may occur. The sampling process is shown in Fig. 4.

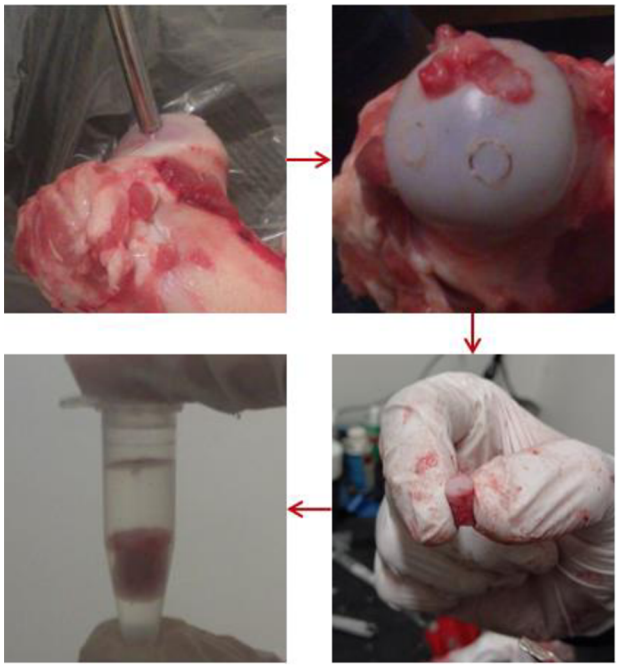

Fig. 4. Specimen preparation process.

Three variants of lubricant were used. The composition of all the used lubricants is shown in Tab. 1.

Table 1. Composition of the used lubricants.

	Concentration [mg/ml]		
	γ-globulin	**HA**	**Albumin**
Lubricant 1	-	-	20
Lubricant 2	3,6	-	-
Lubricant 3	3,6	2,5	20

In the experiments focused on visualization, lubricant 3 was used. The composition of lubricant 3 was constant for all the visualization experiments, despite the fluorescently stained component varied. In the first case, albumin was marked by Rhodamine-B-isothiocyanate (283924, Sigma-Aldrich) and in the second case, γ globulin was marked by Fluorescein-isothiocyanate (F7250, Sigma-Aldrich).

2.3 Experimental methodology

All of the experiments in this study were measured with one sample to be secured comparability of all individual measurements. Although the samples are removed from one rigorously defined place of cartilage surface, there are significant deviations between friction trends of each cartilage samples. This deviation is caused by different mechanical and structural properties among individual animal bones and therefore measurements were performed with one single sample. The validation of one sample measurements was set in this study. 5% deviation in maximum was found comparing the measurements.

The procedure was strictly specified in order to minimize the results deviation and to compare the measurements. Before each measurement, the sample was stored in PBS to rehydrate the cartilage tissue. First, the run-in procedure (20 reciprocating cycles at 10 N load) was performed before each measurement. This procedure suppresses the effect of previous experiments, especially effect of any previously used lubricants.

In the first section, lubricants 1 and 2 were used considering the friction measurements only. In the second section, the fluorescent microscopy was simultaneously combined with friction measurements. The experiments were focused on finding a correlation between visualization of contact area and friction trends. Model synovial fluid with lubricant 3 was used for all measurements in the second section. It had two configurations; the first with fluorescently

marked albumin and the second with stained γ-globulin. The composition was the same in the both cases. The measurements were performed in identic conditions and procedure.

2.4 Experimental condition

The scope of chosen conditions was to simulate human hip joint, therefore the conditions were defined with respects to it. The contact stress was set to1 MPa, which was achieved by 10 N of load. This conditions provides the medium stress comparable with hip joint. Speed of the movement was se to 10 mm/s, which corresponds to slow walking. Stroke of reciprocating motion was taken from the previous studies and it was chosen to be 20 mm. Lubricant bath was heated to 37 °C.

3. RESULTS AND DISCUSION

The results of friction measurements are shown in Fig. 5.

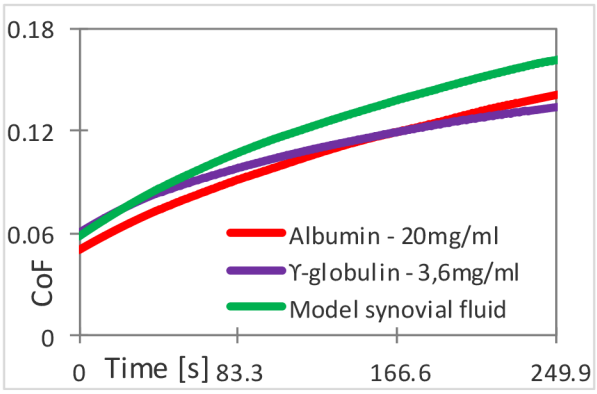

Fig. 5. Friction trends.

Lubricant 1 (albumin 20 mg/ml) exhibits steeper increase of friction than lubricant 2. It can be explained by the presence of higher concentration of proteins and larger size of albumin molecules. This explanation is also supported by images from contact visualization, which show higher light image intensity in the case of measurement with marked albumin. There is only one curve labelled as lubricant 3, which represents both of the performed measurements. In the first case, albumin protein was marked, while in the second case ϒ-globulin protein was visualised. Model synovial lubricant (lubricant 3) shows higher friction than any of the simple protein solutions. The growing global volume of proteins in lubricant leads to apparently higher friction. Very similar lubricant solutions were studied by Murakami et al. [18] who observed higher friction for γ-globulin proteins than for complex synovial fluid. Nevertheless, in the mentioned reference, the authors used different concentration of proteins and different specimens. This can explain the disagreement of the achieved results.

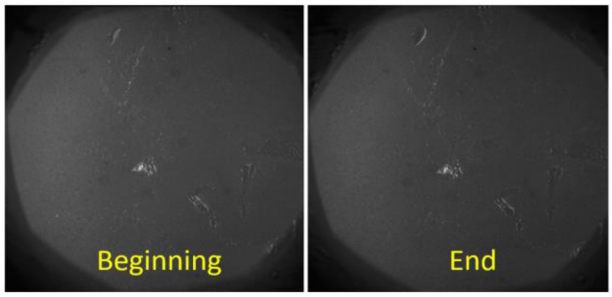

Fig. 6. Contact area visualization – Lubricant 3 with stained albumin at the beginning and at the end of the measurement.

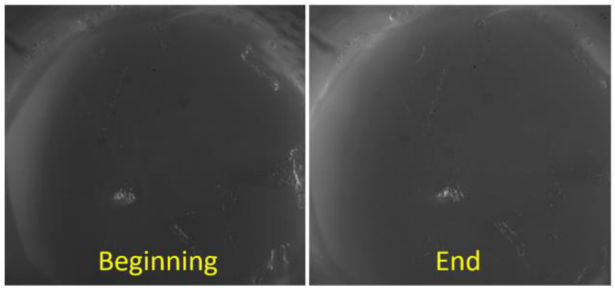

Fig. 7. Contact area visualization – Lubricant 3 with stained ϒ-globulin at the beginning and at the end of the measurement.

In order to visualize the contact area, lubricant 3 was used. The friction measurements were performed simultaneously with the visualization. The visualized contact area shown in Figs. 6 and 7 corresponds to friction curve of lubricant 3 shown in Fig. 5. White spots in in Figs. 6 and 7 are the proteins entrapped within the contact area.

Compared to the Fig. 6, Fig. 7 shows higher global intensity of emitted light. It means, that the thickness of lubricant film formed by lubricant 3 with labelled albumin is higher. Fig. 6 shows more and bigger aggregations of albumin particles. Apparently, the albumin protein is more represented constituent in the contact. The concentration of γ-globulin proteins in lubricant 3 is lower and its molecules are of smaller size at the same time. Comparing the impact of both

marked proteins, we can see that the contribution of albumin is more important in terms of cartilage lubrication.

The proteins are captured in the same location in both experiments (Fig. 6, Fig. 7). It can be assumed, that there are small local damages of the cartilage.

4. CONCLUSION

New specialized reciprocating tribometer for biotribological research was designed. It includes controlling and measuring systems, which allow friction force measurement and contact area visualisation at the same time.

Fluorescence microscopy was chosen as a suitable optical method for visualization of cartilage contact area. It was successfully used for soft contact visualization before and proved again its benefits for such type of visualisations.

The methodology for preparation of the specimens was also demonstrated in the present study.

Calibration and data validation was performed using commercial tribometer Bruker TriboLAB. The capabilities of new device were shown on the set of pilot experiments.

It reveals new unexplored fields in biotribology. Future research may bring a significant contribution, which could be eventually applied in treatment of human joint diseases.

Acknowledgement

This research was carried out under the project LTAUSA17150 with financial support from the Ministry of Education, Youth and Sports of the Czech Republic.

REFERENCES

[1] H. Czichos, D. Klaffke, E. Santner, M. Woydt, *Advances in tribology: the materials point of view,* Wear, vol. 190, iss. 2, pp. 155-161, 1995, doi: 10.1016/0043-1648(96)80014-7

[2] S.V. Eleswarapu, N.D. Leipzig, K.A. Athanasiou, *Gene expression of single articular chondrocytes*, Cell and Tissue Research, vol. 327, iss. 1, pp. 43-54, 2007, doi: 10.1007/s00441-006-0258-5

[3] V.C. Mow, A. Ratcliffe, A.R. Poole, *Cartilage and diarthrodial joints as paradigms for hierarchical materials and structures*, Biomaterials, vol. 13, iss. 2, pp. 67-97, 1992, doi: 10.1016/0142-9612(92)90001-5

[4] J.B. Fitzgerald, M. Jin, A.J. Grodzinsky, *Shear and compression differentially regulate clusters of functionally related temporal transcription patterns in cartilage tissue*, Journal of Biological Chemistry, vol. 281, iss. 34, pp. 24095-24103, 2006, doi: 10.1074/jbc.M510858200

[5] A.J. Almarza, K.A. Athanasiou, *Design characteristics for the tissue engineering of cartilaginous tissues,* Annals of biomedical engineering, vol. 32, iss. 1, pp. 2-17, 2004, doi: 10.1023/B:ABME.0000007786.37957.65

[6] J. Becerra, J.A. Andrades, E. Guerado, P. Zamora-Navas, J.M. López-Puertas, A.H. Reddi, *Articular cartilage: structure and regeneration,* Tissue Engineering Part B: Reviews, vol. 16, iss. 6, pp. 617-627, 2010, doi: 10.1089/ten.teb.2010.0191

[7] T.M. Quinn, E.B. Hunziker, H.J. Häuselmann, *Variation of cell and matrix morphologies in articular cartilage among locations in the adult human knee*, Osteoarthritis and cartilage, vol. 13, iss. 8, pp. 672-678, 2005, doi: 10.1016/j.joca.2005.04.011

[8] S. Yarimitsu, K. Nakashima, Y. Sawae, T. Murakami, *Influences of lubricant composition on forming boundary film composed of synovia constituents*, Tribology International, vol. 42, iss. 11-12, pp. 1615-1623, 2009, doi: 10.1016/j.triboint.2008.11.005

[9] R.W. Forsey, J. Fisher, J. Thompson, M.H. Stone, C. Bell, E. Ingham, *The effect of hyaluronic acid and phospholipid based lubricants on friction within a human cartilage damage model*, Biomaterials, vol. 27, iss. 26, pp. 4581-4590, 2006, doi: 10.1016/j.biomaterials.2006.04.018

[10] T.T. Wu, X.Q. Gan, Z.B. Cai, M.H. Zhu, M.T. Qiao, H.Y. Yu, *The lubrication effect of hyaluronic acid and chondroitin sulfate on the natural temporomandibular cartilage under torsional fretting wear*, Lubrication Science, vol. 27, iss. 1, pp. 29-44, 2015, doi: 10.1002/ls.1253

[11] D. Nečas, M. Vrbka, F. Urban, I. Křupka, M. Hartl, *The effect of lubricant constituents on lubrication mechanisms in hip joint replacements,* Journal of the mechanical behavior of biomedical materials, vol. 55, pp. 295-307, 2016, doi: 10.1016/j.jmbbm.2015.11.006

[12] D. Nečas, M. Vrbka, P. Šperka, M. Druckmüller, P. Skládal, P. Štarha, I. Křupka, M. Hartl, *Qualitative*

analysis of film thickness in rolling EHD contact by fluorescence technique, Modern Methods of Construction Design, pp. 615-622, 2014, doi: 10.1007/978-3-319-05203-8_81

[13] A. Moore, D. Burris, *New Insights Into Joint Lubrication*, Tribology & Lubrication Technology, vol. 72, no. 5, pp. 26-30, 2016.

[14] J. Katta, Z. Jin, E. Ingham, J. Fisher, *Effect of nominal stress on the long term friction, deformation and wear of native and glycosaminoglycan deficient articular cartilage*, Osteoarthritis and Cartilage, vol. 17, iss. 5, pp. 662-668, 2009, doi: 10.1016/j.joca.2008.10.008

[15] A.C. Cilingir, *Effect of Rotational and Sliding Motions on Friction and Degeneration of Articular Cartilage under Dry and Wet Friction*, Journal of Bionic Engineering, vol. 12, iss. 3, pp. 464-472, 2015, doi: 10.1016/S1672-6529(14)60137-2

[16] E. Northwood, J. Fisher, *A multi-directional in vitro investigation into friction, damage and wear of innovative chondroplasty materials against articular cartilage*, Clinical Biomechanics, vol. 22, iss. 7, pp. 834-842, 2007, doi: 10.1016/j.clinbiomech.2007.03.008

[17] J.E. Pickard, J. Fisher, E. Ingham, J. Egan, *Investigation into the effects of proteins and lipids on the frictional properties of articular cartilage*, Biomaterials, vol. 19, iss. 19, pp. 1807-1812, 1998, doi: 10.1016/S0142-9612(98)00147-1

[18] T. Murakami, S. Yarimitsu, N. Sakai, K. Nakashima, T. Yamaguchi, Y. Sawae, *Importance of adaptive multimode lubrication mechanism in natural synovial joints*, Tribology International, vol. 113, pp. 306-315, 2017, doi: 10.1016/j.triboint.2016.12.052

materials

MDPI

Article

Biotribology of Synovial Cartilage: A New Method for Visualization of Lubricating Film and Simultaneous Measurement of the Friction Coefficient

Pavel Čípek *, Martin Vrbka, David Rebenda, David Nečas and Ivan Křupka

Faculty of Mechanical Engineering, Brno University of Technology, 616 69 Brno, Czech Republic; Martin.Vrbka@vut.cz (M.V.); David.Rebenda@vut.cz (D.R.); david.necas@vut.cz (D.N.); krupka@fme.vutbr.cz (I.K.)

* Correspondence: Pavel.Cipek@vut.cz

Received: 7 April 2020; Accepted: 27 April 2020; Published: 30 April 2020

Abstract: A healthy natural synovial joint is very important for painless active movement of the natural musculoskeletal system. The right functioning of natural synovial joints ensures well lubricated contact surfaces with a very low friction coefficient and wear of cartilage tissue. The present paper deals with a new method for visualization of lubricating film with simultaneous measurements of the friction coefficient. This can contribute to better understanding of lubricating film formation in a natural synovial joint. A newly developed device, a reciprocating tribometer, is used to allow for simultaneous measurement of friction forces with contact visualization by fluorescence microscopy. The software allowing for snaps processing and subsequent evaluation of fluorescence records is developed. The evaluation software and the follow-up evaluation procedure are also described. The experiments with cartilage samples and model synovial fluid are carried out, and the new software is applied to provide their evaluation. The primary results explaining a connection between lubrication and friction are presented. The results show a more significant impact of albumin proteins on the lubrication process, whereas its clusters create a more stable lubrication layer. A decreasing trend of protein cluster count, which corresponds to a decrease in the thickness of the lubrication film, is found in all experiments. The results highlight a deeper connection between the cartilage friction and the lubrication film formation, which allows for better understanding of the cartilage lubrication mechanism.

Keywords: biotribology; cartilage; reciprocating tribometer; friction; lubrication; fluorescence microscopy

1. Introduction

Painless movement, i.e., the proper function of our joints, is very important in the active life of a human. Despite advanced medicine, there are many diseases of natural joints (osteoarthritis, arthrosis, arthritis, etc.) that lead to degradation and soreness of these joints [1,2]. The extent of the disease depends on many factors and may result in incurable, irreversible damage of natural joints. In this case, a natural joint has to be replaced by an artificial one. However, these replacements have a limited lifetime, which is a problem especially for young active people [3]. When the artificial joint is worn, it has to be replaced by a new one. This process cannot be repeated many times because of the adverse impacts on human health (bone degradation due to a thorn replacement, mental intensity of the operation for the patient, etc.) [4–6].

Some of the methods of the treatment of damaged natural joints are non-invasive methods, e.g., viscosupplementation (the supplement (a gel-like fluid called hyaluronic acid) is injected into the

joint gap) [7]. The general effort of non-invasive treatments is to postpone the operation of total endoprosthesis as long as possible. Viscosupplementation is a treatment method allowing to restart the lubrication process in a damaged synovial joint, which temporarily stops or at least stabilizes the degradation of natural cartilage [7–9]. So far, the function of the supplements has not been completely understood, and their effects are not fully guaranteed for individual patients [10–13]. To better understand these issues, it is necessary to describe the cartilage lubrication. The cartilage and synovial fluid properties are the basis of articular joint lubrication [14,15].

The cartilage together with a natural lubricant (synovial fluid) are very important parts of the synovial joint for tribology investigation. The cartilage surface along with the synovial fluid distribute load between the opposite bones [16]. Due to the very low elastic modulus of cartilage tissue and unique synovial fluid properties, the contact pressure is distributed over a large area of the cartilage surface; therefore, the friction coefficient (CoF) is very low [17]. The cartilage tissue is formed largely by water, type II collagen fibers, hyaluronic acid (HA), lubricin, etc. [16,18–20]. It is a sectionporous fabric with a varying structure through the thickness of the cartilage divided into three zones [16]. The structure varies especially in the composition, shape, and orientation of fibers [21–24]. Due to a low cell density, the cartilage tissue is nourished through the synovial fluid. The synovial fluid of natural joints normally functions as a natural biological lubricant, as well as a distributor of nutrients to the cartilage tissue [25]. The synovial fluid mainly consists of HA, phospholipids, proteoglycans, etc. [26–29]. The structure of cartilage contains negatively charged particles, which ensure sucking of water (synovial fluid) to the structure pores [30]. The accumulation of water in the structure of cartilage is the principle of the unique lubrication system, and many explanatory theories are based on it. In general, these properties are the basis of the lubrication processes in the synovial joint.

The research exploring the tribology of natural joints is focused on various techniques and methods. Some studies are concerned with artificial joints (joint replacement) and observation of their lubrication [31,32]; others deal with biochemical analysis of materials for the manufacturing of joint replacements and their impact on the lubricating processes [33]. The study experimentally tests the chitosan coating of the artificial prothesis, and the results show that this method causes a decrease in CoF. This is caused by the adsorbed protein layer formed on the surface because the chitosan coating binds the proteins. The publications [34,35] were focused on friction testing of artificial materials: hydrogels. Publication [35] tested the artificial cartilage from hydrogel, and publication [34] carried out friction tests with a lens from the hydrogel. The similar values of CoF as in natural cartilage were reported in both studies; however, the work in [34] showed that the friction forces were composed of three components (viscoelastic dissipation, interfacial shear, and viscous shearing). Other studies also dealt with the articular cartilage; however, their investigation was not directly focused on tribology. The work [36] carried out an extensive study focused on the treatment of mature cartilage, and the growth factor-induced therapy was evaluated using gradually carried out analyses.

There are two main types of works describing the cartilage tribological performance. The first group of works deals with cartilage lubrication, while the second one is focused on the friction between the cartilage tissues.

The first group is concerned with several mechanisms for the lubrication of articular cartilage including hydrodynamic lubrication [37], boundary lubrication [38–41], weeping lubrication [42,43], and boosted lubrication [40]. Other works of this group, which presented complementary information for already published results or describing new lubrication mechanisms, appeared in later years: hydration lubrication [44,45] and adaptive multimode [46–48]. These studies were focused on visualization of natural cartilage or hydrogels by fluorescent microscopy; their aim was to support and verify the above lubrication theories. A great influence of ϒ-globulin in the lubrication of hydrogel has been shown, but it depends on its concentration and the concentration of other lubricant components [35]. HA also seems to be very beneficial for the lubrication of cartilage [49]. It creates a gel-like layer on the cartilage surface and binds with chondrocytes contained in the cartilage structure. The penetration of the cartilage surface depends on the size of the particles; small particles penetrate the cartilage, while larger ones adhere on the cartilage surface and create a gel-like layer

[50]. The fluid leakage from the cartilage structure has also been proven, which supports the presented lubrication theories.

The second group of works is focused on cartilage friction. The number of "friction" studies is higher because the friction measurement methodology is better developed, and these works indicate well the understanding of the cartilage friction behavior. The behavior of cartilage lubricated by synovial fluid was presented in [51–55] showing that the synovial fluid reports a very low CoF. HA helps to lower CoF [54]; CoF grows with time [51,52,54,55–58]; CoF decreases with a rising load [51,57,58]; CoF is influenced by the type of movement depending on the cartilage sampling [52,59]; and the cartilage rehydration has a positive impact on CoF [60].

Obviously, there are many friction studies and also studies focused on the visualization of cartilage contact with a well indicated examined area, but there are no works allowing for simultaneous measurement of friction and visualization of cartilage contact. Fluorescence microscopy is a suitable experimental method for visualization of the cartilage contact owing to a very compliant material (cartilage) and the non-reflective surface of cartilage, which is not possible by traditional methods, e.g., optical interferometry. Another limitation of cartilage contact visualization is the non-conductivity of samples (cartilage-glass); therefore, the electrical methods cannot be used. Fluorescent microscopy is the only applicable method that allows for visualization of non-reflective, non-conductive, and compliant materials. The studies focused on the visualization of cartilage lubrication film are very limited, and the relationship with friction measurements is missing. Moreover, there is no work describing the connection between the friction in synovial joints and the visualization of cartilage contact in order to provide a better description of lubrication processes in the synovial joint. The present study explains the missing relationship to allow for a better understanding of lubrication in the synovial joint. The aim of this study is to carry out the visualization of cartilage contact by fluorescence microscopy simultaneously with the friction measurement and to explain the new methodology for the description of lubrication film in the model of the synovial joint. A similar approach to the processing of results has never been published. In this connection, a designed reciprocating tribometer and evaluating software are presented. The research study submitted offers a description of lubricating film formation in the model of the synovial joint, which can help to develop new treatment supplements along with understanding of their function.

2. Materials and Methods

2.1. Experimental Device

A unique design of the reciprocating tribometer was used; the scheme of the device is shown in Figure 1. This new design allowed for the in situ contact observation simultaneously with friction measurement. The design created was inspired by the concept in [60], where a similar design was used. A detailed description was published in the previous studies [61,62]. The use of the reciprocating tribometer simulates the compliant contact between the cartilage sample and the glass plate to create a simplified model of the synovial joint. The cartilage sample was situated under the glass plate in the static position. This arrangement allowed for the contact area visualization by the fluorescence optical system combined with a high-speed camera. The contact area was flooded with lubricant, and the lubricating bath was heated to the temperature of the human body. The glass plate was a moveable part with a reciprocating motion. Load was applied through the cartilage sample, and the lever measured friction forces. The operating conditions (stroke, sliding velocity, and load) could be modified. The tribometer was situated under the optical microscope based on fluorescence microscopy (Nikon, Eclipse NI, Minato, Tokyo, Japan).

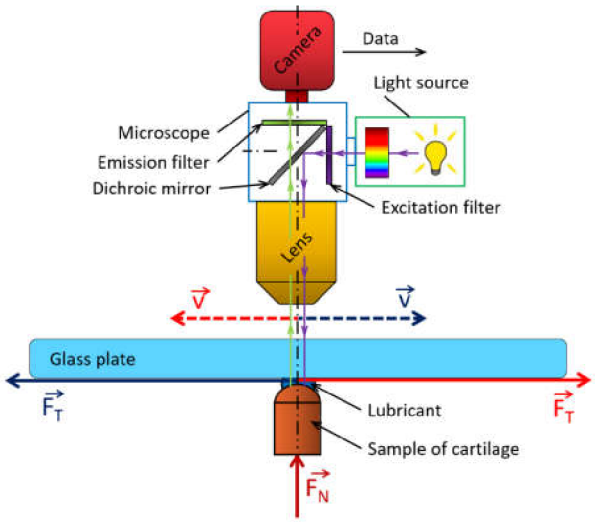

Figure 1. Schema of the experimental apparatus.

The experimental device is shown in Figures 2 and 3. The basis of this concept was a rigid frame where the other components were mounted. The glass plate was fixed to the carriage, which was actuated using a combination of a ball screw and a stepper motor. A clearance-free and accurate reciprocating motion of the carriage was ensured by guide bars and the ball sleeve. The sealing between the glass plate and the heated bath prevented the leakage of lubricant from the bath. The sample was mounted at the end of the lever through which the load was applied and distributed by a linear stepper actuator. This actuator was placed under the lever, at the opposite end to where the sample was mounted. The load sensor was a part of the lever, and the friction sensor was connected in parallel to the lever. The c control system was based on Arduino, which controlled the movement and the loading system. The input parameters were entered through an LCD interface. The measuring system worked separately and was fitted with two single-point tensometric sensors to allow for recording of loading and friction forces. Force curves were saved to the data files; CoF was calculated therefrom.

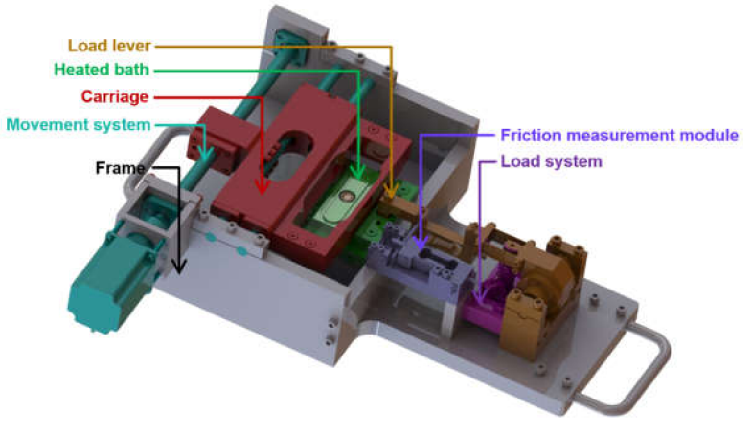

Figure 2. Digital model of the reciprocating tribometer.

Figure 3. Experimental apparatus.

2.2. Experimental Method: Fluorescence Microscopy

In this paper, the optical method based on the principle of mercury lamp inducted fluorescence was used. Fluorescence is the light emission of a substance; it is excited by light or other electromagnetic radiation. The fluorescence phenomenon can be described in three steps: excitation (the excitation photon emitted by the excitation light source is absorbed by the fluorophore contained in the fluorescent dye), excitation state period (dissipation of energy to ensure the emission of fluorescence), and emission (due to the dissipation of energy in the excitation state period, the photon emitted by the dye has a lower energy; therefore, it emits radiation at longer wavelengths). A full description of the fluorescence method was given in [63]. The mercury lamp emitting white light was used as an excitation source. The carousel with various excitation and emission filters were placed in front of the light source. For the purpose of this study, Fluorescein Isothiocyanate (FITC) and Tetramethylrhodamine (TRITC) filters were used; they allowed for a change in the wavelength of excitation and emission light, FITC (excitation on 490 nm, emission on 525 nm) and TRITC (excitation on 557 nm, emission on 576 nm). The double magnification lens was used for the observation of contact. The analysis of the apparatus was carried out, and the axial resolution was approximately 290 μm for the FITC filter and 320 μm for the TRITC filter. The field depth of the apparatus was approximately 200 μm, which was sufficient with respect to the sliding speed and estimated film thickness. Focusing of the image (contact) was carried out by the field diaphragm and slight re-focusing by the z-feed of the microscope. The focusing procedure was realized before each experiment, and it was immutable during the experiments. The fluorescence method was introduced and described in previous studies visualizing joint replacements for different material combinations [31,32]. The glass plate, through which the contact was visualized, was made from optical glass B270; therefore, the light excitation and emission were not affected. The scheme of the apparatus is shown in Figure 1.

2.3. Specimens and Lubricants

Samples were removed from the femoral hip head of mature pigs. The sampling process was realized as early as possible after the slaughter of the animal. The samples were removed from the canopy of the most loaded site of the femoral head, which ensured the best mechanical properties. This site was selected for all sample bones to achieve a low deviation of mechanical and tribological properties. The samples were removed by a hollow punch with an internal diameter of 9.7 mm and stored in phosphate-buffered saline (PBS), deeply frozen (−20 °C), and defrosted immediately before the experiments. The same sampling procedure was used in [55,58] and verified in [64,65]. The sampling process is shown in Figure 4. The opposite sample to the cartilage was the glass plate, which fulfilled the immediate requirement for insight into the contact area. The dimension of the glass

sample was 154 mm long, 43 mm wide, and 4 mm thick, which allowed for a sufficient stroke without leakage of testing fluid.

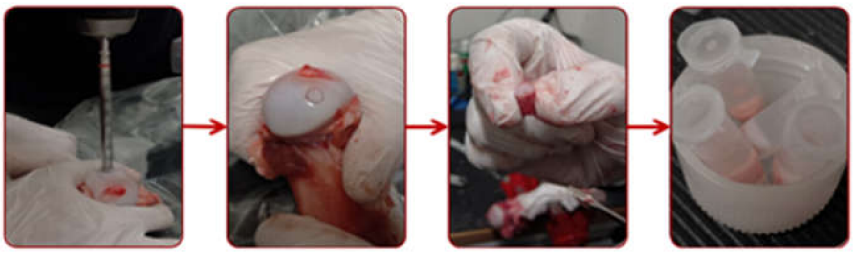

Figure 4. Sampling process.

As an experimental lubricant, a model synovial fluid was used. The composition of the model synovial fluid corresponded to the physiological synovial fluid; see Table 1. Bovine serum (BS) albumin (powder, ≥96%; A2153, Sigma-Aldrich, St. Louis, MO, USA) was labelled by Rhodamine-B-isothiocyanate (283924, Sigma-Aldrich, St. Louis, MO, USA) in this case, and the other components were mixed without dye. The protein solution was further comprised of Ƴ-globulin from bovine blood (powder, ≥99%; G5009, Sigma-Aldrich, St. Louis, MO, USA) and HA with a molecular weight of 1000 kDa. All these components were mixed in PBS solution. The lubricant degraded in air; therefore, the lubricant specimens were stored in a frozen state at −20 °C and defrosted immediately before the experiments. A single lubricant was used for each experiment, and after that, the lubricant sample was discarded. The duration of each experiment (see Table 2) was too short to degrade the lubricant sample. The other conditions of the experiments (especially contact pressure and temperature) did not speed up the degradation.

Table 1. Lubricants' composition.

Lubricant	Albumin (mg/mL)	Ƴ-globulin (mg/mL)	HA (mg/mL)	Labelled Component
Model Synovial Fluid 1	20	3.6	2.5	Albumin
Model Synovial Fluid 2	20	3.6	2.5	Ƴ-globulin
Calibration Fluid 1	20	-	-	Albumin

2.4. Methodology and Conditions

A strictly-defined procedure of the preparation of each experiment was defined for adherence to the repeatability of the results as described in the previous study [61]. All experiments were carried out under the same experimental conditions; see Table 2. These conditions were defined based on the previous studies and inspired by natural synovial joints [20,66,67]. The contact pressure was approximately 0.8 MPa. The value of the contact pressure was determined by the Hertz theory. This value was strongly dependent on the modulus of elasticity of removed cartilage, which varied through all specimens. The contact pressure was applied as 10 N of load. Similar conditions were used for example in [54,60]. The tribometer allowed for a constant majority of the velocity trend, as shown in Figure 5, where one cycle of reciprocating motion can be seen. The constant part of the velocity trend was 96.5% of every cycle.

Table 2. Experimental conditions.

Load	Contact Pressure	Velocity	Stroke	Total Distance	Number of Cycles	Duration	Temperature
10 N	0.8 MPa	10 mm/s	20 mm	1200 mm	60	approximately 4.5 min	37 °C

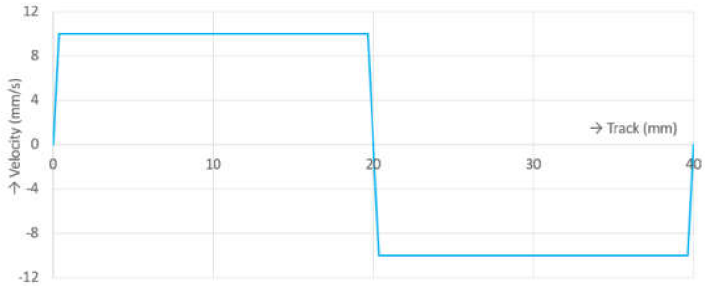

Figure 5. Sliding velocity trend.

The output of each experiment was a force record and recorded snaps of the contact area. Each experiment had to be post-processed in two ways: the effect of the forces and the visualization (snaps of contact); however, both processed results were linked at the end of post-processing. The schema of the experiments' evaluation is shown in Figure 6. The raw data from the effects of forces needed to be edited and filtered for further processing. Due to the preloaded friction sensor, the raw signal had to be offset in the first step (Figure 6A), and after that, CoF could be calculated (Figure 6B) (ratio of friction force and normal force). The complete procedure for evaluation of the effect of forces was published in [52]. The CoF trend was determined from each measurement, and the percentage difference of the CoF value from the beginning to the end was evaluated for each experiment; see Figure 6C. The percentage difference was determined from the average of the last 1000 values of CoF and subtracted from the average of the first 1000 values; this was the first evaluation parameter for the final evaluation.

The record of contact from the camera was the second parallel way of input from the experiments. The raw record from the camera was exported to the particular snaps in the first step (Figure 6D). The snaps were in a resolution of 2560 × 2140 pixels, and the pixel size while using the double magnification lens was 3.75 micrometers. The individual snaps are processed by specially designed software, which filtered out the background of each snap and highlighted the lighter points; see Figure 6E. A description of the software is given in the paragraph below. The lighter points show the labelled proteins in the lubricant; this was a significant evaluation parameter. The background noise was caused by the lubricant, which was sucked in the cartilage pores. The particle count in the contact was an output of each snap. The dependence of particle count on time was an output of the entire record; see Figure 6F. The software processed every snap in every recording according to the input parameters. The difference between the initial and final particle counts in the contact was the second evaluation parameter for final evaluation; see Figure 6G. The dependence between the particles' difference and the friction difference led to a lubrication description, especially the determination of the influence of synovial fluid individual components on the lubrication of cartilage.

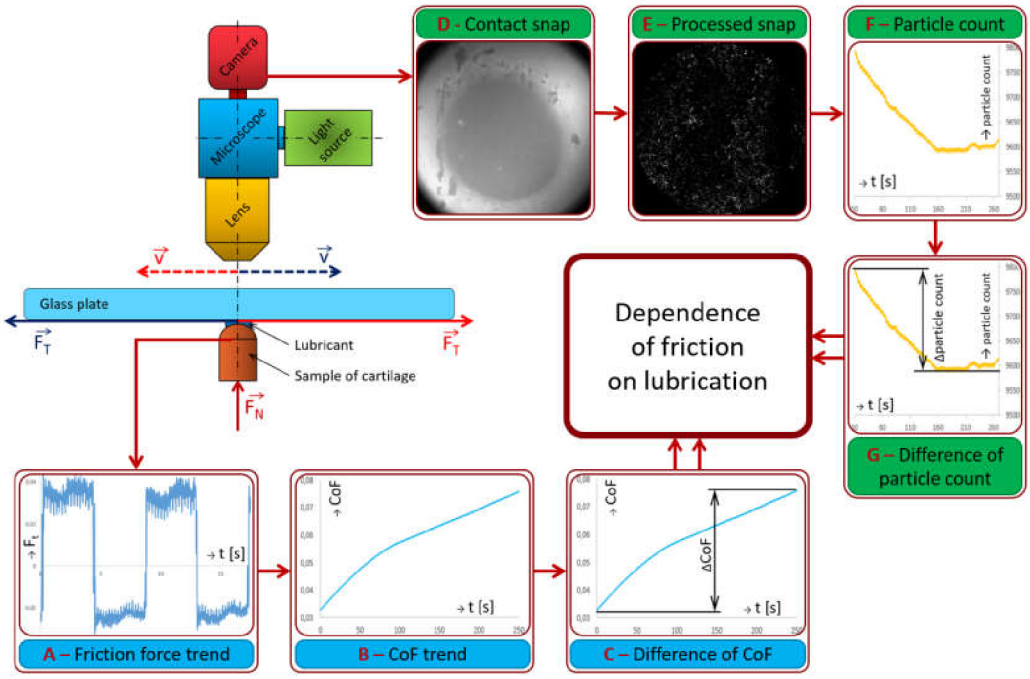

Figure 6. Evaluation schema. (**A**) Friction force trend (**B**) CoF trend (**C**) Difference of CoF (**D**): Contact snap (**E**) Processed snap (**F**) Particle count (**G**) Difference of particle count.

The processing of snaps was based on the unique software design (Figure 8) using the segmentation principle of image processing. Segmentation is the process of transforming the individual parts of the snap into meaningful regions or objects [68,69]. This software removed the background and highlighted the labelled proteins from snaps in several steps. The whole procedure of snap processing is shown in the diagram in Figure 7. First, the contact area was defined by a circle, Steps 7B and 7C, and the surrounding area was suppressed, i.e., the surrounding area did not enter the future processing. The contact area was defined based on visual observation; the contact area was clearly visible in each snap. In the second step, dual operations, erosion and dilation, were carried out (this combination is called morphological opening, Step 7D); therefore, at first, structuring element (SE) was searched in the examined area, and if SE was detected, the pixel was added into the center of SE (i.e., the examined area was reduced by the SE radius). After that, the overlap of SE in the examined area was determined. If SE, at least partially, overlapped the examined area, the center of the resulting area was added (i.e., the examined area was magnified by the SE radius) [69]. The opened snap was subtracted from the original snap (Steps 7D–E). Finally, thresholding was carried out; see Steps 7F and 7G in Figure 7; according to the threshold value, all points that were below the threshold were suppressed. This principle was used in [70]. The author used the morphological opening for processing of microscope snaps of a metallic alloy to highlight some parts of the snap and remove the background.

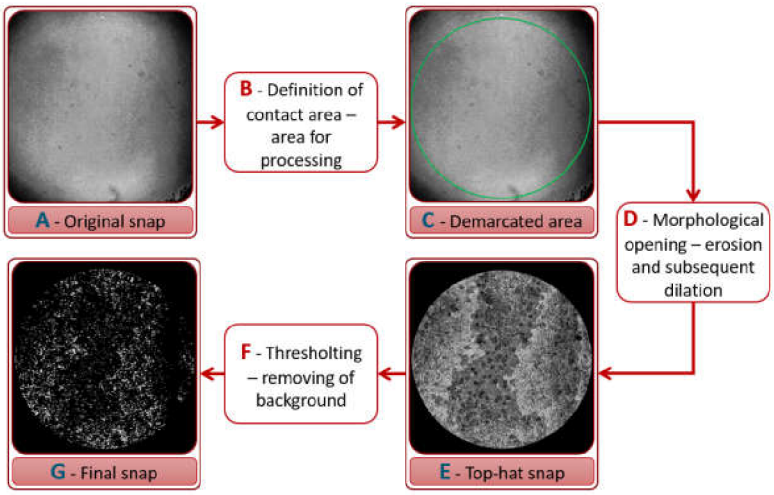

Figure 7. Snap processing diagram. (**A**) Original Snap (**B**) Definition of contact area-area for processing (**C**) Demarcated area (**D**) Morphological opening-erosion and subsequent dilation (**E**) Top-hat snap (**F**) Thresholting-removing of background (**G**) Final snap.

A snapshot of the software with its description is shown in Figure 8. In the top right corner, there are fields for input parameters. Functions "Mask width" and "Mask center" define the circular area by which the size and position of the contact are defined. The "TopHat width" value defines sensitivity to the local snap maximum, and consequently, the areas for morphological opening are defined. The last box "Threshold" defines the threshold to determine the background. The processing steps of snaps are shown under the boxes with input parameters. The software determined the count of detected proteins and their average size; this is shown under the images with processing steps. The graph in the lower right corner describes the count and the size of particles found. The final processed snap is shown on the left side of the software window.

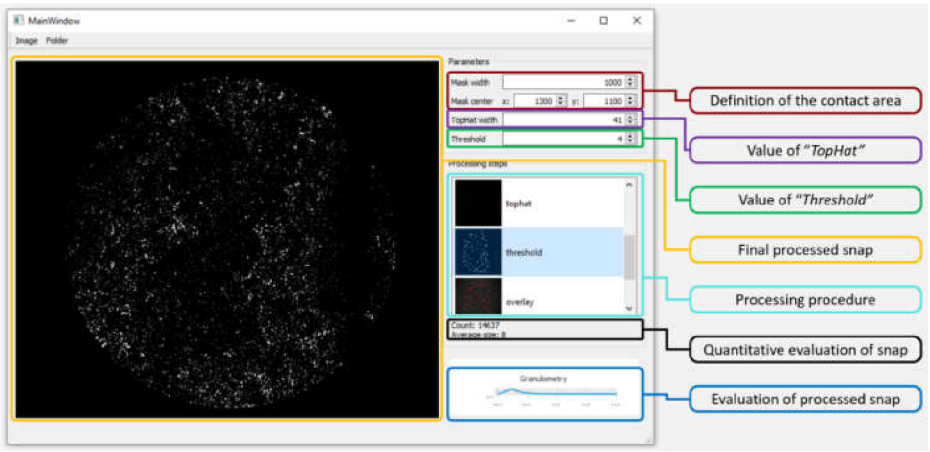

Figure 8. Evaluation software.

3. Results and Discussion

3.1. Verification and Calibration of the Method

The cartilage contact was verified by a spectrometer. The individual lubricants and their combinations with the cartilage were tested by spectral analysis. They were radiated using TRITC

and FITC filters, and their emissions were monitored. The results are shown in Figure 9. Obviously, no emission was detected if the cartilage alone was excited using both filters, as shown by Curves E and F in Figure 9. The cartilage in combination with labelled lubricants always emitted only at wavelengths of the filter used, which was obvious from Curves B and D. The labelled lubricant alone also emitted only at wavelengths of the filter used (see Curves A and C); however, the emission was stronger than in the case of lubricant with cartilage. The chart in Figure 9 shows that the individual lubricants and cartilage combinations were not mutually affected throughout measurements because their emissions were offset relative to each other.

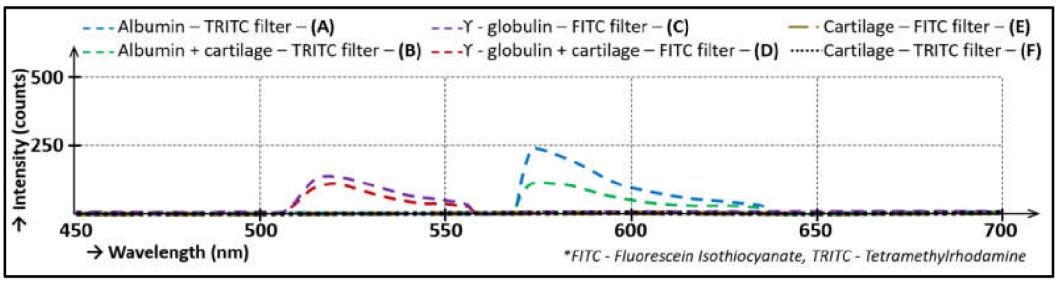

Figure 9. Lubricant emission.

The software was calibrated based on the fluorescence intensity trend, which was directly exported from camera records. The recording device was a high-speed camera allowing for recording with a high framerate. The originally delivered camera software was used to export the intensity and to convert the video record into individual snaps. These snaps must then be processed by the newly designed software. A wide spectrum of combinations of input parameters for processing by this software was compiled; however, only a small section of the spectrum was selected using the knockout chart in Figure 10. This chart shows the entire spectrum of different combinations of software input settings. Each individual point represents one input combination, and the whole chart shows a percentage decrease of particle counts throughout the experiments. The total percentage decrease was determined similarly to the CoF difference (Section 2.4), specifically from the average of the last six cycles of particle counts, and it was subtracted from the average of the first six cycles. The value from the middle of each cycle was used for average calculation. The points, which report the opposite trends to fluorescent microscopy, were eliminated (points in Figure 10 under the red line). From the remaining trends, only the points reporting similar trends as the fluorescent intensity trend were used for the following step.

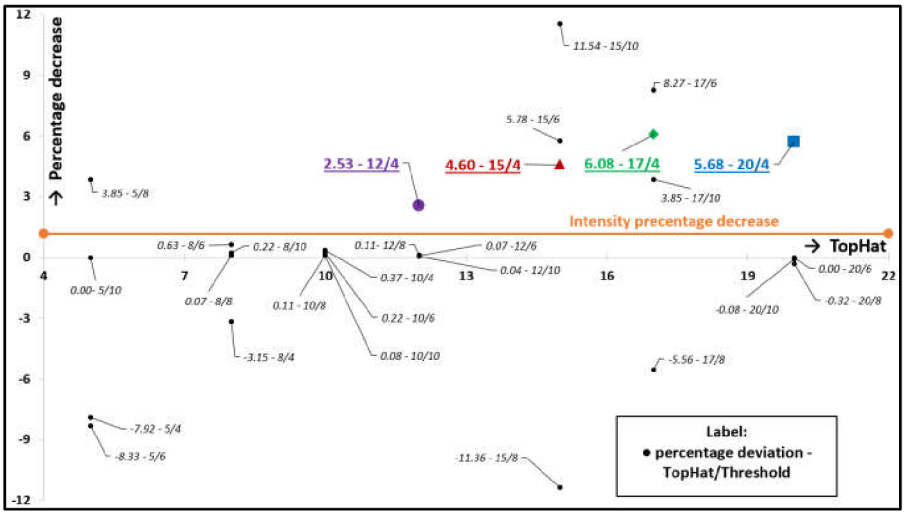

Figure 10. Knockout chart.

In this step, the similarity of the percentage decrease of particle count trends and fluorescence intensity was compared. For the next step, only the results closest to the fluorescence percentage decrease trend were used; therefore, the two y axis graph was compiled. The y axis on the right represents fluorescence intensity (Fluorescence microscopy (FLM) in Figure 11). The y axis on the left represents the particle count. The x axis is time. This dependency is shown in Figure 11. These trends were interpolated by a linear curve, and the tangent directions of these curves were compared. The most similar settings were Quantification Monitoring software (QM) 15/4 and QM 17/4; both of them well described the intensity trend, and their tangent directions were the most similar ones. As the final setting of software, setting 15/4 was defined, which meant TopHat 15 and Threshold 4. However, this setting was valid only for measurement with labelled albumin. A new calibration was necessary for each measurement to validate the data from the new software. The independent calibrations of evaluation software were carried out for both model synovial fluids, and the determined calibration inputs are shown in Table 3.

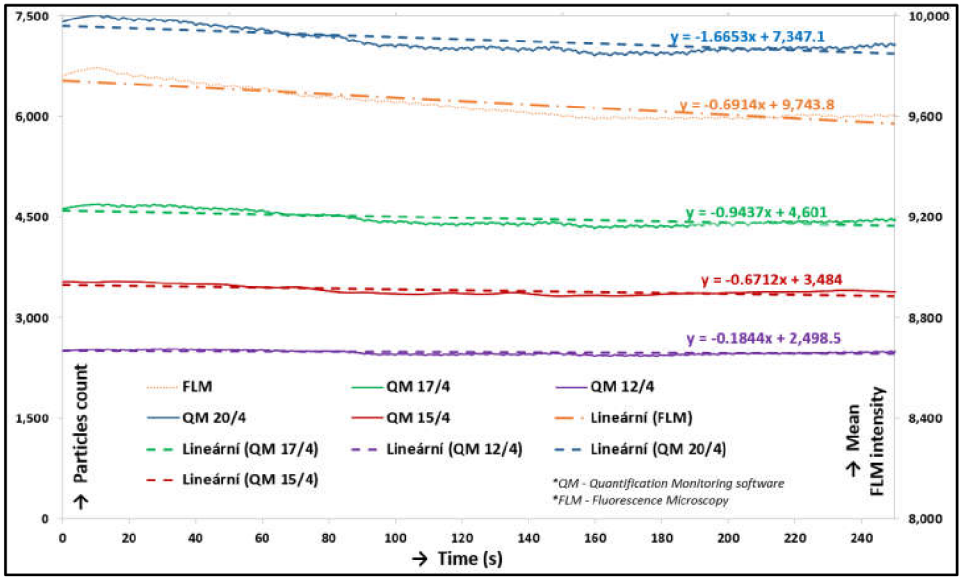

Figure 11. Comparison chart of individual input parameters.

Table 3. Percentage deviation of CoF.

Lubricant	Mask Radius (pixel)	Contact Center x/y (pixel)	Top Hat	Threshold	Labelled Component	Fluorescence Filter
Model Synovial Fluid 1	1000	1300/1100	15	4	Albumin	TRITC
Model Synovial Fluid 2	1000	1300/1100	13	4	Ɣ-globulin	FITC

3.2. Friction and Lubrication in Cartilage Contact

At first, prior to all experiments focused on lubrication analysis, the static experiment without reciprocating motion was carried out. The cartilage specimen was gradually loaded from the unloaded state to the load of 10 N by a linearly rising loading process. The contact was recorded simultaneously. This experiment was carried out only with the solution of albumin and PBS (Calibration Fluid 1; see Table 1). Figure 12 shows the states immediately before the contact was loaded (12A), immediately after the contact was loaded (12B), and after the contact was fully loaded (12C). The red circle in the snaps represents a cartilage contact area, and the white points represent clusters of labelled proteins; in this case, albumin. The lower snaps in Figure 12 show the original snaps, and the clusters of proteins are obstructed by thin red curves. The decrease of the count of particles in contact was obvious throughout loading. The particle count curve (Figure 13) showed a

strong fall during the loading process; nevertheless, the following particle count trend did not vary much and reported only a slight decrease. A decreasing trend of particle count corresponded to a decreasing trend of fluorescence intensity (Figure 14). However, the size of protein clusters sharply rose during the loading process, i.e., the size of protein clusters increased with rising load. This trend corresponded to the contact snaps in Figure 12. Conclusions from these experiments confirmed the presence of protein clusters in cartilage contact and their squeezing out from the cartilage pore structure, and subsequently from the contact. This confirmed a decreasing trend of particle count and fluorescence intensity. A similar theory, the escape of proteins from the contact and synovial fluid from the cartilage tissue during loading, was suggested and described in [40–43]; nevertheless, this phenomenon was described only at the theoretical level in connection with lubrication theories. The study [71] described similar results, the extrusion of lubricant during load, but based on different experiments.

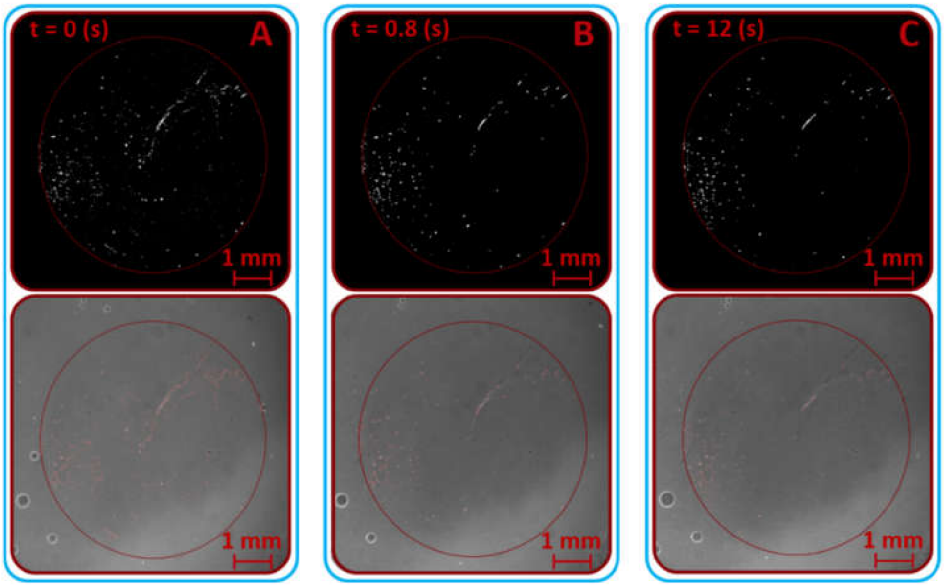

Figure 12. Loading of contact snaps – highlighted protein clusters by the software. (**A**)—protein clusters at the beginning of the experiment (in the time 0 s), (**B**)—protein clusters in the time 0.8 s, (**C**)—protein clusters at the end of experiment (in the time 12 s).

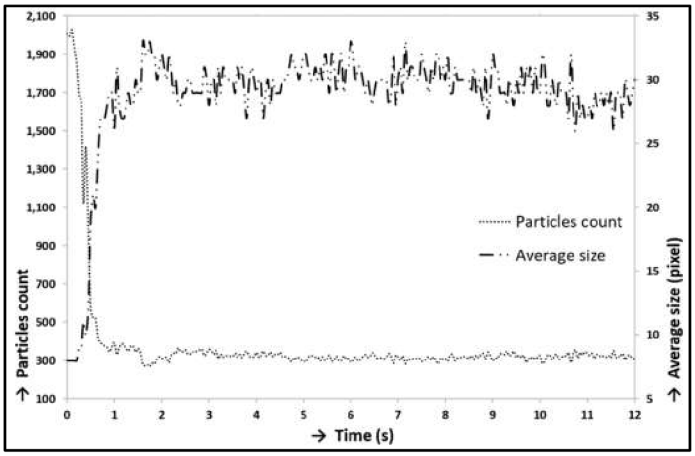

Figure 13 Loading of contact–particles count/average size.

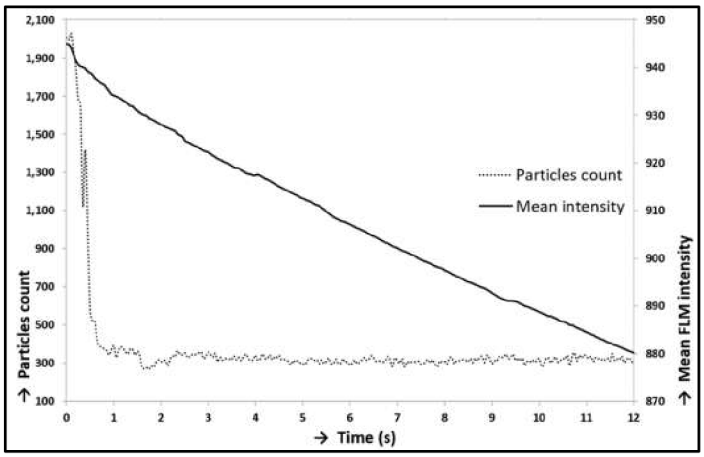

Figure 14. Loading of contact–particles count/FLM (fluorescence microscopy) intensity.

Two different measurements were carried out. The variation of experiments lied on two model synovial fluid variants with the same composition; nevertheless, a different labelled component was used (see Table 1). Both measurements were carried out under the conditions in Table 2 and focused on simultaneous recording of friction forces and visualization. The particle count trends and the trends of average size of protein clusters were evaluated and shown in Figure 15. Decreasing trends of particle counts were obvious from both curve trends. The percentage deviation of the decreases is given in Table 4. Model Synovial Fluid 1 showed a more significant decrease of particle count than Fluid 2 (see Figure 15) and also on deviation (Table 4). The average size of ϒ-globulin clusters (Model Synovial Fluid 2) decreased simultaneously with the decrease of the ϒ-globulin particle count; however, the average size of albumin protein clusters (Model Synovial Fluid 1) was unchangeable. The opposite deviations were shown by the simultaneous friction measurements. The deviation (percentage increase) of CoF trends was evaluated (see Table 4). This parameter was the second main output from the experiments. The correlation between CoF and particle count trends, measurement with Model Synovial Fluid 1, is shown in Figure 16. These trends implied the dependency between the initial increase in CoF and the decrease in particle count; i.e., the trends did not change much, and their changes were gradual. In the second measurement, a similar dependency was not distinct (measurement with Synovial Fluid 2, labelled ϒ-globulin).

Table 4. evaluation outputs from experiments: percentage deviations of measured magnitude.

Lubricant	Deviation of CoF	Deviation of Particle Count
Model Synovial Fluid 1	61.55%-Increase	3.73%-Decrease
Model Synovial Fluid 2	56.96%-Increase	23.33%-Decrease

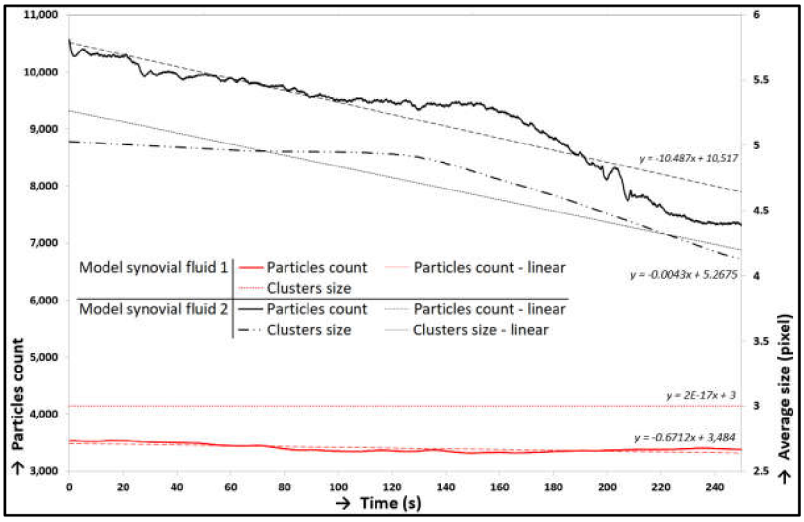

Figure 15. Particle count/average size/time-dependence: Model Synovial Fluids 1 and 2.

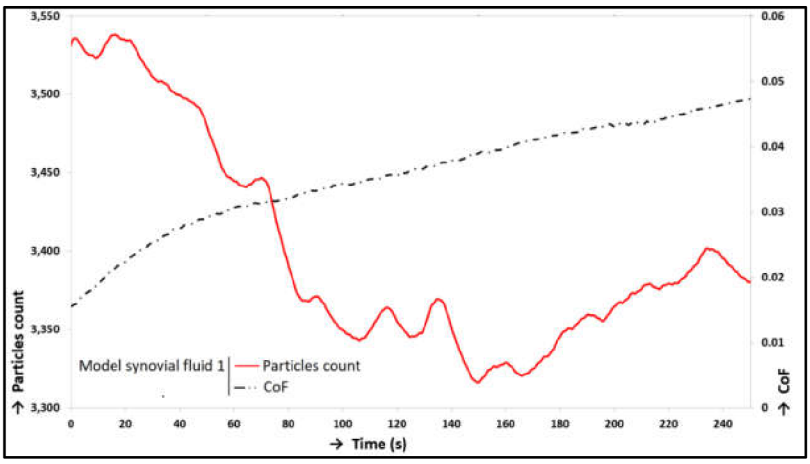

Figure 16. CoF trend: Model Synovial Fluid 1.

A comparison of particle count trends showed that the Υ-globulin protein clusters were wiped off faster from the contact than the albumin; thus, the lubrication film was formed especially by albumin clusters. Υ-globulin helped with the forming of the lubrication film at the beginning of the experiments, and the size of its clusters was much larger than that of the clusters formed by albumin; nevertheless, the lubrication film formed by albumin was more stable. The results suggested a greater influence of albumin proteins on lubrication because of their higher stability in contact, but the clusters formed by Υ-globulin were more numerous. Similar conclusions were also presented in [35], but different lubrication compositions of the fluids were used with the same labelled components. The study suggested more Υ-globulin clusters in the contact, but the trends of particle counts with both labelled components were different. This could be caused by the different composition of the experimental fluids, experimental conditions, and in particular different specimens (PVA hydrogel was used instead of cartilage samples). The decreasing trends of particle counts were shown in both measurements, although the trend of CoF was increasing. The measurement with Model Synovial Fluid 2 showed a steeper decline of particle counts, which indicated a connection with the growing trend of CoF (see Figure 15), but with a smaller impact on lubrication film forming. However, measurement with Fluid 1 showed a very gradual decrease of particle counts, which indicated a greater impact on lubrication, but a smaller impact on the increasing trend of CoF. These results showed that, in this case, the albumin proteins represented the main component responsible for

lubrication film formation. In general, a decrease in particle counts in both measurements indicated squeezing out of lubricant from the contact area, i.e., weeping and squeezing out of protein clusters from the contact, which weakened the adsorbed film formed by the proteins. In general, the connection between the rising CoF trend and the decreasing trend of particle count pointed out that the adsorbed lubricating film on the cartilage surface, which was created by the protein clusters, was a key factor for the low friction in the contact and protected the cartilage surface from damage [50]. When the adsorbed lubricating film covered the cartilage surface, the motion (friction) took place inside or between the protein layers, i.e., lower CoF. The results showed that the albumin clusters were the basis of the lubricating film; they were adsorbed at first on the cartilage surface, and the Υ-globulin clusters were bonded to them. The protein clusters were gradually wiped off from the contact; at first, the Υ-globulin clusters and after that, the albumin clusters. This caused, in the extreme case, the contact of raw cartilage tissue, which damaged the cartilage tissue and increases the CoF. The presence of protein clusters was partly due to weeping of lubricant from cartilage pores, which was proven by the static loading experiment in correspondence with the lubrication theories published in [42,43]. These theories describe the cartilage lubrication based on the weeping of lubricant from cartilage pores during motion. The pores serve as a lubrication stack, and this is exhausted during motion, which causes a CoF increasing trend. In general, the decreasing trends of particle counts caused a decreasing thickness of lubrication film until the proteins were completely removed from the contact. According to the indications, it was expected that the carried-out experiment worked at the transition of the boundary and mixed lubrication regime depending on the value of CoF. A decrease in lubrication film led to an increasing CoF trend. Albumin had a greater effect on the CoF change from this perspective, but Υ-globulin showed a greater change of particle count. Albumin showed a greater impact on lubrication in both cases (lubrication and friction). The values of CoF started approximately between 0.01 and 0.02 and ended at approximately 0.05 after 250 s of testing. Other publications showed slightly different values and also in comparison with these findings above. Publication [60] showed similar values of CoF with a similar configuration of the tribometer; nevertheless, different operating conditions and lubricants were tested. Publications [46–48] showed experiments with a similar model of synovial fluids providing similar results of CoF. Different cartilages were also tested: a cartilage removed from guinea pigs [38], bovine bones [57], and human specimens [51]. Though the samples were removed from different animals, the values and trends of CoF were comparable; nevertheless, the deviation of CoF depended on the combination of friction samples, testing conditions, etc. A rise in CoF trends, which was shown in this study, has been known from other publications [46–60, 38], and the values of CoF were comparable depending on the processing conditions, configuration of specimens, and lubricants.

3.3. Methodology and its limits

All measurements were carried out with one cartilage specimen. The reason is a great variation of tribological and mechanical properties across cartilage samples removed from different bones. Mechanical properties, especially elasticity modulus, depend on the site of sample removal, which is connected with the deviation of tribological properties [72,73]. Mechanical and tribological properties are better when the specimens are removed from the most loaded site of the bone surface. Specimen properties also deviate due to the type of joint because each joint is differently loaded [17,66,74]. Tribological properties also depend on the age of the animal from which the specimen is removed [38]. The use of only one specimen declared the comparability of the percentage deviations of measurement values. The cartilage as a biological material tissue is also sensitive to degradation in air; therefore, all experiments were carried out consecutively in one day [75]. The lubricant was also a biological specimen so there was a risk of degradation. Moreover, there was also a risk of gradual loss of the fluorescence properties of the dye contained in the lubricant specimens. When the lubricant was excited by the light source, the emitted light from the dye gradually decreased. It could be assumed that the measured fluorescence intensity, which was the basis for the evaluation of the particle count by the new software, was thus affected.

Real natural synovial joints operate under various conditions (load, sliding speed between cartilages) depending on the type of movement (walk, trot, run, etc.) [73]. The direction and type of movement between the surfaces of cartilages vary depending on the type of joint (knee, hip, etc.); each joint operates under special kinematic conditions [73,76,77]. The present study used a simplified model of the synovial joint. The kinematic operating conditions were simplified to the reciprocating motion with a constant velocity (see Figure 5); i.e., the kinematic operating conditions were simplified from the multi-axis motion with various velocity and load to the single-axis motion with constant velocity and load. This simplified model of the synovial joint with a reciprocating tribometer used the cartilage as a testing specimen and the glass plate as the friction specimen. The glass plate ensured insight into the contact; however, the modulus of elasticity of glass is of a larger order than that of cartilage tissue. The performed experiments used model synovial fluids that did not contain all of the components of physiological synovial fluid. The compositions of the fluids were adapted to the possibilities of fluorescence labelling of synovial fluid components. Previous research studies used different fluid compositions; moreover, each animal has a unique synovial fluid composition.

4. Conclusions

The present research showed a new approach to cartilage friction and lubrication evaluation. Friction measurement was connected with simultaneous visualization of cartilage contact, which helped to better understand the cartilage lubrication processes. This opened a new look at the evaluation of individual components of the lubricant and the correlation with the friction coefficient. The newly designed evaluation software and experimental device were presented. The evaluation of lubrication was based on the processing of the contact record provided by this software, which evaluated records (snaps) from the fluorescence microscope. Friction measurements simultaneously with visualization were carried out for on-off loaded contact and the reciprocating test with the model synovial fluid. The conclusions from the measurements were as follows:

The on-off loaded contact showed a decreasing trend of particle count in the contact, which pointed to weeping of lubricant out of the contact.

The albumin protein played a major role in lubrication and created a stable lubrication film in the contact.

The connection between the rising trend of friction and the trend of albumin particle count was indicated.

The Ɣ-globulin protein showed a significant decrease of particle count in the contact, which pointed to its smaller role in the cartilage lubrication.

This methodology represented great potential for understanding the lubrication system in human synovial joints, which will help to treat joint diseases. Our research assumed the future experiments to be focused on the analysis of the impact of individual components of synovial fluid on lubrication and friction, and also the rehydration of cartilage will be examined. The newly designed experimental apparatus together with the newly developed evaluation methodology could open new possibilities for testing of other soft contacts, such as contact lenses, rubbers, or soft polymers.

Author Contributions: Conceptualization, P.Č. and D.N.; methodology, P.Č., D.R. and D.N.; software, P.Č.; validation, D.R., D.N. and M.V.; formal analysis, P.Č.; investigation, P.Č., D.R. and D.N.; resources, M.V. and I.K.; data curation, P.Č. and D.R.; writing—original draft preparation, P.Č.; writing—review and editing, P.Č. and D.N.; visualization, M.V.; supervision, D.N. and M.V.; project administration, M.V. and I.K.; funding acquisition, M.V. and I.K. All authors have read and agreed to the published version of the manuscript.

Funding: This research was founded by Czech Science Foundation, grant number 20-00483S. The research was also founded by the CEITEC 2020 (Central European Institute of Technology), project number LQ1601, with financial support from the Ministry of Education, Youth and Sports of the Czech Republic under the National Sustainability Programme II.

Acknowledgments: Thanks to Michal Plch for helping with the development of the data processing software.

Conflicts of Interest: The authors declare no conflict of interest.

References

1. Walker-Bone, K.; Javaid, K.; Arden, N.; Cooper, C. Regular review: Medical management of osteoarthritis.*BMJ* **2000**, *321*, 936–940.
2. Pendleton, A.; Arden, N.; Dougados, M.; Doherty, M.; Bannwarth, B.; Bijlsma, J.W.J.; Cluzeau, F.; Cooper, C.; Dieppe, P.A.; Günther, K.-P; et al. EULAR recommendations for the management of knee osteoarthritis: Report of a task force of the Standing Committee for International Clinical Studies Including Therapeutic Trials (ESCISIT). *Ann. Rheum. Diseases* **2000**, *59*, 936–944.
3. Lewis, G. Polyethylene wear in total hip and knee arthroplasties. *J. Biomed. Mater. Res.* **1997**, *38*, 55–75.
4. Kurtz, S.M.; Muratoglu, O.K.; Evans, M.; Edidin, A.A. Advances in the processing, sterilization, and crosslinking of ultra-high molecular weight polyethylene for total joint arthroplasty. *Biomaterials* **1999**, *20*, 1659–1688.
5. Schmalzried, T.P.; Kwong, L.M.; Jasty, M.; Sedlacek, R.C.; Haire, T.C.; O'Connor, D.O.; Bragdon, C.R.; Kabo, J.M.; Malcolm, A.J.; Harris, W.H. The mechanism of loosening of cemented acetabular components in total hip arthroplasty. Analysis of specimens retrieved at autopsy. *Clin. Orthop. Relat. Res.* **1992**, *274*, 60–78.
6. Piconi, C.; Maccauro, G.; Muratori, F.; Del Prever, E.B. Alumina and Zirconia Ceramics in Joint Replacements. *J. Appl. Biomater. Biomech.* **2003**, *1*, 19–32.
7. Balazs, E.A.; Denlinger, J.L. Viscosupplementation: A new concept in the treatment of osteoarthritis. *J. Rheumatol.* **1993**, *39*, 3–9.
8. Laurent, C. Biology and Medical Applications of Hyaluronan and Its Derivatives. *Wenner Gren Symp. Series* **1998**, *72*, 3.
9. Weiss, C.; Band, P. Basic principles underlying the development of viscosupplementation for the treatment of osteoarthritis. *JCR J. Clin. Rheumatol.* **1999**, *5.6*, S2–S11.
10. Rutjes, A.W.S.; Jüni, P.; da Costa, B.R.; Trelle, S.; Nüesch, E.; Reichenbach, S. Viscosupplementation for Osteoarthritis of the Knee. *Ann. Int. Med.* **2012**, *157*, 180–191.
11. Jevsevar, D.; Donnelly, P.; Brown, G.A.; Cummins, D.S. Viscosupplementation for Osteoarthritis of the Knee. *J. Bone Joint Surg. Am. Vol.* **2015**, *97*, 2047–2060.
12. Bannuru, R.R.; Vaysbrot, E.E.; Sullivan, M.C.; McAlindon, T.E. Relative efficacy of hyaluronic acid in comparison with NSAIDs for knee osteoarthritis: A systematic review and meta-analysis. *Semin. Arthr. Rheum.* **2014**, *43*, 593–599.
13. Arrich, J.; Piribauer, F.; Mad, P.; Schmid, D.; Klaushofer, K.; Müllner, M. Intra-articular hyaluronic acid for the treatment of osteoarthritis of the knee: Systematic review and meta-analysis. *Can. Med. Assoc. J.* **2005**, *172*, 1039–1043.
14. Jahn, S.; Seror, J.; Klein, J. Lubrication of Articular Cartilage. *Ann. Rev. Biomed. Eng.* **2016**, *18*, 235–258.
15. Wright, V.; Dowson, D. Lubrication and cartilage. *J. Anat.* **1976**, *121*, 107–118.
16. Eleswarapu, S.V.; Leipzig, N.D.; Athanasiou, K.A. Gene expression of single articular chondrocytes. *Cell Tissue Res.* **2006**, *327*, 43–54.
17. Almarza, A.J.; Athanasiou, K.A. Design Characteristics for the Tissue Engineering of Cartilaginous Tissues. *Ann. Biomed.Eng.* **2004**, *32*, 2–17.
18. Knobloch, T.J.; Madhavan, S.; Nam, J.; Agarwal, S., Jr.; Agarwal, S. Regulation of Chondrocytic Gene Expression by Biomechanical Signals. *Crit. Rev. Eukaryot. Gene Expr.* **2008**, *18*, 139–150.
19. Mow, V.C.; Ratcliffe, A.; Robin Poole, A. Cartilage and diarthrodial joints as paradigms for hierarchical materials and structures. *Biomaterials* **1992**, *13*, 67–97.
20. Fitzgerald, J.B.; Jin, M.; Grodzinsky, A.J. Shear and Compression Differentially Regulate Clusters of Functionally Related Temporal Transcription Patterns in Cartilage Tissue. *J. Biological Chem.* **2006**, *281*, 24095–24103.
21. Dunn, W.; DuRaine, G.; Reddi, A.H. Profiling microRNA expression in bovine articular cartilage and implications for mechanotransduction.*Arthr. Rheum.* **2009**, *60*, 2333–2339.
22. Becerra, J.; Andrades, J.A.; Guerado, E.; Zamora-Navas, P.; López-Puertas, J.M.; Reddi, A.H. Articular Cartilage: Structure and Regeneration. *Tissue Eng. Part B Rev.* **2010**, *16*, 617–627.
23. Quinn, T.M.; Hunziker, E.B.; Häuselmann, H.-J. Variation of cell and matrix morphologies in articular cartilage among locations in the adult human knee. *Osteoarthr. Cartil.* **2005**, *13*, 672–678.
24. Darling, E.M.; Athanasiou, K.A. Rapid phenotypic changes in passaged articular chondrocyte subpopulations.*J. Orthop. Res.* **2005**, *23*, 425–432.

25. Blewis, M.E.; Nugent-Derfus, G.E.; Schmidt, T.A.; Schumacher, B.L.; Sah, R.L. A model of synovial fluid lubricant composition in normal and injured joints. *Eur. Cells Mater.* **2007**, *13*, 26–39.
26. Swann, D.A.; Silver, F.H.; Slayter, H.S.; Stafford, W.; Shore, E. The molecular structure and lubricating activity of lubricin isolated from bovine and human synovial fluids. *Biochem. J.* **1985**, *225*, 195–201.
27. Schmid, T.M.; Su, J.-L.; Lindley, K.M.; Soloveychik, V.; Madsen, L.; Block, J.A.; Kuettner, K.E.; Schumacher, B.L. Superficial zone protein (SZP) is an abundant glycoprotein in human synovial fluid with lubricating properties. In *The Many Faces of Osteoarthritis*; Birkhäuser Basel: Basel, 2002; pp. 159–161. ISBN 978-3-0348-9450-0.
28. Ogston, A.G.; Stanier, J.E. The physiological function of hyaluronic acid in synovial fluid; viscous, elastic and lubricant properties. *J. Physiol.* **1953**, *119*, 244–252.
29. Schwarz, I.M.; Hills, B.A. Surface-active phospholipid as the lubricating component of lubricin. *Rheumatology* **1998**, *37*, 21–26.
30. Athanasiou, K.A.; Rosenwasser, M.P.; Buckwalter, J.A.; Malinin, T.I.; Mow, V.C. Interspecies comparisons of in situ intrinsic mechanical properties of distal femoral cartilage. *J. Orthop. Res.* **1991**, *9*, 330–340.
31. Nečas, D.; Vrbka, M.; Urban, F.; Křupka, I.; Hartl, M. The effect of lubricant constituents on lubrication mechanisms in hip joint replacements. *J. Mech. Behav. Biomed. Mater.* **2016**, *55*, 295–307.
32. Nečas, D.; Vrbka, M.; Galandáková, A.; Křupka, I.; Hartl, M. On the observation of lubrication mechanisms within hip joint replacements. Part I: Hard-on-soft bearing pairs. *J. Mech. Behav. Biomed. Mater.* **2019**, *89*, 237–248.
33. Qin, L.; Feng, X.; Hafezi, M.; Zhang, Y.; Guo, J.; Dong, G.; Qin, Y. Investigating the tribological and biological performance of covalently grafted chitosan coatings on Co–Cr–Mo alloy. *Tribol. Int.* **2018**, *127*, 302–312.
34. Rennie, A.C.; Dickrell, P.L.; Sawyer, W.G. Friction coefficient of soft contact lenses: Measurements and modeling. *Tribol. Lett.* **2005**, *18*, 499–504.
35. Yarimitsu, S.; Nakashima, K.; Sawae, Y.; Murakami, T. Influences of lubricant composition on forming boundary film composed of synovia constituents. *Tribol. Int.* **2009**, *42*, 1615–1623.
36. Khan, I.M.; Francis, L.; Theobald, P.S.; Perni, S.; Young, R.D.; Prokopovich, P.; Conlan, R.S.; Archer, C.W. In vitro growth factor-induced bio engineering of mature articular cartilage. *Biomaterials* **2013**, *34*, 1478–1487.
37. Anat, J. The Function of Intra-Articular Fibrocartilages, with Special Reference to the Knee and Inferior Radio-Ulnar Joints. *J. Anat.* **1932**, *66*, 210–227.
38. Teeple, E.; Elsaid, K.A.; Fleming, B.C.; Jay, G.D.; Aslani, K.; Crisco, J.J.; Mechrefe, A.P. Coefficients of friction, lubricin, and cartilage damage in the anterior cruciate ligament-deficient guinea pig knee. *Journal of Orthopaedic Research* **2008**, *26*, 231-237.
39. Hills, B.A. Oligolamellar lubrication of joints by surface active phospholipid. *J. Rheumatol.* **1989**, *16*, 82–91.
40. Radin, E.L.; Swann, D.A.; Weisser, P.A. Separation of a Hyaluronate-free Lubricating Fraction from Synovial Fluid. *Nature* **1970**, *228*, 377–378.
41. Swann, D.A.; Bloch, K.J.; Swindell, D.; Shore, E. The lubricating activity of human synovial fluids. *Arthr. Rheum.* **1984**, *27*, 552–556.
42. McCutchen, C.W. The frictional properties of animal joints. *Wear* **1962**, *5*, 1–17.
43. McCutchen, C.W. Mechanism of Animal Joints: Sponge-hydrostatic and Weeping Bearings. *Nature* **1959**, *184*, 1284–1285.
44. Ikeuchi, K. Origin and future of hydration lubrication. *Proc. Inst. Mech. Eng. J. Eng. Tribol.* **2007**, *221*, 301–305.
45. Klein, J. Hydration lubrication. *Friction* **2013**, *1*, 1–23.
46. Murakami, T.; Higaki, H.; Sawae, Y.; Ohtsuki, N.; Moriyama, S.; Nakanishi, Y. Adaptive multimode lubrication in natural synovial joints and artificial joints. *Proc. Inst. Mech. Eng. Part H J. Eng. Med.* **2006**, *212*, 23–35.
47. Murakami, T. Importance of adaptive multimode lubrication mechanism in natural and artificial joints. *Proc. Inst. Mech. Eng. J. Eng. Tribol.* **2012**, *226*, 827–837.
48. Murakami, T.; Yarimitsu, S.; Sakai, N.; Nakashima, K.; Yamaguchi, T.; Sawae, Y. Importance of adaptive multimode lubrication mechanism in natural synovial joints. *Tribol. Int.* **2017**, *113*, 306–315.

49. Forsey, R.W.; Fisher, J.; Thompson, J.; Stone, M.H.; Bell, C.; Ingham, E. The effect of hyaluronic acid and phospholipid based lubricants on friction within a human cartilage damage model. *Biomaterials* **2006**, *27*, 4581–4590.
50. Wu, T.; Gan, X.-Q.; Cai, Z.-B.; Zhu, M.-H.; Qiao, M.-T.; Yu, H.-Y. The lubrication effect of hyaluronic acid and chondroitin sulfate on the natural temporomandibular cartilage under torsional fretting wear. *Lubr. Sci.* **2015**, *27*, 29–44.
51. Merkher, Y.; Sivan, S.; Etsion, I.; Maroudas, A.; Halperin, G.; Yosef, A. A rational human joint friction test using a human cartilage-on-cartilage arrangement. *Tribol. Lett.* **2006**, *22*, 29–36.
52. Caligaris, M.; Ateshian, G.A. Effects of sustained interstitial fluid pressurization under migrating contact area, and boundary lubrication by synovial fluid, on cartilage friction. *Osteoarthr. Cartil.* **2008**, *16*, 1220–1227.
53. Cilingir, A.C. Effect of rotational and sliding motions on friction and degeneration of articular cartilage under dry and wet friction. *J. Bionic Eng.* **2015**, *12*, 464–472.
54. Li, F.; Wang, A.; Wang, C. Analysis of friction between articular cartilage and polyvinyl alcohol hydrogel artificial cartilage. *J. Mater. Sci. Mater. Med.* **2016**, *27*, 87.
55. Furmann, D.; Nečas, D.; Rebenda, D.; Čípek, P.; Vrbka, M.; Křupka, I.; Hartl, M. The Effect of Synovial Fluid Composition, Speed and Load on Frictional Behaviour of Articular Cartilage. *Materials* **2020**, *13*, 1334–1350.
56. Stachowiak, G.W.; Batchelor, A.W.; Griffiths, L.J. Friction and wear changes in synovial joints. *Wear* **1994**, *171*, 135–142.
57. McCann, L.; Udofia, I.; Graindorge, S.; Ingham, E.; Jin, Z.; Fisher, J. Tribological testing of articular cartilage of the medial compartment of the knee using a friction simulator. *Tribol. Int.* **2008**, *41*, 1126–1133.
58. Katta, J.; Jin, Z.; Ingham, E.; Fisher, J. Effect of nominal stress on the long term friction, deformation and wear of native and glycosaminoglycan deficient articular cartilage. *Osteoarthr. Cartil.* **2009**, *17*, 662–668.
59. Chan, S.M.T.; Neu, C.P.; Komvopoulos, K.; Reddi, A.H. The role of lubricant entrapment at biological interfaces: Reduction of friction and adhesion in articular cartilage. *J. Biomech.* **2011**, *44*, 2015–2020.
60. Moore, A.C.; Burris, D.L. New Insights Into Joint Lubrication. *Tribol. Lubr. Technol.* **2016**, *72*, 26–30.
61. Čípek, P.; Rebenda, D.; Nečas, D.; Vrbka, M.; Křupka, I.; Hartl, M. Visualization of Lubrication Film in Model of Synovial Joint. *Tribol. Ind.* **2019**, *41*, 387–393.
62. Development of reciprocating tribometer for testing synovial joint. In Proceedings of the Engineering Mechanics, Svratka, Czech Republic, 2018; pp. 169–172.
63. Lakowicz, J.R. *Principles of Fluorescence Spectroscopy*, 3rd ed.; Springer: New York, 2006; ISBN 978-0387-31278-1.
64. Northwood, E.; Fisher, J. A multi-directional in vitro investigation into friction, damage and wear of innovative chondroplasty materials against articular cartilage. *Clin. Biomech.* **2007**, *22*, 834–842.
65. Pickard, J.E.; Fisher, J.; Ingham, E.; Egan, J. Investigation into the effects of proteins and lipids on the frictional properties of articular cartilage. *Biomaterials* **1998**, *19*, 1807–1812.
66. Hodge, W.A.; Fijan, R.S.; Carlson, K.L.; Burgess, R.G.; Harris, W.H.; Mann, R.W. Contact pressures in the human hip joint measured in vivo. *Proc. Natl. Acad. Sci. USA* **1986**, *83*, 2879–2883.
67. Mow, V.C.; Kuei, S.C.; Lai, W.M.; Armstrong, C.G. Biphasic Creep and Stress Relaxation of Articular Cartilage in Compression: Theory and Experiments. *J. Biomech. Eng.* **1980**, *102*, 73–84.
68. Vala, H.J.; Baxi, A. A review on Otsu image segmentation algorithm. *Int. J. Adv. Res. Comput. Eng. Technol.* **2013**, *2*, 387–389.
69. Acharya, T.; Ray, A.K. *Image Processing: Principles and Applications*; John Wiley: Hoboken, NJ, 2005; ISBN 978-0-471-71998-4.
70. Vincent, L. Morphological Area Openings and Closings for Grey-scale Images. In *Shape in Picture*; Springer: Berlin/Heidelberg, Germany, 1994; pp. 197–208. ISBN 978–3-642-08188-0.
71. Greene, G.W.; Zappone, B.; Zhao, B.; Söderman, O.; Topgaard, D.; Rata, G.; Israelachvili, J.N. Changes in pore morphology and fluid transport in compressed articular cartilage and the implications for joint lubrication. *Biomaterials* **2008**, *29*, 4455–4462.
72. McNary, S.M.; Athanasiou, K.A.; Reddi, A.H. Engineering Lubrication in Articular Cartilage. *Tissue Eng. Part B Rev.* **2012**, *18*, 88–100.
73. Chan, S.M.T.; Neu, C.P.; DuRaine, G.; Komvopoulos, K.; Reddi, A.H. Tribological altruism: A sacrificial layer mechanism of synovial joint lubrication in articular cartilage. *J. Biomech.* **2012**, *45*, 2426–2431.

74. Chan, S.M.T.; Neu, C.P.; DuRaine, G.; Komvopoulos, K.; Reddi, A.H. Atomic force microscope investigation of the boundary-lubricant layer in articular cartilage. *Osteoarth. Cartil.* **2010**, *18*, 956–963.
75. Karran, E.H.; Young, T.J.; Markwell, R.E.; Harper, G.P. In vivo model of cartilage degradation—Effects of a matrix metalloproteinase inhibitor. *Ann. Rheum. Diseases* **1995**, *54*, 662–669.
76. Ramsey, D.K.; Wretenberg, P.F. Biomechanics of the knee: Methodological considerations in the in vivo kinematic analysis of the tibiofemoral and patellofemoral joint. *Clin. Biomech.* **1999**, *14*, 595–611.
77. Sahara, W.; Sugamoto, K.; Murai, M.; Tanaka, H.; Yoshikawa, H. 3D kinematic analysis of the acromioclavicular joint during arm abduction using vertically open MRI. *J. Orthop. Res.* **2006**, *24*, 1823–1831.

Engineering Science and Technology, an International Journal 34 (2022) 101090

HOSTED BY

Contents lists available at ScienceDirect

Engineering Science and Technology, an International Journal

journal homepage: www.elsevier.com/locate/jestch

Biotribology of synovial cartilage: Role of albumin in adsorbed film formation

Pavel Čípek *, Martin Vrbka, David Rebenda, David Nečas, Ivan Křupka

Department of Tribology, Faculty of Mechanical Engineering, Brno University of Technology, Technická 2896/2, Brno 616 69, Czech Republic

ARTICLE INFO

Article history:
Received 9 June 2021
Revised 30 November 2021
Accepted 23 December 2021

Keywords:
Biotribology
Cartilage
Reciprocating tribometer
Friction
Lubrication
Fluorescence microscopy

ABSTRACT

A properly lubricated natural synovial joint is the basis of the proper function of the natural musculoskeletal system to lead an active and painless life. A properly lubricated natural synovial joint is the basis of the proper function of the natural movement system to lead an active and painless life. Well lubricated synovial joints are expressed, in particular, by an extremely low coefficient of friction and wear between cartilage surfaces. The presented manuscript is focused on the impact of albumin protein on the formation of adsorbed boundary layer in the contact of cartilage – a simplified model of synovial joint. This can contribute to better understanding of the lubrication in synovial joints. All presented experimental tasks were performed using a reciprocating tribometer along with fluorescence microscopy – friction forces were measured simultaneously with fluorescence records of contact. This unique experimental approach used a newly designed evaluating procedure based on image processing. The experimental results show a great impact of hyaluronic acid; adding of hyaluronic acid leads to a reduction in friction and a larger area of albumin adsorbed boundary layer; however, the phospholipids show the opposite effect. A combination of the individual protein solutions, albumin and γ-globulin, has no significant effect on the particles count of albumin clusters adsorbed in the contact; however, the area of albumin adsorbed boundary layer with simple albumin solution was much larger than the solution combining both proteins. The conclusions and discussion of this study describe the role of albumin protein in the lubricating process prevailing in a simplified model of synovial joint under conditions corresponding to slow human gait.

1. Introduction

The comfortable and active human life needs a proper functioning of the musculoskeletal system; however, despite a high level of current state of healthcare, we suffer from a number of joint diseases [1]. The progression of joint diseases may vary depending on many factors and can reach the state when the joint is incurable. So far, the most common solution for the incurable natural joint is its removal and replacement by an artificial one [2]. Although the advanced joint prosthesis has a long lifetime, sometimes it has to be replaced repeatedly. A reoperation of the prosthesis is a considerable burden for the human body. It has the impact on bone degradation, mental health of patients, etc. [3–5]. This is enormously stressful for people who prefer an active life but are afraid of reoperation; therefore, the general effort is to postpone the necessity of operation of prosthetics as long as possible.

One of more contemporary ways of how to treat or, at least, delay or stabilize the disease of the natural joints which are not completely destroyed, is a non-invasive treatment (the intervention does not require surgery) using viscosuplementation (supplement – a gel-like fluid consisting mostly of hyaluronic acid (HA) is injected into the joint gap) [6]. Due to the limited lifetime of the prosthesis, the common endeavor of viscosuplementation is to defer the urgency of operation of prosthetics as long as possible. The supplements should restart the lubrication processes in degraded natural joints, which ideally stops future damaging of joints or, at least, slows down the process of degradation of natural joints (natural cartilage) [6,7]. The supplement therapy is usually effective, but the same therapeutic effect is not guaranteed for all patients, and how exactly the supplement works has not yet been proven [8–10]. To better understand this issue, the full principle of lubrication in natural synovial joints needs to be described, i.e., it is necessary to describe the adsorbed boundary layer formation in

* Corresponding author.
E-mail address: Pavel.Cipek@vut.cz (P. Čípek).
Peer review under responsibility of Karabuk University.

https://doi.org/10.1016/j.jestch.2021.101090
2215-0986/

the contact realized by the articular cartilage and lubricated by synovial fluid (SF) [11].

The basis of the unique tribological and mechanical properties of natural synovial joints is the contact of two bones, whose surfaces are covered by the articular cartilage, and the lubrication is realized by SF [12]. Due to the specific mechanical and tribological properties of cartilage, the contact pressure is dispersed over a large area on the surface of cartilage where the SF ensures a very low friction coefficient (CoF) [13]. An alternative to a natural cartilage is a hydrogel, which represents an artificial model of cartilage with similar tribological properties [14]. Most of natural cartilage tissue consists of water and of type II collagen fibres as a matrix, HA, and lubricin [12,15]. The tissue of a fabric structure is filled with water and its thickness is divided into three zones, varying especially in orientation, shape, and amount of collagen fibres [12,16]. The cartilage tissue is characterized by low cell density; therefore, the tissue of cartilage is nourished through the SF [17]. The SF is mainly formed by proteins, HA, phospholipids and proteoglycans [18–20]. Based on the study [20], the albumin protein is the most abundant in the SF. The porous cartilage structure contains negatively charged components which provide the attraction and detention of water (SF) to the pores [21]. The lubrication system in natural synovial joints works on the principle of porous structure and absorption of water, on which is based the synovial joints lubrication system. There are many theories which seek to explain this principle, but so far there is no work that would give a comprehensive overview of the lubrication function in the synovial joint.

The research focused on tribology of cartilage can be divided into two main groups. The first one is focused on cartilage lubrication and the other one describes the friction performance of cartilage. The main discussed topic in the lubrication studies is the lubrication regime, where there are several theories attempting to explain the lubrication mechanism including hydrodynamic lubrication [22], boundary lubrication [23,24], weeping lubrication [25,24], and boosted lubrication [26]. Some studies published in later years show more advanced lubrication theories or present new theories of lubrication mechanisms – hydration lubrication [27], and adaptive multimode [28,29]. Although the studies on visualization are less common, the published ones mostly describe the use of hydrogel instead of cartilage. These studies seek to support and verify the mentioned theories, and the authors try to classify the influence of individual components of SF. The γ-globulin protein was shown as a significant component in the lubrication process of hydrogel; nevertheless, a degree of influence depends on the γ-globulin protein concentration and the concentrations of remaining components of the lubricant [30]. The gel–like layer on the surface of cartilage is also essential for lubrication processes, because it can protect the surface from wear. HA is the main component of gel-like layer. This layer is formed on the cartilage surface due to bonding of HA with chondrocytes contained in the structure of cartilage [31]. The thickness and composition of gel-like layers depend on the size of individual molecules and the pore sizes. Large molecules cling to the surface of cartilage and the cartilage structure is penetrated only by smaller particles. [32]. All presented studies reflect the fluid leakage from the cartilage structure, which is the basis of all theories.

Another topic discussed by the researchers is focused on the friction properties of cartilage. The "friction" issues of cartilage are better understood due to a simpler but more developed methodology related to the experiments and evaluation of data. These "friction" studies indicate the understanding of cartilage behaviour due to friction. They deal with the behaviour of cartilage contact lubricated by SF and indicate very good friction properties [33,34,35], which is expressed by very low CoF. The positive impact of friction (lower CoF) may be expressed by a larger volume of HA in SF [34], rehydration [36], higher load [33,37,36]. There is the dependence between the level of CoF and the type of movement [37]. The change of the sampling point on the cartilage surface has a significant impact on CoF; this depends on the mechanical properties of cartilage samples [38]. The general CoF trend has a growing character [33,34,37].

As is obvious, many studies are focused only on friction of cartilage contacts while the studies dealing with visualization are less common. Moreover, there are no studies connecting these two issues into one experimental task; i.e., the experimental device and methodology, which allow for simultaneous measurement of friction forces and visualization of cartilage contact (a simplified model of synovial joint). Some authors used a fluorescence microscopy for visualization of cartilage or hydrogel contacts, from which it follows that this method is the most appropriate for the visualization of compliant (cartilage) contacts on non-reflective surfaces. Studies dealing with visualization of cartilage contact are not frequent and the link with measurement of frictional forces is missing. The present study supplements the relationship between the cartilage visualization and friction measurement in the simplified model of synovial joint; therefore, a better description of cartilage lubrication processes will be replenishing, which can help to better understand the cartilage lubricating processes. The previous study [39] presents the methodology for the evaluation of simultaneous visualization of cartilage contact together with friction measurement. This study is a follow-up one and extends the research dealing with the experimental task focused on the behaviour of albumin protein in the formation of adsorbed boundary layer in the cartilage contact and the methodology presented in [39] is used. This study aims to clarify the link between the influence of albumin protein (as the protein with the highest concentration in SF [20]) in the formation of adsorbed boundary layer and the change of CoF trends. An explanation of the lubricating processes and the adsorbed boundary layer formation in the synovial joint contact can contribute to understanding of viscosupplements function and ensuring the right effect on all patients.

2. Materials and methods

2.1. Experimental device

A pin-on-plate tribometer of a unique own design was used as described in detail in [39–41]. The basis of the experimental device (schema is shown in Fig. 1A) is a cartilage sample in contact with a reciprocating glass plate (material B270). The contact is loaded using a lever through the cartilage sample and this is placed under the glass plate. The optical system is located above the contact and the observation record is obtained by camera. The contact is flooded with lubricant – in this case, the SF model. The lubricating bath is heated to the human body temperature (37C) by temperature controller Hotset C448 together with heating cartridges. These are placed under the bath and the temperature sensor is placed as close to the lubricant as possible. This arrangement prevents the lubricant from overheating (overheating of lubricant would cause rapid degradation of used components). A rigid frame of tribometer is the basis of the whole device and, together with the ball screw, allows for the reciprocating motion without clearance. The loading mechanism is based on the principle of a lever mounted on two preloaded bearings. The loading lever is equipped with a deformation member allowing for a minimum deformation in the loading direction and a high deformation in the friction direction, which permits the measurement of very low friction forces. Both forces (normal and friction) are measured by tensometric sensors. The reciprocating motion and loading are ensured by the stepper motors - rotational in the reciprocation case, and linear in the other

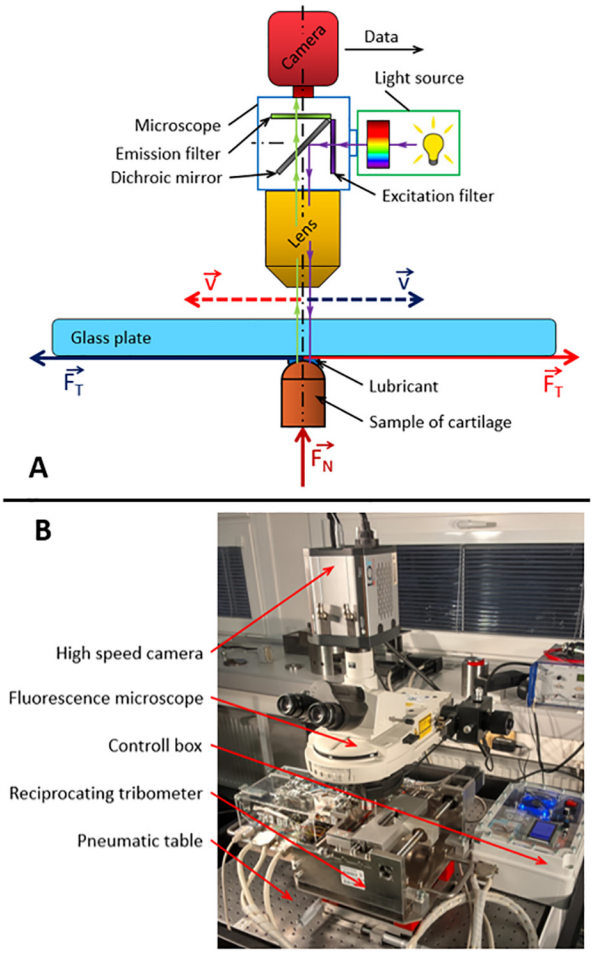

Fig. 1. Experimental apparatus. (A) schema of experimental apparatus, (B) experimental apparatus in laboratory.

case. The reciprocating tribometer is placed on the pneumatically balanced table, where the fluorescence microscope is also anchored. The entire experimental device is shown in Fig. 1B. The outputs of each experiment are the record of contact area and the friction and load forces trends.

2.2. Fluorescence microscopy

The fluorescence microscopy was used as an optical (observation) method for the experiments presented in this study. The basis of this method is a light emission of a substance excited by radiation. The fluorescence principle can be divided into three steps. First, it is excitation, when the excitation photon is absorbed by the fluorophore contained in the fluorescent dye. It is followed by the excitation state period; the absorbed energy is dissipated to ensure the emission of fluorescence. The last step is emission – the dye emits radiation; however, the level of energy is lower due to dissipation of energy in the excitation state period, which is the reason why the emitted radiation has a longer wavelength. A detailed description of fluorescence principle is shown in [42]. The mercury lamp allowing for the emission of a white light was used as a light source. The FITC and TRITC filters placed behind the mercury lamp were used to achieve the required wavelength of emitted and excited light for the dyes. The FITC filter has an excitation wavelength of 490 nm and the emission wavelength of 525 nm, the TRITC filter has an excitation wavelength of 557 nm and the emission wavelength of 576 nm. The optical method and the fluorescence microscope were described in detail in previous studies, where the methodology of visualization of joint replacement for different material combinations was published [43,42]. The visualization (recording of the contact area) is performed through the glass plate, the material of which ensures that the excitation and emission of the contact are not affected. The schema of the optical system is shown in Fig. 1A.

2.3. Specimens and lubricants

The femoral hip heads of mature pigs were utilized for samples removal. The area with the highest contact pressure on the surface of femoral head of hip joint was defined as a sampling area; this definition provides the most mechanical properties of cartilage sample. Due to a compliance of the same placement of removed samples (for all removed bones), the deviation between all samples was minimized, and the mechanical properties were comparable. The samples were removed by the ejector with internal diameter of 9.7 mm. The sampling was performed without delay after the slaughter of the animal. The samples were inspected after sampling with a focus on the preservation of the cartilage surface and on the cartilage edges damage (not to be frayed) to avoid influencing the experiments. The samples were deep frozen (−20 ℃) in phosphate buffered saline (PBS) immediately after sampling. Samples were defrosted immediately before the experiments to avoid degradation. Defrosting of cartilage samples was performed without heating at laboratory temperature, after that the sample is removed from the test tube and placed to the tribometer and flooded by lubricant. The same sampling process was verified in [44]. The sampling process used in this study is shown in Fig. 2. Due to the variability of cartilage samples, the samples were preselected before the experiments. The used cartilage sample was selected using a strict laboratory protocol. The second sample from the contact pair was the glass plate, which fulfils the important premise of transparency in order to observe the contact. The glass plate is 154 mm long, 43 mm wide, and 4 mm thick.

The model of physiological SF and its partial solutions were used as an experimental lubricant. The composition of synovial fluid was inspired by the native synovial fluid. The analysis of native synovial fluid was performed in [20] and the used composition of lubricants was inspired by this article. The variation and composition of all experimental lubricants are shown in Table 1. As is obvious from Table 1, the most represented component of synovial fluid is the albumin protein. Due to this fact, the albumin protein was defined as one of the most important components of synovial fluid; therefore, this article is focused on visualization and behaviour of albumin protein - the albumin protein was examined across all experiments. A bovine serum (BS) albumin (Sigma-Aldrich, A7030) was labelled by Rhodamine B isothiocyanate (283924, Sigma-Aldrich) in this case. The magnetic stirrer was used to stir the other components without dye with the labelled component. The other component of the experimental solutions was γ-globulin from bovine blood (Sigma-Aldrich, G5009), HA = Sodium Hyaluronate HySilk (powder, quality class-cosmetic; molecular weight = 820–1020 kDa, Contipro, Dolní Dobrouč, Czech Republic) and phospholipids = L - α - Phosphatidylcholine (powder, Type XVI-E, lyophilized powder; ≥ 99%; vesicles form; P3556, Sigma-Aldrich, St. Louis, MO, USA). The final solution was prepared by mixing all components with PBS solution. Solutions were mixed using a magnetic stirrer at a maintained laboratory temperature – without heating. The mixing process performs without air access (to avoid degradation) – the laboratory vessel is covered with a nontoxic parafilm foil. The process takes approximately 2 h, until all lubricant components are complete dispersion. The prepared protein solutions were kept in a deep-frozen state (−20 ℃) in opaque and darkened test tubes to prevent degradation and ordination

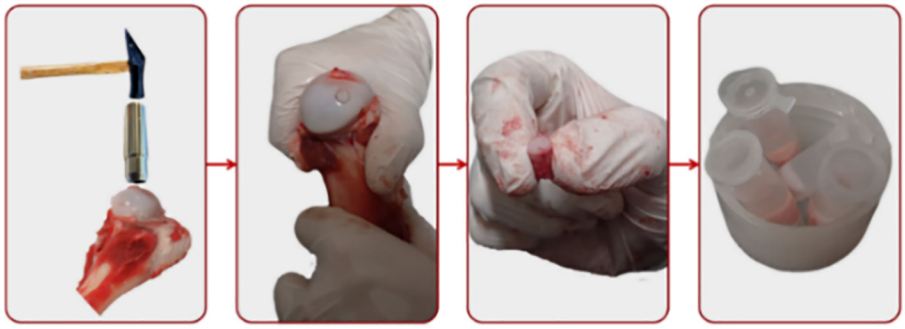

Fig. 2. Sampling process.

Table 1
Lubricants composition, labelled component - albumin.

Lubricant label	Albumin (mg/ml)	γ-globulin (mg/ml)	HA (mg/ml)	Phospholipids (mg/ml)
Lubricant 1	20	–	–	–
Lubricant 2	20	3.6	–	–
Lubricant 3	20	3.6	2.5	–
Lubricant 4	20	3.6	2.5	0.15

of lubricants. Defrosting was performed immediately before the experiments.

2.4. Methodology and conditions

The performed experiments followed a strictly defined procedure for preventing the undesired errors in the results and to help a sufficient repeatability of results. The established procedure of each experiment was described in detail in previous works [41,39]. The same experimental conditions were used for all performed experiments to make the results comparable, see Table 2. The conditions laid down are based on the presented studies in this field regarding the prevailing conditions in the natural synovial joint [45,46]. The load was set at 10 N, which corresponds approximately to 0.8 MPa of contact pressure and 10 mm/s of sliding speed. These conditions correspond to a very slow human gait and average joint pressure [45,46], which is a joint regime corresponding to a large part of human joint life. The experimental temperature was maintained at 37C. A similar condition was used for experiments in previously published studies; it allows to compare the results between this study and the studies that have already been published [34, [36]. Each experiment, i.e., the experiment with one type of lubricant, was carried out 9 times (3 experiments, where one experiment counts 3 repetitive experiments with an in - between hydration cycle, together with 9 individual experiments). The schema of one set of experiments is shown in Fig. 3. The selected count of experimental tasks allows to determine the repeatability of the experiments and the impact of rehydration. All experiments were performed on one sample so that the results of the individual experimental sections can be compared; especially, the recordings of the contact area. To ensure the same state of the cartilage sample before each experimental set, the run – in a cycle was carried out before each set of experiments, which helps to bring the cartilage structure and surface to the same state before each experimental section.

Output procedures are described in detail in the previous work [39]. The process to evaluate the results is shown in Fig. 4. As is obvious, the evaluation process is divided into two parts – CoF processing (Fig. 4A – C) and processing of the record of contact area snaps (Fig. 4D – G), which finally shows the dependency between friction and lubrication. The raw main data output from each experiment are friction forces measured in the contact and the record of the contact area through the fluorescence microscope. This data was further processed. The friction trend is transformed to CoF and is fitted by the straight line. The tangent slope is determined for each CoF trend and it is the evaluation value for the connection with lubrication.

The record of the contact area from each experiment whose output are the snaps, is an input for the processing by the specially designed software described in detail in [39]. This software is based on the principle of image segmentation, allowing for the removal of the background and highlighting particles that have an order of magnitude higher intensity. This processing ensures that only the marked particles to be monitored are left in the snap. The software calculates the particle count and the average size of particles in each snap. These values are determined for all snaps; therefore, the particle count trend was defined for each experiment. This trend is fitted by a straight line and the tangent slope was determined, whereby it is expressed as the relative difference of particle count and it is the output evaluation value from visualization, the second evaluation parameter.

The culmination of the evaluation process is the linking of both relative differences which form the final output from each experiment – dependency between the particle count and CoF. Both differences are relative to allow for a comparison between both output parameters and also between all performed experiments. The final CoF and the particle count dependency allows to determine the impact of the individual compositions of the lubricant on the lubrication process.

Table 2
Experimental conditions.

Load	Velocity	Stroke	Number of cycles	Duration	T
10 N	10 mm/s	20 mm	25	2 min	37 C

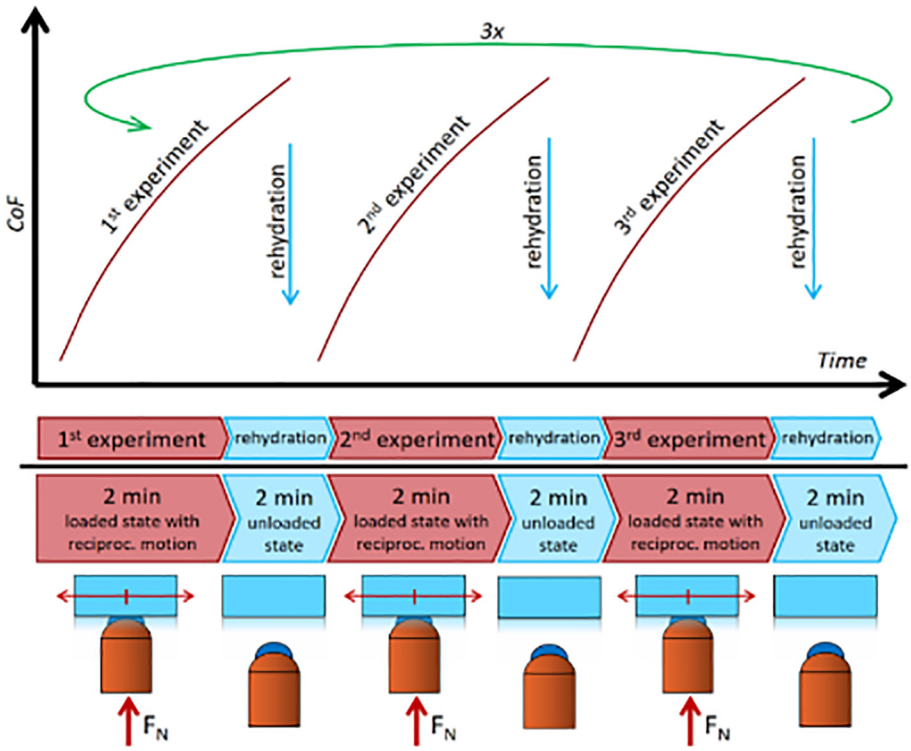

Fig. 3. Schema of each experimental set.

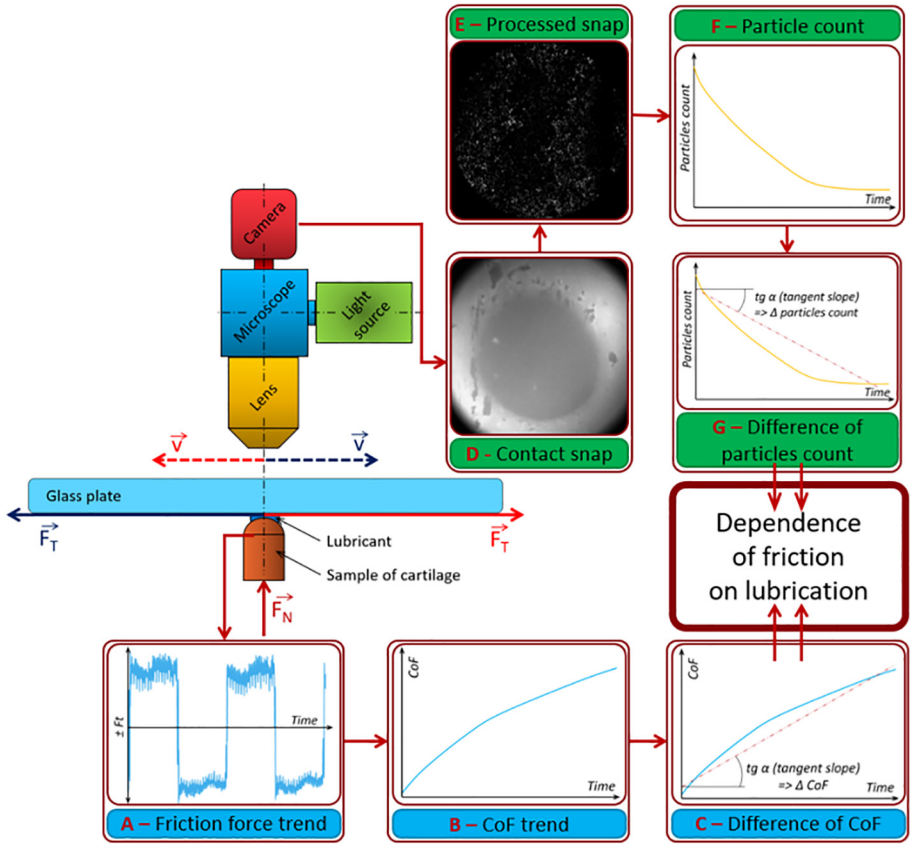

Fig. 4. Evaluation schema.

3. Results

3.1. The toolbar and its menus

Four sets of experimental tasks were carried out and each set was performed with one modification of lubricant (lubricant 1 – 4, see Table 1). Each lubricant was used for 3 replicate measurements consisting of 3 consecutive measurements with rehydration between each experiment, 9 individual experimental tasks in total (see Fig. 3). The friction trends for all modifications of lubricant are shown in Fig. 5. One curve in this graph represents 3 averaged measurements, and each type of curves represents one set of experiment (1,2,3) with in–between rehydration (see Fig. 3). The lowest fiction is reported by lubricant 3, although it is not the complex SF. However, the lubricant 4 (complex SF model - adding of phospholipids to the lubricant unlike a lubricant 3) causes deterioration of friction properties; nevertheless, this lubricant reports a lower CoF than lubricants 1 and 2, which represent the proteins solutions (lubricant 1 – simple albumin and lubricant 2 - albumin + γ-globulin solution). The worst CoF is reported by lubricant 1 – simple albumin solution. The rehydration has an expected impact on CoF trend, the CoF value is restarted after each rehydration.

3.2. Visualization of contact

The albumin protein was labelled with all modifications of the lubricant (see Table 1); therefore, all records of the contact area show only albumin dependencies. Snaps were processed by the evaluation software [39] and correspond to one value of CoF; consequently, each snap shows the count of albumin protein clusters and their average size. The evaluation software was calibrated by comparing the trend (tangent slope) of emission intensity (raw output from the experiment – measured by a fluorescent microscope) and the trend (tangent slope) of particle count [39]. The sensitivity of the calibration process to the setting of input parameters is analysed in chapter 4.3. The examples of processed snaps (the protein clusters are highlighted) are shown in Fig. 6; they were taken with lubricant 3 (albumin + γ-globulin + HA – measuring number 5/9). Fig. 6A shows the beginning of the experiment (particles – protein clusters, nearly 1600 clusters of albumin proteins), Fig. 6B represents the state in time t = 25 s (the particle count has increased, nearly 1700 clusters of albumin proteins) and the last

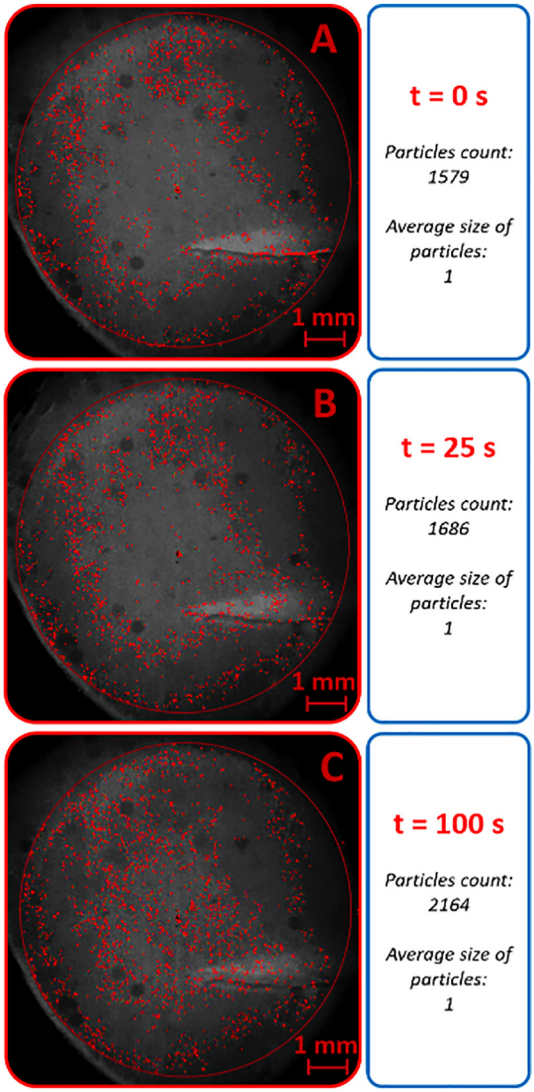

Fig. 6. Snaps of contact area of cartilage – highlighted protein clusters. Experiment with lubricant 3 (albumin + γ-globulin + HA). (A) the start of the experiment – time 0 s, (B) time 25 s, (C) the end of experiment –time 100 s.

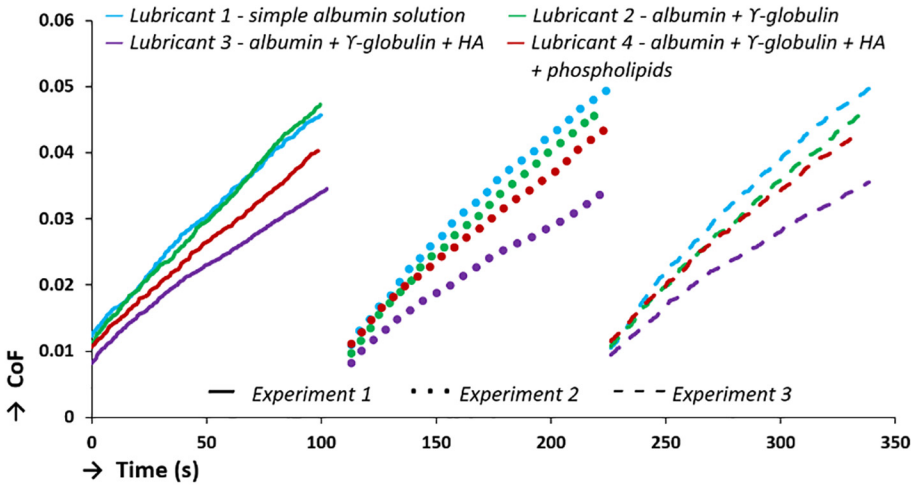

Fig. 5. CoF trends - comparison of all experiments.

snap (Fig. 6C) represents the state at the end of the experiment (the count of protein cluster is the largest, nearly 2200 clusters of albumin proteins). Each of these values belong to one snap. The average size of the detected particles does not change during this experiment. The increase in the particle count is clear from Fig. 6 (the difference between Fig. 6A and Fig. 6B).

The output of evaluation software was determined for each snap in each experimental task so that the particle count trend for each experimental task can be depicted – see Fig. 7. As with CoF trends, one curve in this graph represents 3 averaged measurements, and each type of curve represents one set of experiment (1,2,3) with an in - between rehydration (see Fig. 3). The trends representing protein solutions (lubricant 1 and lubricant 2) show a lower total count of albumin protein clusters than the more complex modification of lubricant 3 and complex SF model – lubricant 4. The trends of lubricant 1 and lubricant 2 mostly show a declining character; however, trends representing more complex modifications of lubricants (lubricant 3 and lubricant 4) show a rising trend of particle count of albumin clusters. Lubricant 3 and lubricant 4 (representing a more complex SF model) show a higher total count of albumin protein clusters than simpler modifications of lubricants (lubricant 1 and lubricant 2). The largest count of albumin protein clusters is shown by lubricant 3 (partial SF – albumin + γ -globulin + HA), although the complex SF model (lubricant 4) reports lower values of protein cluster count.

The particle count does not always have to be an authoritative benchmark for evaluation, quality and quantification of the adsorbed boundary layer; nevertheless, the area of adsorbed boundary layer formed by the labelled component of the lubricant (in this case by albumin protein) has a higher strength of value. The area of the adsorbed boundary layer in the contact is calculated by the multiplication of the particle count and the average size of particles in the contact and is then specified in pixel units. Trends of the albumin adsorbed boundary layer area are shown in Fig. 8. As with CoF trends, one curve in this graph represents 3 averaged measurements, and each type of curve represents one set of experiments (1,2,3) with an in - between rehydration (see Fig. 3). Lubricant 3 (partial SF - albumin + γ-globulin + HA) shows the largest area of the adsorbed boundary layer, although it is not a complex SF model which reports the adsorbed boundary layer mostly with the smallest area. The albumin solution (lubricant 1) shows only a slight reduction in the area of the adsorbed boundary layer. Lubricant 2 (albumin + γ-globulin solution) shows slightly higher values in the area of the adsorbed boundary layer. The adsorbed boundary layer area is further used as an evaluation value for linking the friction in the cartilage contact and its lubrication.

3.3. Connection between friction and lubrication

This study joints two approaches to the evaluation of tribological properties of cartilage - friction evaluation and visualization of cartilage contact. The final output is shown in Fig. 9, where a dependency of friction on lubrication can be seen. The graph shows the impact of friction and also the impact of adsorbed boundary layer; nevertheless, the quality and quantity of adsorbed boundary layer is shown. The larger points in the graph represent the arithmetic mean from one set of measurements (3 individual measurements) and the smaller points represent all experiments carried out. The friction property is represented by *the arithmetic mean of CoF* (x–axis), and the lubrication impact is represented by *the albumin adsorbed boundary layer area* (y-axis). Lubrication is represented by the area of albumin adsorbed boundary layer (count of albumin protein clusters × average size of clusters), which is a representative value expressing formed adsorbed boundary layer. Four shapes can be seen in Fig. 9; each of them represents one lubricant. When the shape is moved closer to the left (closer to the y–axis), the lubricant reports better friction properties and when the shape is moved up (further from the x–axis), the labelled part of the lubricant reports better lubricating properties. The goal is to move the shape as close as possible to the y–axis and as far as possible from the x-axis - as shown by the dashed arrow. Therefore, the best lubricant is number 3 – it is moved further in the direction of the dashed arrow. This lubricant shows the best friction properties while the larger albumin adsorbed boundary layer is formed. Lubricant 4 (complex SF model) shows good tribological properties; however, the adsorbed boundary layer formed by albumin is smaller. Partial SFs (lubricant 1 and lubricant 2) show both inferior frictional and lubricating properties, although the lubricant 1 turns to be slightly better in the area of adsorbed boundary layer. The graph also suggests that the lubricant 3 forms the most stable adsorbed boundary layer because the area of its shape is the smallest; therefore, the measured points are closest to each other. On the contrary, the least stable adsorbed boundary layer is formed by simple albumin solution.

4. Discussion

4.1. Global discussion

A healthy natural synovial joint ensures painless human movement with the phenomenal low friction. The proper function of natural joints is based on the unique properties of cartilage tissue in connection with natural SF [12]. Unfortunately, many diseases

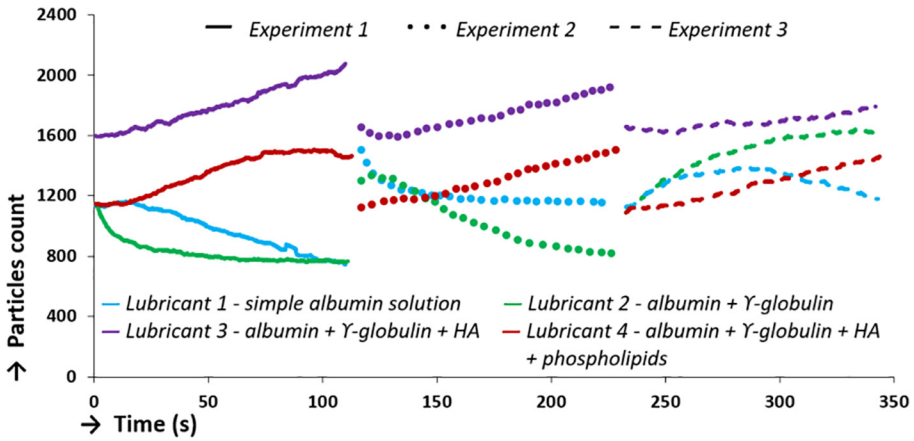

Fig. 7. Particles count trend - comparison of all experiments.

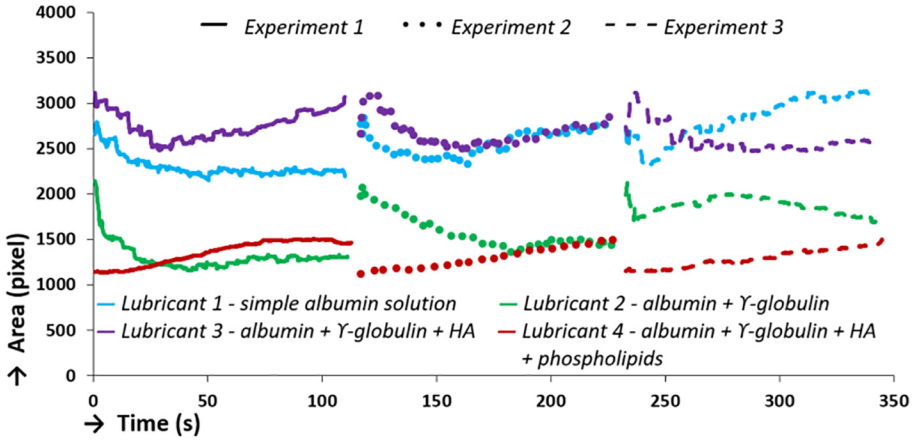

Fig. 8. Trend of adsorbed boundary layer area of albumin - comparison of all experiments.

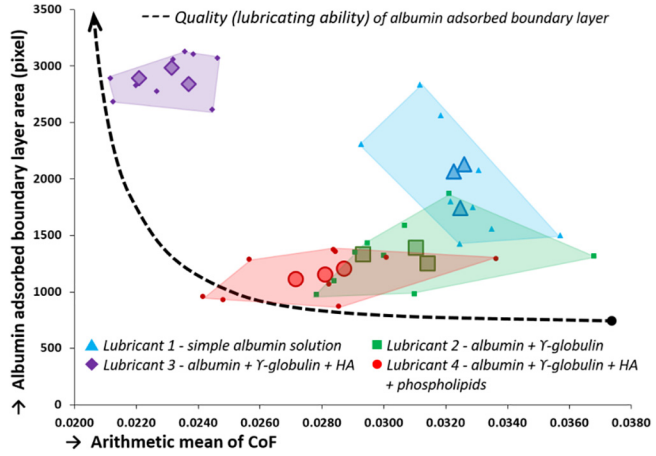

Fig. 9. Dependence of friction on lubrication - arithmetic mean of CoF represent impact of friction and albumin adsorbed boundary layer area represents impact of adsorbed boundary layer.

Table 3
Albumin impact on the lubrication process.

CoF		
Lubricant label deviation	Arithmetic mean	Standard deviation
Lubricant 1	0.0324	0.0016
Lubricant 2	0.0306	0.0025
Lubricant 3	0.0230	0.0012
Lubricant 4	0.0280	0.0027
Particles count in the contact		
Lubricant label	Arithmetic mean	Standard deviation
Lubricant 1	656	485
Lubricant 2	772	291
Lubricant 3	1908	138
Lubricant 4	1155	188
Lubrication film area		
Lubricant label	Arithmetic mean	Standard deviation
Lubricant 1	1980	471
Lubricant 2	1321	276
Lubricant 3	2907	183
Lubricant 4	1158	190

cause degradation and painfulness of joints [1]. The diseases affecting the joints can degrade up to the state when the human movement is not possible without pain. In this case, it is necessary to replace the degraded joint by the artificial one using surgery [2]. The artificial joints do not have an unlimited lifetime; the reoperation is possible but not indefinitely [3]. This is the reason why it is beneficial to postpone the necessity of surgery and stabilize the disease as early as possible. The explanation of cartilage lubricating system is exceedingly substantial for description of lubricating system in natural synovial joint; this knowledge helps to find effective drugs to cure in the best case or, at least, to stabilize or slowdown the disease of natural joints. This study deals with the adsorbed boundary layer formation in the simplified model of synovial joint and describe the role of albumin protein in the SF model.

The global impact of albumin on the lubricating process can be seen in Fig. 9; it is obvious from the shape size that the adsorbed boundary layer formed by the albumin protein is not stable when a simple protein solution is used as lubricant (lubricants 1 and 2). These lubricants show a high standard deviation (see Fig. 9 and Table 3); however, it drops when the lubricants are more complex (lubricants 3 and 4), which is also evident from the area size of individual shapes in Fig. 9. The complex SF model (lubricant 4) and lubricant 3 show lower values of average CoF than simple protein solutions representing lubricants 1 and 2. When the simple albumin solution was used (lubricant 1), the number of protein clusters is declining during the experiment (see in Fig. 7); nevertheless, the average size of its clusters is rising (see in Fig. 8), which causes a slightly increasing area of albumin adsorbed boundary layer in the contact. Simple albumin creates an adsorbed film on hydrophilic surfaces [47]. The cartilage tissue is of a porous structure, whose polarity attracts and absorbs water solutions [48]; therefore, the cartilage surface is suitable for albumin protein adsorption. One part of the lubricant flows through the contact, where the proteins adsorb on the cartilage surface and the other parts flow through the cartilage pores [49]. The albumin proteins create larger clusters when the pressure gradient is higher (in the centre of the contact). It is the reason why the protein clusters on the cartilage contact are smaller than in the case of artificial joints [42]. The increase in the size of albumin protein clusters, and thus also in the area of albumin film, causes, in our opinion, the CoF trend to grow faster and due to the average value of CoF, it is the highest (Fig. 5 and Table 3). The schema of adsorbed boundary layer formation in the case of lubrication by a simple albumin solution (lubricant 1) is shown in Fig. 10-A.

The second variant of the lubricant (lubricant 2) with an added γ–globulin component (see Table 1) shows lower values of CoF than lubricant 1 with albumin only. The particle count also always declines during the experiment (Fig. 7), but the decline is slightly steeper. However, this lubricant shows smaller protein clusters, which causes a lower area of albumin protein film in the contact (Fig. 8). The γ-globulin proteins are much larger than albumin proteins and bind with albumin, as Nečas published in [42]. The albu-

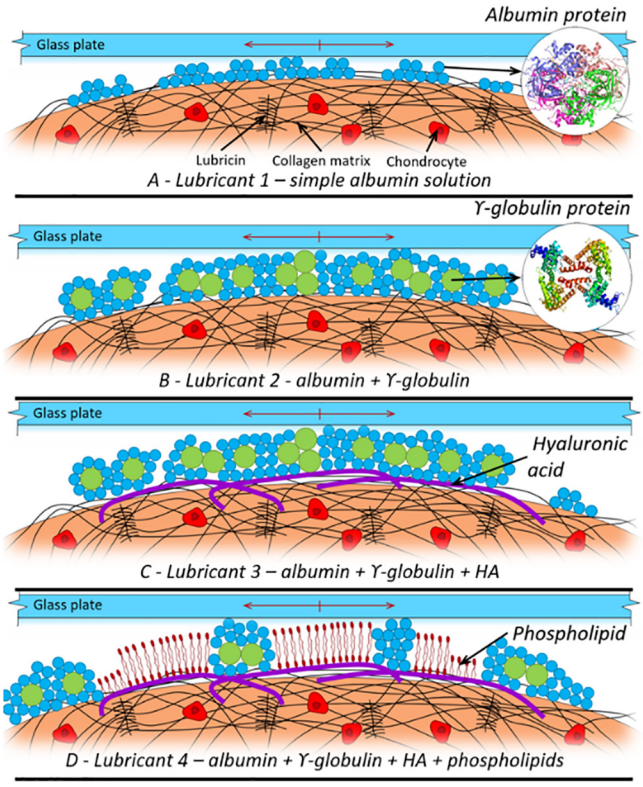

Fig. 10. Schema of adsorbed boundary layer formation. (A) lubricant 1, (B) lubricant 2, (C) lubricant 3, (D) lubricant 4.

min and γ-globulin are proteins characterized by a "string-like" structure. The albumin protein is predominantly characterised by α-helix structure and γ-globulin predominantly by β-sheet [50,51]. These proteins bond together due to their structure - "the string structure becomes entangled in itself" [42,50,51]; therefore, the albumin proteins can bind to the γ-globulin proteins and also the γ-globulin proteins can bond to each other. The adsorbed boundary layer is formed by the albumin cluster, which is divided by γ–globulins; therefore, the cluster formed by albumin is smaller (see Fig. 10-B), where the schema of adsorbed boundary layer formed by lubricant 2 is shown. In our opinion, the combination of albumin clusters and larger γ–globulins causes a greater thickness of the adsorbed boundary layer, leading to lower values of CoF. This deduction is supported also by [35], where the simple γ-globulin shows lower values of CoF.

The lowest values of CoF are produced by lubricant 3, where HA was added. The HA plays an extremely important role in the lubricating system of cartilage [35,49,10] and forms the gel-like layer on the cartilage surface [29]. The surface layers formed by HA protect the cartilage surface against damage [32] and, due to strong hydrophilicity, create an attracting environment for albumin proteins, which adsorb on the surface with better and stronger hydrophilicity. The lubricant 3 (albumin + γ-globulin + HA) shows the best values of CoF (Fig. 5), but also the best values of the number of albumin clusters in the contact (Fig. 7) and the best area of the adsorbed boundary layer formed by albumin (Fig. 8). The number of albumin protein clusters increases during each experiment with lubricant 3; this indicates that the albumin clusters are trapped on the contact mode during experiments. The area of the albumin film formed in the contact decreases in all experiments, though it seems to increase slightly in the other section. The albumin protein clusters are better bonded to the hyaluronic surface layer, which causes a more appropriate fastening of albumin in the contact. The interaction with protein is most present in high molecular weight HA, which also forms the gel-like layer on the cartilage surface. The HA fraction with lower molecular weight penetrated the cartilage structure, in particular the collagen fibres contained in the cartilage structure [31,32,52]. The connection of constitution units of HA causes a firm grip of HA gel–like layer on the cartilage surface. The highest number of albumin clusters in the contact causes a higher thickness of adsorbed boundary layer; therefore, the hyaluronic protecting surface layer is not present in the contact with the raw cartilage surface on the glass plate. In our opinion, it is the reason of the rapid decline of CoF values. The schema of the adsorbed boundary layer provided by lubricant 3 is shown in Fig. 10-C. As is obvious from Fig. 8, the area of lubricant 3 shape is the smallest, i.e., the HA acts as a stabilizer of the adsorbed boundary layer to achieve the same quality of adsorbed boundary layer in each experiment.

The experiments with complex SF (lubricant 4) showed slightly higher values of CoF and lower values of adsorbed boundary layer area formed by albumin, protein, and particle count. In general, it seems that the complex SF has worse tribological properties than the partial complex SF (lubricant 3); nevertheless, the complex SF model is the only one which shows an increasing trend in the number of albumin protein clusters in the contact and an increasing trend of the area of albumin adsorbed boundary layer. This indicates the increasing amount of adsorbed boundary layer during the experiment, which provides a complete protection against cartilage wear. The phospholipids added to the lubricant bind to the HA surface layer on the cartilage. The phospholipids also interbond by lipid tails [27], which allows for the hydration lubrication. However, this is based on the lipid bilayer on each side of the contact, which assumes the same or, at least, similar hydrophilic surface on the other side of the contact. The experimental model used in our study allows for the visualization of the contact of the glass transparent plate; nevertheless, the glass does not meet the requirement for hydrophilicity of surface. The phospholipids bind only to the cartilage surface, or to HA surface layer; therefore, the hydration lubrication is not applied in this case. The schema of the adsorbed boundary layer formation by lubricant 4 is shown in Fig. 10-D. In our opinion, the albumin clusters bind to the cartilage surface and they are imprisoned between a bilayer of phospholipids, which cause a gradual attachment of albumin proteins in the contact. The interaction between proteins and phospholipids is minimal because the phospholipids are strongly bound to the high polar hydration gel-like HA layer; therefore, the phospholipids do not attract low polar albumin and Y-globulin proteins. The phospholipids contain a negative charge phosphate residue of phosphatidic acid and nonpolar lipids residue. In polar solutions (SF), phospholipids are oriented in bilayers or have a micellar orientation, while the phosphate residue is oriented outside of the layer [11,27,53]. The presence of phospholipids causes the increase in CoF [35]; nevertheless, it depends on the amount of all components of the lubricant. In complex SF model (lubricant 4), the presence of phospholipids causes a higher CoF value but the number of protein clusters and the area of albumin film increases during the experiment. The phosphate nuclei bind to water [27,53], and this, without the presence of the second bilayer, together with the structure of phospholipids, causes the lubricant to flow through the contact with higher resistance. The increasing amount of albumin in the contact seems to be the reason of higher value of CoF, as confirmed in [35], where the result shows the same conclusion. The lubrication provided by the complex SF model (lubricant 4) is the only one that allows for long-term operation while avoiding the stable adsorbed boundary layer in the contact.

One of the unique properties of cartilage is the ability of rehydration. As is obvious from Fig. 5, the rehydration between the individual steps of experiment causes the CoF trend to return to

the initial value after each rehydration. Trends showing the adsorbed boundary layer quality (Fig. 7 and Fig. 8) are obviously also affected by rehydration; the trend of adsorbed boundary layer area formed by albumin protein returns to the initial value after each rehydration unlike in the case of particles count in the contact. The regularity of behaviour is better when the lubricant composition is more complex (lubricant 3 and 4). In our opinion, the irregular influence of albumin particle counts in the contact area by the rehydration after each experiment is caused by the count of albumin particles that are nearby the contact area when the experiment is started. The reason is probably that the albumin and γ-globulin proteins in the simpler protein solutions (lubricants 1 and 2) are not as hydrophilic as HA, which causes less ability of individual proteins to bind to the cartilage surface. The regular behaviour of the CoF trends (the value of CoF after rehydration restores to the initial value) in connection with not entirely regular behaviour of trends of particles count through experiments (the value of particles count after rehydration does not always restore to the initial value) point out that the regularity of CoF is not caused only by albumin proteins but it is also affected by other components of synovial fluid. Future research will offer a complete study of each component of synovial fluid. This can contribute to determination of complete dependency of individual components of synovial fluid on the lubricating behaviour and CoF.

4.2. Methodology limitation

The main aim of this study is measuring of friction effects while visualizing the cartilage contact area. The main premiss of this measurement is that one of the contact pairs has to be transparent (the glass plate). The glass plate allows for the reciprocating tribometer to create the model of the synovial joint and allows for the in-situ view of the lubricating processes in the contact. This study admits that the simplified model of synovial joints represents only a very simplified natural synovial joint; however, neither friction measurement nor visualization in-situ can be carried out. In this case, only half of the real joint is preserved – the cartilage sample. The limitation is the elasticity modulus of the glass plate, which is many times higher than the modulus of the second real joint pair, and of different structural, tribological, and hydrophilic properties. Another limitation is the operating condition, which respects the actual pressure in the human joints and the average sliding speed between bones; nevertheless, the variable load cycle, as in the natural joint, is not applied. The values of contact pressure were determined on the basis of maximum values prevailing in the human hip joint; however, the cartilage samples were removed from pigs' joint. To sum up, considering all limitations, the results can only zoom the real adsorbed boundary layer formed in the synovial joint.

As with all experimental bio-tribological tasks, there is a problem with repeatability of measurements performed with the same lubricant but another cartilage sample because each cartilage has a different modulus of elasticity, geometry, and other properties [38]. It is the reason why the measurements were performed on cartilage samples. The aim of this study is to compare the performed measurements and evaluate the data obtained in experiments. The use of a unique sample of cartilage for each measurement could cause the difference between the data from each experiment, especially in visualization, which makes the comparison very difficult. The risk of using one sample is that it can affect consecutive measurements due to the clinging of individual components of the lubricant in the porous structure of cartilage. The components can have a chemical bond to its structure which is very difficult to remove. This study tries to prevent this influence by the initial run-in cycle before each experiment in order to remove all undesired residues from the cartilage structure.

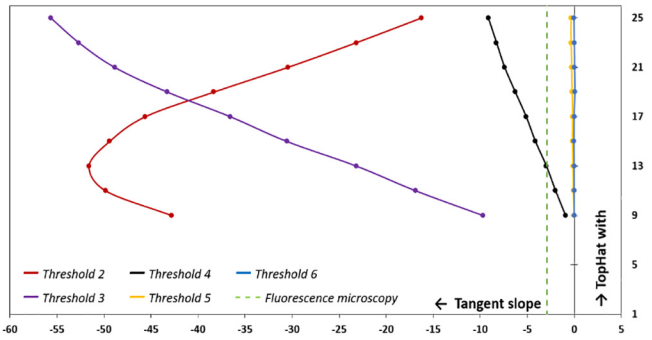

Fig. 11. Sensitivity of processing software settings.

Another provision how to protect the experiment from being influenced by the previous experiment is to determine the lubricant with gradual addition of individual components. Thus the acceptable repeatability can be achieved, see Table 3. The standard deviations of frictional measurements – expected by the CoF, report a magnitude smaller value than the CoF average value – in units of percent. The corresponding value from the assessment of friction/lubrication properties of the lubricant is the CoF; in both cases, it is the area of albumin adsorbed boundary layer calculated from the particle count of albumin protein clusters in the contact and the average size. The arithmetic average and its standard deviation are shown in Table 3.

A part of the experimental apparatus is a specially designed software for processing the snaps from the visualization by fluorescence microscope; a detailed description was published in [39]. For the processed snaps, the software results (particle count and average size of protein clusters) depend on the setting of the input parameters, especially "*TopHat width*" and "*Threshold*". The important input parameters affect the processed snaps; nevertheless, a degree of influence depends on the settings of software. It is calibrated before each experimental set based on the fluorescence trend; however, the calibration may vary depending on the quality of records from the camera, etc. To clarify the magnitude of the effect of variation of input parameters on the software, the sensitivity analysis was performed. The graph in Fig. 11 shows the dependency of the software input parameters in correlation with fluorescence microscopy (dashed green line in Fig. 11). The setting determined for this study is *Threshold* 13, *TopHat width* 4 and the calibration parameter is the tangent slope of intensity trend gained from the fluorescence record; therefore, the settings for these experiments are almost ideal. The set input parameters respond very well; nevertheless, it is not possible to set absolutely the same input parameters as has the intensity trend. Although the input parameters are set to "error", the dependency of other sets is linear; at least in the area (*Threshold* 4). If different input parameters were set (the processing error is linear), the processing error would be deducted because the whole set is processed by one set of input parameters of software.

5. Conclusions

The presented results used the new evaluation procedure introduced in the previous study [39]. This evaluation method allows for simultaneous friction measurement and visualization of contact. The connection of these two previously unconnected tribological approaches contributes to a deeper understanding of tribological behaviour of natural synovial joint including the impact of lubrication on the friction. This research presents a complex study of the impact of albumin protein on the lubrication process of natural cartilage. Fluorescence microscopy, a specially

designed tribometer and evaluation software allow to determine the amount of albumin clusters in the active contact and their average size. The output of visualization is connected to simultaneously measured friction forces, which allows to determine the impact of individual components of the lubricant (albumin in the SF) on the CoF and adsorbed boundary layer formation. Four sets of experiments were carried out, each with one lubricant. The SF model was gradually built from a simple albumin solution to a complex SF model. The concentration corresponds to physiological SF.

The basis of the results are trends of CoF and their relationship with trends represent a lubrication behaviour – the particles count of albumin in the contact and the area of adsorbed boundary layer formed by the albumin protein. The best tribological behaviour was found with lubricant 4, which represents a complex model of synovial fluid. This is the only lubricant which shows low values of friction and a stable adsorbed boundary layer – a permanently rising area of adsorbed boundary layer created by albumin protein. The lubricating behaviour of complex synovial fluid is apparently caused by the presence of HA in combination with phospholipids. In our opinion, HA, due to high hydrophilicity, binds to phospholipids, which causes detention of proteins in the contact. Although the fully complex lubricant represents a good long - term protection of cartilage surface, better friction properties were shown by the lubricant without phospholipids (albumin + γ-globulin + HA). However, a long - term protection of raw cartilage surface is not guaranteed. Although the trends of particles count of albumin in the contact rise quite steeply, the area of albumin adsorbed boundary layer is not always rising over time; the adsorbed boundary layer is likely to break and the raw cartilage surface comes into contact with the glass – the cartilage tissue can be damaged. In the case of protein solutions (simple albumin on one hand and a combination of albumin + γ-globulin on the other hand), a stable adsorbed boundary layer was not observed. In the both cases, the trends of albumin particle counts were decreasing; however, relatively high values of albumin adsorbed boundary layer area were observed, especially for simple albumin lubrication. The trends representing the lubricating quantity in these two cases are not guaranteed. This behaviour seems to be caused by absence of HA, which allows for stronger bonding of proteins with the cartilage surface in the contact. The particles count of albumin and also the area of albumin adsorbed boundary layer show low values for the lubricant combining albumin and γ-globulin. The adsorbed boundary layer consists of a smaller number of particles with a smaller size. The γ–globulin protein is compared to the albumin protein much larger and, based on the previous studies, the γ-globulin binds with albumin. This indicates γ–globulin as a separator of albumin adsorbed boundary layer. The impact of rehydration was also evaluated. The CoF trends return to the initial values after each experiment but the trends representing the adsorbed boundary layer do not show the same trend. This indicates that the restart of CoF values is not only affected by the albumin protein lubrication, but another component is also involved.

The authors presented the first study where the visualization of albumin protein in cartilage contact was performed simultaneously with friction measurement and a newly developed method [39] was used for evaluation of adsorbed boundary layer in a simplified synovial joint model. These methodologies and experimental devices allow for certain limitations and represent not only a simplified model of synovial joints; regardless of this knowledge, this can contribute to the understanding of the lubrication system prevalent in the human synovial joint. In order to approximate the real situation on the nature synovial joint, the future experiments will focus on the evaluation of all components contained in SF. Furthermore, our research assumes the improvement of the experimental equipment using a hydrogel instead of glass, which bring the experimental device closer to the real synovial joint. Newly acquired knowledge gained through a special evaluation method and experimental equipment also allows for a new opportunity in the field of soft contact research (tribology of the eyes, fascia or tissue).

Declaration of Competing Interest

The authors declare that they have no known competing financial interests or personal relationships that could have appeared to influence the work reported in this paper.

Acknowledgement

This research was funded by Czech Science Foundation, grant number 20-00483S.

References

[1] P.A. Simkin, D.O. Graney, J.J. Fiechtner, Roman arches, human joints, and disease, Arthritis Rheum. 23 (11) (1980) 1308–1311, https://doi.org/10.1002/art.1780231114.
[2] J. Buckwalter, J. Martin, Osteoarthritis☆, Adv. Drug Deliv. Rev. 58 (2) (2006) 150–167, https://doi.org/10.1016/j.addr.2006.01.006.
[3] A. Threlkeld, D. Currier, Osteoarthritis, Phys. Ther. 68 (1988) 364–370, https://doi.org/10.1093/ptj/68.3.364.
[4] A. Suckel, F. Geiger, L. Kinzl, N. Wulker, M. Garbrecht, Long-term Results for the Uncemented Zweymuller/Alloclassic Hip Endoprosthesis, J. Arthroplast. 24 (6) (2009) 846–853, https://doi.org/10.1016/j.arth.2008.03.021.
[5] PICONI C, MACCAURO1 G, MURATORI1 F, BRACH DEL PREVER E. Alumina and Zirconia Ceramics in Joint Replacements. Journal of Applied Biomaterials & Biomechanics 2003:19-32. https://doi.org/10.1177/228080000300100103.
[6] N. Bellamy, J. Campbell, V. Welch, T. Gee, R. Bourne, G. Wells, Viscosupplementation for the treatment of osteoarthritis of the knee, Cochrane Database of Systematic Reviews (2006), https://doi.org/10.1002/14651858.CD005321.pub2.
[7] K.D. Brandt, J.A. Block, J.P. Michalski, L.W. Moreland, J.R. Caldwell, P.T. Lavin, Cite Share Favorites Permissions Efficacy and Safety of Intraarticular Sodium Hyaluronate in Knee Osteoarthritis, Clin. Orthop. Relat. Res. 385 (2001) 130–143.
[8] J.A. Jarcho, D.J. Hunter, Viscosupplementation for Osteoarthritis of the Knee, N. Engl. J. Med. 372 (11) (2015) 1040–1047, https://doi.org/10.1056/NEJMct1215534.
[9] R.R. Bannuru, E.E. Vaysbrot, M.C. Sullivan, T.E. McAlindon, Relative efficacy of hyaluronic acid in comparison with NSAIDs for knee osteoarthritis: A systematic review and meta-analysis, Semin. Arthritis Rheum. 43 (5) (2014) 593–599, https://doi.org/10.1016/j.semarthrit.2013.10.002.
[10] D. Rebenda, M. Vrbka, P. Čípek, E. Toropitsyn, D. Nečas, M. Pravda, M. Hartl, On the Dependence of Rheology of Hyaluronic Acid Solutions and Frictional Behavior of Articular Cartilage, Materials 13 (2020) 1–14, https://doi.org/10.3390/ma13112659.
[11] S. Jahn, J. Seror, J. Klein, Lubrication of Articular Cartilage, Annu. Rev. Biomed. Eng. 18 (1) (2016) 235–258, https://doi.org/10.1146/annurev-bioeng-081514-123305.
[12] S.V. Eleswarapu, N.D. Leipzig, K.A. Athanasiou, Gene expression of single articular chondrocytes, Cell Tissue Res. 327 (1) (2006) 43–54, https://doi.org/10.1007/s00441-006-0258-5.
[13] A.J. Almarza, K.A. Athanasiou, Design Characteristics for the Tissue Engineering of Cartilaginous Tissues, Ann. Biomed. Eng. 32 (1) (2004) 2–17, https://doi.org/10.1023/B:ABME.0000007786.37957.65.
[14] M.M. Blum, T.C. Ovaert, Investigation of friction and surface degradation of innovative boundary lubricant functionalized hydrogel material for use as artificial articular cartilage, Wear 301 (1-2) (2013) 201–209, https://doi.org/10.1016/j.wear.2012.11.042.
[15] T.J. Knobloch, S. Madhavan, J. Nam, S. Agarwal, Jr., S. Agarwal, Regulation of Chondrocytic Gene Expression by Biomechanical Signals. Critical Reviews™ in Eukaryotic, Gene Expr. 18 (2) (2008) 139–150, https://doi.org/10.1615/CritRevEukarGeneExpr.v18.i2.30.
[16] J. Becerra, J.A. Andrades, E. Guerado, P. Zamora-Navas, J.M. López-Puertas, A.H. Reddi, Articular Cartilage: Structure and Regeneration, Tissue Eng. Part B Rev. 16 (6) (2010) 617–627, https://doi.org/10.1089/ten.teb.2010.0191.
[17] M.E. Blewis, G.E. Nugent-Derfus, T.A. Schmidt, B.L. Schumacher, R.L. Sah, A MODEL OF SYNOVIAL FLUID LUBRICANT COMPOSITION IN NORMAL AND INJURED JOINTS, Eur. Cells Mater. 13 (2007) 26–39.
[18] T. Schmid, J. Su, K. Lindley, V. Soloveychik, L. Madsen, J. Block, K. Kuettner, B. Schumacher, Superficial zone protein (SZP) is an abundant glycoprotein in human synovial fluid with lubricating properties, in: V. Hascall, K. Kuettner (Eds.), The Many Faces of Osteoarthritis, 1 ed.,., Birkhäuser Basel, Basel, 2002, pp. 159–161, https://doi.org/10.1007/978-3-0348-8133-3_16.

[19] I.M. Schwarz, B.A. Hills, Surface-active phospholipid as the lubricating component of lubricin, Rheumatology 37 (1) (1998) 21–26, https://doi.org/10.1093/rheumatology/37.1.21.
[20] A. Galandáková, J. Ulrichová, K. Langová, A. Hanáková, M. Vrbka, M. Hartl, J. Gallo, Characteristics of synovial fluid required for optimization of lubrication fluid for biotribological experiments, J. Biomed. Mater. Res. B Appl. Biomater. 105 (6) (2017) 1422–1431, https://doi.org/10.1002/jbm.b.33663.
[21] K.A. Athanasiou, M.P. Rosenwasser, J.A. Buckwalter, T.I. Malinin, V.C. Mow, Interspecies comparisons of in situ intrinsic mechanical properties of distal femoral cartilage, J. Orthop. Res. 9 (3) (1991) 330–340, https://doi.org/10.1002/jor.1100090304.
[22] M. MacConaill, The Function of Intra-Articular Fibrocartilages, with Special Reference to the Knee and Inferior Radio-Ulnar Joints, Jurnal of Anatomy 1932 (1932) 220–227.
[23] B.A. Hills, Boundary lubrication in vivo, Proc. Inst. Mech. Eng. [H] 214 (1) (2000) 83–94, https://doi.org/10.1243/0954411001535264.
[24] E.L. Radin, D.A. Swann, P.A. Weisser, Separation of a Hyaluronate-free Lubricating Fraction from Synovial Fluid, Nature 228 (5269) (1970) 377–378, https://doi.org/10.1038/228377a0.
[25] C.W. McCUTCHEN, Mechanism of Animal Joints: Sponge-hydrostatic and Weeping Bearings, Nature 184 (4695) (1959) 1284–1285, https://doi.org/10.1038/1841284a0.
[26] K. Ikeuchi, Origin and future of hydration lubrication, Proceed. Instit. Mech. Eng. Part J: J. Eng. Tribol. 221 (3) (2007) 301–305, https://doi.org/10.1243/13506501JET214.
[27] J. Klein, Hydration lubrication, Hydration lubrication. Friction 1 (1) (2013) 1–23, https://doi.org/10.1007/s40544-013-0001-7.
[28] T. Murakami, Importance of adaptive multimode lubrication mechanism in natural and artificial joints, Proceed. Instit. Mech. Eng. Part J J. Eng. Tribol. 226 (10) (2012) 827–837, https://doi.org/10.1177/1350650112451377.
[29] T. Murakami, S. Yarimitsu, N. Sakai, K. Nakashima, T. Yamaguchi, Y. Sawae, Importance of adaptive multimode lubrication mechanism in natural synovial joints, Tribol. Int. 113 (2017) 306–315, https://doi.org/10.1016/j.triboint.2016.12.052.
[30] S. Yarimitsu, K. Nakashima, Y. Sawae, T. Murakami, Influences of lubricant composition on forming boundary film composed of synovia constituents, Tribol. Int. 42 (11-12) (2009) 1615–1623, https://doi.org/10.1016/j.triboint.2008.11.005.
[31] R. Forsey, J. Fisher, J. Thompson, M. Stone, C. Bell, E. Ingham, The effect of hyaluronic acid and phospholipid based lubricants on friction within a human cartilage damage model, Biomaterials 27 (26) (2006) 4581–4590, https://doi.org/10.1016/j.biomaterials.2006.04.018.
[32] T.-T. Wu, X.-q. Gan, Z.-B. Cai, M.-H. Zhu, M.-T. Qiao, H.-Y. Yu, The lubrication effect of hyaluronic acid and chondroitin sulfate on the natural temporomandibular cartilage under torsional fretting wear, Lubr. Sci. 27 (1) (2015) 29–44, https://doi.org/10.1002/ls.1253.
[33] Y. Merkher, S. Sivan, I. Etsion, A. Maroudas, G. Halperin, A. Yosef, A rational human joint friction test using a human cartilage-on-cartilage arrangement, Tribol. Lett. 22 (1) (2006) 29–36, https://doi.org/10.1007/s11249-006-9069-9.
[34] F. Li, A. Wang, C. Wang, Analysis of friction between articular cartilage and polyvinyl alcohol hydrogel artificial cartilage, J. Mater. Sci. - Mater. Med. 27 (2016) 1–8, https://doi.org/10.1007/s10856-016-5700-y.
[35] D. Furmann, D. Nečas, D. Rebenda, P. Čípek, M. Vrbka, I. Křupka, M. Hartl, The Effect of Synovial Fluid Composition, Speed and Load on Frictional Behaviour of Articular Cartilage, Materials 13 (2020) 1–16, https://doi.org/10.3390/ma13061334.
[36] A. Moore, D. Burris, New Insights Into Joint Lubrication, Tribol. Lubricat. Technol. 72 (2016) 26–30.
[37] A.C. Cilingir, Effect of rotational and sliding motions on friction and degeneration of articular cartilage under dry and wet friction, J. Bionic Eng. 12 (3) (2015) 464–472, https://doi.org/10.1016/S1672-6529(14)60137-2.
[38] S.M.T. Chan, C.P. Neu, G. DuRaine, K. Komvopoulos, A.H. Reddi, Atomic force microscope investigation of the boundary-lubricant layer in articular cartilage, Osteoarth. Cartil. 18 (7) (2010) 956–963, https://doi.org/10.1016/j.joca.2010.03.012.
[39] P. Čípek, M. Vrbka, D. Rebenda, D. Nečas, I. Křupka, Biotribology of Synovial Cartilage: A New Method for Visualization of Adsorbed boundary layer and Simultaneous Measurement of the Friction Coefficient, Materials 13 (2020) 1–19, https://doi.org/10.3390/ma13092075.
[40] Development of reciprocating tribometer for testing synovial joint. ENGINEERING MECHANICS 2018, Svratka, Czech republic: Engineering Mechanics; 2018, pp. 169-172. https://doi.org/10.21495/91-8-169.
[41] P. Čípek, D. Rebenda, D. Nečas, M. Vrbka, I. Křupka, M. Hartl, Visualization of Adsorbed boundary layer in Model of Synovial Joint, Tribol. Industry 41 (2019) 387–393.
[42] D. Nečas, M. Vrbka, A. Galandáková, I. Křupka, M. Hartl, On the observation of lubrication mechanisms within hip joint replacements. Part I: Hard-on-soft bearing pairs, J. Mech. Behav. Biomed. Mater. 89 (2019) 237–248, https://doi.org/10.1016/j.jmbbm.2018.09.022.
[43] D. Nečas, M. Vrbka, F. Urban, I. Křupka, M. Hartl, The effect of lubricant constituents on lubrication mechanisms in hip joint replacements, J. Mech. Behav. Biomed. Mater. 55 (2016) 295–307, https://doi.org/10.1016/j.jmbbm.2015.11.006.
[44] J.E. Pickard, J. Fisher, E. Ingham, J. Egan, Investigation into the effects of proteins and lipids on the frictional properties of articular cartilage, Biomaterials 19 (19) (1998) 1807–1812, https://doi.org/10.1016/S0142-9612(98)00147-1.
[45] W. Hodge, R. Fijan, K. Carlson, R. Burgess, W. Harris, R. Mann, Contact pressures in the human hip joint measured in vivo, Proc. Natl. Acad. Sci. 83 (2879–2883) (1986) 2879–2883, https://doi.org/10.1073/pnas.83.9.2879.
[46] V.C. Mow, A. Ratcliffe, A. Robin Poole, Cartilage and diarthrodial joints as paradigms for hierarchical materials and structures, Biomaterials 13 (2) (1992) 67–97, https://doi.org/10.1016/0142-9612(92)90001-5.
[47] Y.L. Jeyachandran, E. Mielczarski, B. Rai, J.A. Mielczarski, Quantitative and Qualitative Evaluation of Adsorption/Desorption of Bovine Serum Albumin on Hydrophilic and Hydrophobic Surfaces, Langmuir 25 (19) (2009) 11614–11620, https://doi.org/10.1021/la901453a.
[48] S.M. McNary, K.A. Athanasiou, A.H. Reddi, Engineering Lubrication in Articular Cartilage, Tissue Eng. Part B: Rev. 18 (2) (2012) 88–100, https://doi.org/10.1089/ten.teb.2011.0394.
[49] G.W. Greene, B. Zappone, B. Zhao, O. Söderman, D. Topgaard, G. Rata, J.N. Israelachvili, Changes in pore morphology and fluid transport in compressed articular cartilage and the implications for joint lubrication, Biomaterials 29 (33) (2008) 4455–4462, https://doi.org/10.1016/j.biomaterials.2008.07.046.
[50] S.B. Dev, J.T. Keller, C.K. Rha, Secondary structure of 11 S globulin in aqueous solution investigated by FT-IR derivative spectroscopy, Biochim. et Biophys. Acta (BBA) - Protein Struct. Molecul. Enzymol. 957 (2) (1988) 272–280, https://doi.org/10.1016/0167-4838(88)90283-X.
[51] M.J. Howard, C.M. Smales, NMR Analysis of Synthetic Human Serum Albumin α-Helix 28 Identifies Structural Distortion upon Amadori Modification, J. Biol. Chem. 280 (24) (2005) 22582–22589, https://doi.org/10.1074/jbc.M501480200.
[52] Z. Liu, W. Lin, Y. Fan, N. Kampf, Y. Wang, J. Klein, Effects of Hyaluronan Molecular Weight on the Lubrication of Cartilage-Emulating Boundary Layers, Biomacromolecules 21 (10) (2020) 4345–4354, https://doi.org/10.1021/acs.biomac.0c0115110.1021/acs.biomac.0c01151.s001.
[53] R. Murray, D. Granner, P. Mayes, V. Rodwell, Harper's Illustrated Biochemistry, 28 ed., McGraw-Hill, New York, United States, 2018.

7 CONCLUSIONS

A healthy NSJ ensures painless human movement with uniquely low friction as a result of unique tribological properties of the AC. Movement activities are very important for enjoyable and stress-free life but it can be interrupted by many kinds of joint diseases, which can lead to irreversible destruction of the NSJ. This is often solved by application of artificial joints. Unfortunately, they have a limited service life, which leads to the necessity of replacing the artificial joint repeatedly. If this occurs in young age, there is a potential problem with its reoperation, after the service life has elapsed. The general effort is to postpone the necessity of replacement of the NSJ with artificial joint as long as possible, because the human organism is not able to withstand the frequently repeated surgery. The surgery influences the psychological state of the patient and also the subchondral bone degradation occurs. In order to avoid the necessity of replacing the NSJ with artificial joint, scientists discovered viscosuplementation (the supplement based on HA, which is needled to the joint gap). This supplement allows restarting of the lubricating processes of NSJ, which ideally stops the disease progression, or at least slows it down. The same effect of supplements in all patients is not guaranteed, which points to incomplete understanding of NSJ lubricating. Full understanding of lubrication processes in the NSJ allows us to develop an effective treatment for all patients with diseased joints.

The research focused on the biotribology of NSJ contains many studies dealing with the frictional properties of the NSJ. Various experimental configurations and their impact to friction properties were observed. It can be said that the frictional behaviour of the AC is described in detail. Studies dealing with the lubrication processes appear in a smaller number. The authors observe the impact of composition or experimental conditions on the lubricating film formation, using frictional or optical methods. The theoretical models of lubrication mechanism were developed within these studies, but they usually do not have a fully experimental background. The visualization of the AC contact is not commonly discussed. If so, the authors describe the influence of the composition of lubricants on lubrication, and also the impact of concentration of individual components of model SF was observed. The simultaneous contact visualization and friction measurement are discussed very rarely with the exception of a few studies. These studies almost always used the PVA hydrogel instead of AC sample, and the visualization was performed either after the experiments or was not performed continuously. There is no work performing the simultaneous AC contact visualization and friction measurements. This thesis strives to fill this white space, which can help to better understand the lubrication system prevailing in the NSJ, and the gained knowledge can contribute to the development of effective treatment of diseased NSJ.

A novice evaluation approach of a contact provided by the model of NSJ is introduced and used in this thesis, the description of lubricating film formation is provided. This system of

AC contact evaluation has not yet been published. The main conclusions of this thesis can be summarized as follows:

- A new evaluating methodology of articular cartilage contact was developed, including a specially designed reciprocating tribometer, evaluation software, and experimental data procedure
- Due to the new evaluation methodology of articular cartilage contact, the lubricating film formation in the model of synovial joint was performed, and the impact of individual components using the albumin protein observation was described

Regarding the scientific questions, the obtained knowledge can be summarized in the following concluding remarks:

- From the performed investigation, a simple albumin solution creates a lubricating film with high number of particles in the contact; however, this film is gradually wiped, which confirms that the simple albumin solution does not create a stabile lubrication film. The lubricant which consists of the mixture of albumin and γ-globulin proteins, gives better lubricating and frictional properties, which was expected based on previous studies. The count of albumin clusters in the contact was lower than in the simple albumin solution, which is attributed to the bonding between albumin and γ-globulin. Due to the γ globulin protein having a larger size than albumin, the γ globulin surface is covered with albumin proteins which bind to the cartilage surface, optionally to a gel-like layer of hyaluronic acid. Hyaluronic acid is used in the lubricant with a mixture of proteins and causes a significant reduction of friction, and the cartilage contact area shows much more particles of albumin. Hyaluronic acid creates the gel-like layer on the cartilage surface; due to high hydrophilicity of hyaluronic acid, the protein adsorption on the cartilage surface (gel-like layer) is more significant. The complex model synovial fluid containing protein components, hyaluronic acid, and phospholipids gives higher values of friction than the lubricant without phospholipids; however, the lubricating film area increases, which was indicated only for this lubricant composition.
  (HYPOTHESIS WAS NOT FALSIFIED WHITIN THIS THESIS)

- The best frictional properties were observed for the lubricant with a composition of protein components and hyaluronic acid, which was also the lubricant that shows the highest number of particles in the cartilage contact. Nevertheless, the simple albumin solution showed a higher particle count in the contact than the mixture of albumin and γ-globulin, which gives better values of friction coefficient.
  (HYPOTHESIS WAS FALSIFIED WHITIN THIS THESIS)

8 LIST OF PUBLICATIONS

8.1 Papers published in journals with impact factor

ČÍPEK, P.; VRBKA, M.; REBENDA, D.; NEČAS, D.; KŘUPKA, I. Biotribology of Synovial Cartilage: A New Method for Visualization of Lubricating Film and Simultaneous Measurement of the Friction Coefficient. *Materials,* 2020, **13**(9), 1-20. ISSN: 1996-1944.

REBENDA, D.; VRBKA, M.; ČÍPEK, P.; TOROPITSYN, E.; NEČAS, D.; PRAVDA, M.; HARTL, M. On the Dependence of Rheology of Hyaluronic Acid Solutions and Frictional Behavior of Articular Cartilage. *Materials,* 2020, **13**(11), 1-14. ISSN: 1996-1944.

FURMANN, D.; NEČAS, D.; REBENDA, D.; ČÍPEK, P.; VRBKA, M.; KŘUPKA, I.; HARTL, M. The effect of synovial fluid composition, speed and load on frictional behaviour of articular cartilage. *Materials,* 2020, **13**(6), 1-16. ISSN: 1996-1944.

ČÍPEK, P.; VRBKA, M.; REBENDA, D.; NEČAS, D.; KŘUPKA, I. Biotribology of Synovial Cartilage: Role of Albumin in Adsorbed Film Formation. *Engineering Science and Technology, an International Journal*. 2022, **34**, 101090. ISSN: 22150986

8.2 Papers published in peer-reviewed journals

ČÍPEK, P.; REBENDA, D.; NEČAS, D.; VRBKA, M.; KŘUPKA, I.; HARTL, M. Visualization of Lubrication Film in Model of Synovial Joint. *Tribology in Industry,* 2019, **41**(3), 387-393. ISSN: 0354-8996.

8.3 Papers in conference proceedings

ČÍPEK, P.; REBENDA, D.; VRBKA, M.; HARTL, M. OBSERVATION OF LUBRICATION FILM IN SYNOVIAL JOINT. In *Proceedings on Engineering Science. Proceedings on Engineering Sciences - 16th International Conference on Tribology*. Kragujevac: University of Kragujevac, Faculty of Engineering, 2019, 687-692. ISSN: 2620-2832.

REBENDA, D.; ČÍPEK, P.; VRBKA, M.; KŘUPKA, I. Effect of Hyaluronic Acid Molecular Weight on Friction of Articular Cartilage. In *Proceedings on Engineering Sciences - 16th International Conference on Tribology*. *Proceedings on Engineering Sciences - 16th International Conference on Tribology*. Kragujevac: University of Kragujevac, Faculty of Engineering, 2019, 693-697. ISSN: 2620-2832.

ČÍPEK, P.; REBENDA, D.; NEČAS, D.; VRBKA, M.; KŘUPKA, I. Development of reciprocating tribometer for testing synovial joint. In *Engineering Mechanics 2018*. *Engineering Mechanics 2018*. First edition. Praha: Institute of Theoretical and Applied Mechanics of the Czech Academy of Sciences, Prague, 2018, 169-172. ISBN: 978-80-86246-88-8. ISSN: 1805-8256.

REBENDA, D.; ČÍPEK, P.; NEČAS, D.; VRBKA, M.; HARTL, M. Effect of Hyaluronic Acid on Friction of Articular Cartilage. In *Engineering Mechanics 2018*. First. Praha: Institute of Theretical and Applied Mechanics of the Czech Academy of Sciences, 2018, 709-712. ISBN: 978-80-86246-91-8.

9 LITERATURE

[1] VAN DER ZWAN, Judith, Wieke DE VENTE, Anja HUIZINK, Susan BÖGELS a Esther DE BRUIN. Physical Activity, Mindfulness Meditation, or Heart Rate Variability Biofeedback for Stress Reduction: A Randomized Controlled Trial. *Applied Psychophysiology and Biofeedback*. 2015, **40**(4), 257-268

[2] HAMER, Mark, Romano ENDRIGHI a Lydia POOLE. Physical Activity, Stress Reduction, and Mood: Insight into Immunological Mechanisms. YAN, Qing, ed., Qing YAN. *Psychoneuroimmunology*. Totowa, NJ: Humana Press, 2012, s. 89-102

[3] BUCKWALTER, J a J MARTIN. Osteoarthritis☆. *Advanced Drug Delivery Reviews*. 2006, **58**(2), 150-167

[4] ACKERMAN, Ilana, Megan BOHENSKY, Richard DE STEIGER et al. Lifetime Risk of Primary Total Hip Replacement Surgery for Osteoarthritis From 2003 to 2013: A Multinational Analysis Using National Registry Data. *Arthritis Care & Research*. 2017, **69**(11), 1659-1667

[5] THRELKELD, A. a Dean CURRIER. Osteoarthritis. *Physical Therapy*. 1988, **68**(3), 364-370

[6] PICONI, C., G. MACCAURO1, F. MURATORI1 a E. BRACH DEL PREVER. Alumina and Zirconia Ceramics in Joint Replacements. *Journal of Applied Biomaterials & Biomechanics*. 2003, (1), 19-32

[7] BELLAMY, Nicholas, Jane CAMPBELL, Vivian WELCH, Travis GEE, Robert BOURNE a George WELLS. Viscosupplementation for the treatment of osteoarthritis of the knee. *Cochrane Database of Systematic Reviews*

[8] BRANDT, Kenneth, Joel BLOCK, Joseph MICHALSKI, Larry MORELAND, Jacques CALDWELL a Philip LAVIN. Cite Share Favorites Permissions Efficacy and Safety of Intraarticular Sodium Hyaluronate in Knee Osteoarthritis. *Clinical Orthopaedics and Related Research*. 2001, **2001**(285), 130-143

[9] REBENDA, David, Martin VRBKA, Pavel ČÍPEK, Evgeniy TOROPITSYN, David NEČAS, Martin PRAVDA a Martin HARTL. On the Dependence of Rheology of Hyaluronic Acid Solutions and Frictional Behavior of Articular Cartilage. *Materials*. 2020, **13**(11), 1-14

[10] BANNURU, Raveendhara, Elizaveta VAYSBROT, Matthew SULLIVAN a Timothy MCALINDON. Relative efficacy of hyaluronic acid in comparison with NSAIDs for knee osteoarthritis: A systematic review and meta-analysis. *Seminars in Arthritis and Rheumatism*. 2014, **43**(5), 593-599

[11] JARCHO, John a David HUNTER. Viscosupplementation for Osteoarthritis of the Knee. *New England Journal of Medicine*. 2015, **372**(11), 1040-1047

[12] ELESWARAPU, Sriram, Nic LEIPZIG a Kyriacos ATHANASIOU. Gene expression of single articular chondrocytes. *Cell and Tissue Research*. 2006, **327**(1), 43-54

[13] ALMARZA, Alejandro a Kyriacos ATHANASIOU. Design Characteristics for the Tissue Engineering of Cartilaginous Tissues. *Annals of Biomedical Engineering*. 2004, **32**(1), 2-17

[14] TAMER, Tamer Mahmoud. Hyaluronan and synovial joint: function, distribution and healing. *Interdisciplinary Toxicology*. 2013, **6**(3), 111-125

[15] KNOBLOCH, Thomas, Shashi MADHAVAN, Jin NAM, Jr., AGARWAL a Sudha AGARWAL. Regulation of Chondrocytic Gene Expression by Biomechanical Signals. *Critical Reviews™ in Eukaryotic Gene Expression*. 2008, **18**(2), 139-150

[16] MOW, Van, Anthony RATCLIFFE a A. ROBIN POOLE. Cartilage and diarthrodial joints as paradigms for hierarchical materials and structures. *Biomaterials*. 1992, **13**(2), 67-97

[17] FITZGERALD, Jonathan, Moonsoo JIN a Alan GRODZINSKY. Shear and Compression Differentially Regulate Clusters of Functionally Related Temporal Transcription Patterns in Cartilage Tissue. *Journal of Biological Chemistry*. 2006, **281**(34), 24095-24103

[18] BECERRA, José, José ANDRADES, Enrique GUERADO, Plácido ZAMORA-NAVAS, José LÓPEZ-PUERTAS a A. REDDI. Articular Cartilage: Structure and Regeneration. *Tissue Engineering Part B: Reviews*. 2010, **16**(6), 617-627

[19] HODGE, W., R. FIJAN, K. CARLSON, R. BURGESS, W. HARRIS a R. MANN. Contact pressures in the human hip joint measured in vivo. *Proceedings of the National Academy of Sciences*. 1986, **83**(9), 2879-2883

[20] CHAN, S.M.T., C.P. NEU, G. DURAINE, K. KOMVOPOULOS a A.H. REDDI. Atomic force microscope investigation of the boundary-lubricant layer in articular cartilage. *Osteoarthritis and Cartilage*. 2010, **18**(7), 956-963

[21] POOLE, A, I PIDOUX, A REINER a L ROSENBERG. An immunoelectron microscope study of the organization of proteoglycan monomer, link protein, and collagen in the matrix of articular cartilage. *Journal of Cell Biology*. 1982, **93**(3), 921-937

[22] GREENE, George, Bruno ZAPPONE, Boxin ZHAO, Olle SÖDERMAN, Daniel TOPGAARD, Gabriel RATA a Jacob ISRAELACHVILI. Changes in pore morphology and fluid transport in compressed articular cartilage and the implications for joint lubrication. *Biomaterials*. 2008, **29**(33), 4455-4462

[23] LAI, W., S. KUEI a V. MOW. Rheological Equations for Synovial Fluids. *Journal of Biomechanical Engineering*. 1978, **100**(4), 169-186

[24] PRETE, P, A GURAKAROSBORNE a M KASHYAP. Synovial fluid lipoproteins: Review of current concepts and new directions. *Seminars in Arthritis and Rheumatism*. 1993, **23**(2), 79-89

[25] PREKASAN, D. a K.K. SAJU. Review of the Tribological Characteristics of Synovial Fluid. *Procedia Technology*. 2016, **25**, 1170-1174

[26] GOLDSTEIN, Aaron S. Basic Transport Phenomena in Biomedical Engineering, Second Edition Basic Transport Phenomena in Biomedical Engineering, Second Edition Ronald L.Fournier Taylor and Francis Group, New York, 2007. 440 pp. ISBN 1-59169-026-9. *Tissue Engineering*. 2006, **12**(12), 3567-3567

[27] SCHMIDT, T.A. a R.L. SAH. Effect of synovial fluid on boundary lubrication of articular cartilage. *Osteoarthritis and Cartilage*. 2007, **15**(1), 35-47

[28] STAFFORD, C., W. NIEDERMEIER, H. HOLLEY a W. PIGMAN. Studies on the Concentration and Intrinsic Viscosity of Hyaluronic Acid in Synovial Fluids of Patients with Rheumatic Diseases. *Annals of the Rheumatic Diseases*. 1964, **23**(2), 152-157

[29] LINK, Jarrett, Evelia SALINAS, Jerry HU a Kyriacos ATHANASIOU. The tribology of cartilage: Mechanisms, experimental techniques, and relevance to translational tissue engineering. *Clinical Biomechanics*. 2020, **79**

[30] STACHOWIAK, G.W., A.W. BATCHELOR a L.J. GRIFFITHS. Friction and wear changes in synovial joints. *Wear*. 1994, **171**(1-2), 135-142

[31] MERKHER, Y., S. SIVAN, I. ETSION, A. MAROUDAS, G. HALPERIN a A. YOSEF. A rational human joint friction test using a human cartilage-on-cartilage arrangement. *Tribology Letters*. 2006, **22**(1), 29-36

[32] TEEPLE, Erin, Khaled ELSAID, Braden FLEMING, Gregory JAY, Koosha ASLANI, Joseph CRISCO a Anthony MECHREFE. Coefficients of friction, lubricin, and cartilage damage in the anterior cruciate ligament-deficient guinea pig knee. *Journal of Orthopaedic Research*. Hoboken: Wiley Subscription Services, Inc., A Wiley Company, 2008, **26**(2), 231-237

[33] MCCANN, L., I. UDOFIA, S. GRAINDORGE, E. INGHAM, Z. JIN a J. FISHER. Tribological testing of articular cartilage of the medial compartment of the knee using a friction simulator. *Tribology International*. 2008, **41**(11), 1126-1133

[34] CHAN, S.M.T., C.P. NEU, K. KOMVOPOULOS a A.H. REDDI. The role of lubricant entrapment at biological interfaces: Reduction of friction and adhesion in articular cartilage. *Journal of Biomechanics*. 2011, **44**(11), 2015-2020

[35] OUNGOULIAN, Sevan, Krista DURNEY, Brian JONES, Christopher AHMAD, Clark HUNG a Gerard ATESHIAN. Wear and damage of articular cartilage with friction against orthopedic implant materials. *Journal of Biomechanics*. Elsevier Ltd, 2015, **48**(10), 1957-1964

[36] MOORE, Axel a David BURRIS. New Insights Into Joint Lubrication. *Tribology & Lubrication Technology*. 2016, **72**(5), 26-30

[37] LI, Feng, Anmin WANG a Chengtao WANG. Analysis of friction between articular cartilage and polyvinyl alcohol hydrogel artificial cartilage. *Journal of Materials Science: Materials in Medicine*. 2016, **27**(5), 1-8

[38] MOW, Van, Mark HOLMES a W. MICHAEL LAI. Fluid transport and mechanical properties of articular cartilage: A review. *Journal of Biomechanics*. 1984, **17**(5), 377-394

[39] CHEN, A.C., W.C. BAE, R.M. SCHINAGL a R.L. SAH. Depth- and strain-dependent mechanical and electromechanical properties of full-thickness bovine articular cartilage in confined compression. *Journal of Biomechanics*. 2001, **34**(1), 1-12

[40] WU, Ting-ting, Xue-qi GAN, Zhen-bing CAI, Min-hao ZHU, Meng-ting QIAO a Hai-yang YU. The lubrication effect of hyaluronic acid and chondroitin sulfate on the natural temporomandibular cartilage under torsional fretting wear. *Lubrication Science*. 2015, **27**(1), 29-44

[41] ACCARDI, Mario, Daniele DINI a Philippa CANN. Experimental and numerical investigation of the behaviour of articular cartilage under shear loading—Interstitial fluid pressurisation and lubrication mechanisms. *Tribology International*. 2011, **44**(5), 565-578

[42] GLEGHORN, Jason a Lawrence BONASSAR. Lubrication mode analysis of articular cartilage using Stribeck surfaces. *Journal of Biomechanics*. Elsevier Ltd, 2008, **41**(9), 1910-1918

[43] MCCUTCHEN, C.W. The frictional properties of animal joints. *Wear*. 1962, **5**(1), 1-17

[44] WALKER, P, D DOWSON, M LONGFIELD a V WRIGHT. "Boosted lubrication" in synovial joints by fluid entrapment and enrichment. *Annals of the Rheumatic Diseases*. 1968, **27**(6), 512-520

[45] MANSOUR, Joseph a Van MOW. On the Natural Lubrication of Synovial Joints: Normal and Degenerate. *Journal of Lubrication Technology*. 1977, **99**(2), 163-172

[46] SWANN, D.A., H.S. SLAYTER a F.H. SILVER. The molecular structure of lubricating glycoprotein-I, the boundary lubricant for articular cartilage. *Journal of Biological Chemistry*. 1981, **256**(11), 5921-5925

[47] MURAKAMI, Teruo, Seido YARIMITSU, Nobuo SAKAI, Kazuhiro NAKASHIMA, Tetsuo YAMAGUCHI a Yoshinori SAWAE. Importance of adaptive multimode lubrication mechanism in natural synovial joints. *Tribology International*. 2017, **113**, 306-315

[48] JAHN, Sabrina, Jasmine SEROR a Jacob KLEIN. Lubrication of Articular Cartilage. *Annual Review of Biomedical Engineering*. 2016, **18**(1), 235-258

[49] FORSEY, R, J FISHER, J THOMPSON, M STONE, C BELL a E INGHAM. The effect of hyaluronic acid and phospholipid based lubricants on friction within a human cartilage damage model. *Biomaterials*. 2006, **27**(26), 4581-4590

[50] MURAKAMI, T, K NAKASHIMA, Y SAWAE, N SAKAI a N HOSODA. Roles of adsorbed film and gel layer in hydration lubrication for articular cartilage. *Proceedings of the Institution of Mechanical Engineers, Part J: Journal of Engineering Tribology*. 2009, **223**(3), 287-295

[51] HIGAKI, H, T MURAKAMI, Y NAKANISHI, H MIURA, T MAWATARI a Y IWAMOTO. The lubricating ability of biomembrane models with dipalmitoyl phosphatidylcholine and γ-globulin. *Proceedings of the Institution of Mechanical Engineers, Part H: Journal of Engineering in Medicine*. 1998, **212**(5), 337-346

[52] YARIMITSU, Seido, Kazuhiro NAKASHIMA, Yoshinori SAWAE a Teruo MURAKAMI. Influences of lubricant composition on forming boundary film composed of synovia constituents. *Tribology International*. 2009, **42**(11-12), 1615-1623

[53] YARIMITSU, Seido, Kazuhiro NAKASHIMA, Yoshinori SAWAE a Teruo MURAKAMI. Effects of Lubricant Composition on Adsorption Behavior of Proteins on Rubbing Surface and Stability of Protein Boundary Film. *Tribology Online*. 2008, **3**(4), 238-242

[54] NAKASHIMA, K., Y. SAWAE a T. MURAKAMI. Study on wear reduction mechanisms of artificial cartilage by synergistic protein boundary film formation. *JSME International Journal, Series C: Mechanical Systems, Machine Elements and Manufacturing*. 2006, **48**(4), 555-561

[55] ČÍPEK, Pavel, David REBENDA, David NEČAS, Martin VRBKA, Ivan KŘUPKA a Martin HARTL. Visualization of Lubrication Film in Model of Synovial Joint. *Tribology in Industry*. 2019, **41**(3), 387-393

[56] ČÍPEK, Pavel, Martin VRBKA, David REBENDA, David NEČAS a Ivan KŘUPKA. Biotribology of Synovial Cartilage: A New Method for Visualization of Lubricating Film and Simultaneous Measurement of the Friction Coefficient. *Materials*. 2020, **13**(9), 1-19

[57] ČÍPEK, Pavel, Martin VRBKA, David REBENDA, David NEČAS a Ivan KŘUPKA. Biotribology of synovial cartilage: Role of albumin in adsorbed film formation. *Engineering Science and Technology, an International Journal*. 2022, **34**, 1-12

[58] NEČAS, D., M. VRBKA, A. GALANDÁKOVÁ, I. KŘUPKA a M. HARTL. On the observation of lubrication mechanisms within hip joint replacements. Part I: Hard-on-

soft bearing pairs. *Journal of the Mechanical Behavior of Biomedical Materials*. 2019, **89**, 237-248

[59] NEČAS, David, Martin VRBKA, Filip URBAN, Ivan KŘUPKA a Martin HARTL. The effect of lubricant constituents on lubrication mechanisms in hip joint replacements. *Journal of the Mechanical Behavior of Biomedical Materials*. 2016, **55**, 295-307

[60] MOW, V., S. KUEI, W. LAI a C. ARMSTRONG. Biphasic Creep and Stress Relaxation of Articular Cartilage in Compression: Theory and Experiments. *Journal of Biomechanical Engineering*. 1980, **102**(1), 73-84

[61] LAKOWICZ, Joseph R. *Principles of fluorescence spectroscopy*. 3rd ed. New York: Springer, 2006. ISBN 978-0-387-31278-1.

[62] CILINGIR, Ahmet C. Effect of rotational and sliding motions on friction and degeneration of articular cartilage under dry and wet friction. *Journal of Bionic Engineering*. 2015, **12**(3), 464-472

[63] KATTA, J., Z. JIN, E. INGHAM a J. FISHER. Effect of nominal stress on the long term friction, deformation and wear of native and glycosaminoglycan deficient articular cartilage. *Osteoarthritis and Cartilage*. 2009, **17**(5), 662-668

[64] PICKARD, J.E., J. FISHER, E. INGHAM a J. EGAN. Investigation into the effects of proteins and lipids on the frictional properties of articular cartilage. *Biomaterials*. 1998, **19**(19), 1807-1812

[65] NORTHWOOD, Ewen a John FISHER. A multi-directional in vitro investigation into friction, damage and wear of innovative chondroplasty materials against articular cartilage. *Clinical Biomechanics*. 2007, **22**(7), 834-842

[66] CALIGARIS, M. a G.A. ATESHIAN. Effects of sustained interstitial fluid pressurization under migrating contact area, and boundary lubrication by synovial fluid, on cartilage friction. *Osteoarthritis and Cartilage*. 2008, **16**(10), 1220-1227

[67] ACHARYA, Tinku a Ajoy RAY. *Image Processing: Principles and Applications*. 1. NJ: John Wiley: Hoboken, 2005. ISBN 978-0-471-71998-4.

[68] VALA, Hetal a Astha BAXI. A review on Otsu image segmentation algorithm. *International Journal of Advanced Research in Computer Engineering & Technology*. 2013, **2**(2), 387-389

[69] VINCENT, Luc. Morphological Area Openings and Closings for Grey-scale Images. O, Ying-Lie, Alexander TOET, David FOSTER, Henk J. A. M. HEIJMANS a Peter MEER, ed., Ying-Lie O, Alexander TOET, David FOSTER, Henk HEIJMANS, Peter MEER. *Shape in Picture*. 126. Berlin, Heidelberg: Springer Berlin Heidelberg, 1994, s. 197-20

[70] RADIN, ERIC, DAVID SWANN a PAUL WEISSER. Separation of a Hyaluronate-free Lubricating Fraction from Synovial Fluid. *Nature*. 1970, **228**(5269), 377-378

[71] SWANN, David, Kurt BLOCH, David SWINDELL a Elizabeth SHORE. The lubricating activity of human synovial fluids. *Arthritis & Rheumatism*. 1984, **27**(5), 552-556

[72] MCCUTCHEN, C. W. Mechanism of Animal Joints: Sponge-hydrostatic and Weeping Bearings. *Nature*. 1959, **184**(4695), 1284-1285

[73] JEYACHANDRAN, Y., E. MIELCZARSKI, B. RAI a J. MIELCZARSKI. Quantitative and Qualitative Evaluation of Adsorption/Desorption of Bovine Serum Albumin on Hydrophilic and Hydrophobic Surfaces. *Langmuir*. 2009, **25**(19), 11614–11620

[74] MCNARY, Sean, Kyriacos ATHANASIOU a A. REDDI. Engineering Lubrication in Articular Cartilage. *Tissue Engineering Part B: Reviews*. 2012, **18**(2), 88-100

[75] FURMANN, Denis, David NEČAS, David REBENDA, Pavel ČÍPEK, Martin VRBKA, Ivan KŘUPKA a Martin HARTL. The Effect of Synovial Fluid Composition, Speed and Load on Frictional Behaviour of Articular Cartilage. *Materials*. 2020, **13**(6)

LIST OF FIGURES AND TABLES

LIST OF SYMBOLS AND ABBREVIATIONS

AC	Articular cartilage
B270	Glass with guaranteed optical properties
BFS	Bovine synovial fluid
CoCr	High carbon stainless steel
CoCrLC	Low carbon stainless steel
CoF	Coefficient of friction
CS	Chondroitin sulphate extracted from beef
ECM	Extracellular matrix
EM	Elasticity modulus
ESF	Unique synovial fluid
FITC	Fluorescein isothiocyanate
H.B.	Histidine buffer
HA	Hyaluronic acid
CH	Chondroitin sulphate extracted from beef + hyaluronic acid + phosphate buffered saline
I.F.S.	Model synovial fluid
LAB	Laboratory
M1	Medial anterior of the knee bone
M4	Medial posterior of the knee bone
MTM	Mini traction machine
NI	National Industry
NSJ	Natural synovial joint
OA	Osteoarthritis
PBS	Phosphate buffered saline

PTFE	Polytetrafluoroethylene
PVA	Poly-vinyl-alcohol
SE	Structural element
SF	Synovial fluid
SS	Stainless steel
TRITC	Tetramethylrhodamine
UMT	Universal mechanical tester
US	United States
USA	United States of America
USB	Universal serial bus
316SS	Low vacuum melt stainless steel

μ, f	[-]	Coefficient of friction (CoF)
F	[N]	Force
F_N	[N]	Normal load
F_t	[N]	Frictional force
v	[mm·s^{-1}]	Velocity
t	[s]	Time
p	[MPa]	Pressure
ε	[-]	Strain, relative deformation
ω	[rad·s^{-1}]	Angular speed